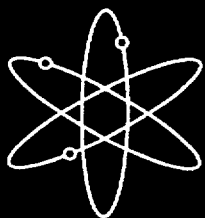


# Analysis of Spent Fuel Heatup Following Loss of Water in a Spent Fuel Pool



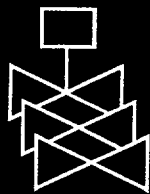
**A Users' Manual for the  
Computer Code SHARP**



Final Report



Energy and Environmental Science, Inc.



**U.S. Nuclear Regulatory Commission  
Office of Nuclear Regulatory Research  
Washington, DC 20555-0001**



## AVAILABILITY OF REFERENCE MATERIALS IN NRC PUBLICATIONS

### NRC Reference Material

As of November 1999, you may electronically access NUREG-series publications and other NRC records at NRC's Public Electronic Reading Room at [www.nrc.gov/NRC/ADAMS/index.html](http://www.nrc.gov/NRC/ADAMS/index.html).

Publicly released records include, to name a few, NUREG-series publications; *Federal Register* notices; applicant, licensee, and vendor documents and correspondence; NRC correspondence and internal memoranda; bulletins and information notices; inspection and investigative reports; licensee event reports; and Commission papers and their attachments.

NRC publications in the NUREG series, NRC regulations, and *Title 10, Energy*, in the Code of *Federal Regulations* may also be purchased from one of these two sources.

1. The Superintendent of Documents  
U.S. Government Printing Office  
Mail Stop SSOP  
Washington, DC 20402-0001  
Internet: [bookstore.gpo.gov](http://bookstore.gpo.gov)  
Telephone: 202-512-1800  
Fax: 202-512-2250
2. The National Technical Information Service  
Springfield, VA 22161-0002  
[www.ntis.gov](http://www.ntis.gov)  
1-800-553-6847 or, locally, 703-605-6000

A single copy of each NRC draft report for comment is available free, to the extent of supply, upon written request as follows:

Address: Office of the Chief Information Officer,  
Reproduction and Distribution  
Services Section  
U.S. Nuclear Regulatory Commission  
Washington, DC 20555-0001  
E-mail: [DISTRIBUTION@nrc.gov](mailto:DISTRIBUTION@nrc.gov)  
Facsimile: 301-415-2289

Some publications in the NUREG series that are posted at NRC's Web site address [www.nrc.gov/NRC/NUREGS/indexnum.html](http://www.nrc.gov/NRC/NUREGS/indexnum.html) are updated periodically and may differ from the last printed version. Although references to material found on a Web site bear the date the material was accessed, the material available on the date cited may subsequently be removed from the site.

### Non-NRC Reference Material

Documents available from public and special technical libraries include all open literature items, such as books, journal articles, and transactions, *Federal Register* notices, Federal and State legislation, and congressional reports. Such documents as theses, dissertations, foreign reports and translations, and non-NRC conference proceedings may be purchased from their sponsoring organization.

Copies of industry codes and standards used in a substantive manner in the NRC regulatory process are maintained at—

The NRC Technical Library  
Two White Flint North  
11545 Rockville Pike  
Rockville, MD 20852-2738

These standards are available in the library for reference use by the public. Codes and standards are usually copyrighted and may be purchased from the originating organization or, if they are American National Standards, from—

American National Standards Institute  
11 West 42<sup>nd</sup> Street  
New York, NY 10036-8002  
[www.ansi.org](http://www.ansi.org)  
212-642-4900

Legally binding regulatory requirements are stated only in laws; NRC regulations; licenses, including technical specifications; or orders, not in NUREG-series publications. The views expressed in contractor-prepared publications in this series are not necessarily those of the NRC.

The NUREG series comprises (1) technical and administrative reports and books prepared by the staff (NUREG-XXXX) or agency contractors (NUREG/CR-XXXX), (2) proceedings of conferences (NUREG/CP-XXXX), (3) reports resulting from international agreements (NUREG/IA-XXXX), (4) brochures (NUREG/BR-XXXX), and (5) compilations of legal decisions and orders of the Commission and Atomic and Safety Licensing Boards and of Directors' decisions under Section 2.206 of NRC's regulations (NUREG-0750).

**DISCLAIMER:** This report was prepared as an account of work sponsored by an agency of the U.S. Government. Neither the U.S. Government nor any agency thereof, nor any employee, makes any warranty, expressed or implied, or assumes any legal liability or responsibility for any third party's use, or the results of such use, of any information, apparatus, product, or process disclosed in this publication, or represents that its use by such third party would not infringe privately owned rights.

**NUREG/CR-6441  
BNL-NUREG-52494**

---

---

# **Analysis of Spent Fuel Heatup Following Loss of Water in a Spent Fuel Pool**

**A User's Manual for the  
Computer Code SHARP**

## **Final Report**

---

---

Manuscript Completed: February 2001

Date Published: March 2002

Prepared by

H.P. Nourbakhsh, G. Miao, and Z. Cheng

Energy and Environmental Science, Inc.

25 East Loop Road

Stony Brook, NY 11790

Under Contract to Brookhaven National Laboratory

Upton, NY 11973-5000

P.Norian, NRC Project Manager

**Prepared for**

**Division of Systems Analysis and Regulatory Effectiveness**

**Office of Nuclear Regulatory Research**

**U.S. Nuclear Regulatory Commission**

**Washington, DC 20555-0001**

**NRC Job Code L2590**



---

**NUREG/CR-6441 has been reproduced  
from the best available copy.**

---

## ABSTRACT

A methodology for predicting the spent fuel heatup in the event of loss of water during storage has been formulated and implemented within a computer code called SHARP (Spent-fuel Heatup: Analytical Response Program). This report documents the overall structure of the computer code SHARP. The code modeling framework, including the mathematical models and solution methods, are described in the report.

The computed results of the spent fuel heatup characteristics using representative design parameters and fuel loading assumptions, are presented. The results of sensitivity calculations to study the effect of fuel burnup, building ventilation rate, baseplate hole size, partial filling of the racks, and the amount of available space to the edge of the pool, are also presented in this report.

# CONTENTS

	Page
ABSTRACT .....	iii
EXECUTIVE SUMMARY .....	ix
FOREWORD .....	xi
NOMENCLATURE .....	xiii
1. INTRODUCTION .....	1-1
1.1 Background .....	1-1
1.2 Scope and Organization of This Report .....	1-2
2. DESIGN CHARACTERISTICS OF SPENT FUEL STORAGE POOLS .....	2-1
3. MODELING REQUIREMENTS .....	3-1
3.1 Technical Issue Specification .....	3-2
3.2 Accident Path Specification .....	3-2
3.3 Spent Fuel Pool Design and Configuration Specification .....	3-2
3.4 Phenomena Evaluation .....	3-2
3.4.1 Spent Fuel Rods .....	3-3
3.4.2 Spent Fuel Storage Rack .....	3-6
3.4.3 Downcomer Next to the Edge of the Pool .....	3-7
3.4.4 Base Region Beneath the Racks .....	3-7
3.4.5 Spent Fuel Storage Building .....	3-7
4. PHYSICAL MODELS .....	4-1
4.1 Heat Transfer in Spent Fuel Elements .....	4-1
4.2 Buoyancy-Driven Air Flows .....	4-4
4.2.1 One Dimensional Conservation Equations .....	4-4
4.2.1.1 Conservation of Mass .....	4-4
4.2.1.2 Conservation of Momentum .....	4-7
4.2.1.3 Conservation of Energy .....	4-7
4.2.2 Solution Procedure .....	4-7
4.3 Thermal-Hydraulics of Spent Fuel Storage Building .....	4-12
4.4 Thermal Hydraulics of the Base Region Beneath the Racks .....	4-12
4.5 Heat Transfer in Structures .....	4-15
4.6 Friction Factor .....	4-16

# CONTENTS

	<b>Page</b>
4.7 Local From Loss Factor Due to Base-Plate Hole .....	4-18
4.8 Pressure Loss at Spacer Grids .....	4-18
4.9 Heat Transfer Coefficient .....	4-18
4.10 Decay Heat .....	4-19
4.11 Overview of SHARP Code .....	4-19
5. CODE VERIFICATION AND VALIDATION .....	5-1
5.1 Comparison with the COBRA-SFS/TEMPEST Codes Predictions .....	5-1
6. RESULTS .....	6-1
7. SUMMARY AND CONCLUSIONS .....	7-1
8. REFERENCES .....	8-1
Appendix A A USER'S MANUAL FOR THE SHARP COMPUTER CODE .....	A-1

## FIGURES

Figure	Page
2.1 Schematic view of a typical spent fuel storage building .....	2-2
2.2 Typical spent fuel storage rack configuration .....	2-3
3.1 Basic components of the methodology for technical issue resolution .....	3-1
4.1 Fuel element geometry .....	4-2
4.2 Effect of decay heat on axial variation of clad temperature .....	4-5
4.3 Effect of inlet air velocity on axial variation of clad temperature .....	4-5
4.4 Schematic of spent fuel storage configuration modeled as parallel channels .....	4-6
4.5 General solution procedure to obtain the buoyancy induced air flow .....	4-9
4.6 Typical hydraulic characteristics of a PWR spent fuel cell .....	4-10
4.7 Typical hydraulic characteristics of a BWR spent fuel cell .....	4-11
4.8 The effect of decay heat on the hydraulic characteristics curves .....	4-13
4.9 The effect of base-plate hole size on the hydraulic characteristics curves .....	4-14
4.10 Decay power characteristics of PWR spent fuel assemblies .....	4-20
4.11 Decay power characteristics of BWR spent fuel assemblies .....	4-21
4.12 SHARP code structure .....	4-22
5.1 Comparison of SHARP code predictions with the steady state results of COBRA-SFS/ TEMPEST code for maximum clad temperature in the Haddam Neck spent fuel .....	5-3
6.1 Maximum clad temperature vs. time after pool drainage for PWR spent fuel .....	6-3
6.2 Building temperature versus time after pool drainage for PWR spent fuel .....	6-4
6.3 Effect of building ventilation rate on heatup of PWR spent fuel .....	6-5
6.4 Effect of baseplate hole size and on heatup of PWR spent fuel .....	6-6
6.5 Effect of downcomer space at the edge of pool on heatup of PWR spent fuel .....	6-7
6.6 Effect of burnup on heatup of PWR spent fuel .....	6-8
6.7 Effect of pool inventory on heatup of PWR spent fuel .....	6-9
6.8 Maximum clad temperature versus time after pool drainage for BWR spent fuel .....	6-10
6.9 Building temperature versus time after pool drainage for BWR spent fuel .....	6-11
6.10 Effect of building ventilation rate on heatup of BWR spent fuel .....	6-12
6.11 Effect of baseplate hole size and on heatup of BWR spent fuel .....	6-13
6.12 Effect of downcomer space at the edge of pool on heatup of BWR spent fuel .....	6-14
6.13 Effect of burnup on heatup of BWR spent fuel .....	6-15
6.14 Effect of pool inventory on heatup of BWR spent fuel .....	6-16

## TABLES

Table		Page
2.1	Design Characteristics of Spent Fuel Pool Used in the Analysis .....	2-4
2.2	Design Characteristics of Fuel Assemblies Used in the Analysis .....	2-4
3.1	Proposed Importance Rankings of Plausible Phenomena Related to Spent Fuel Heatup .....	3-4
4.1	Coefficients in Equation 4.54 for Bare Rod Subchannel Friction Constants $C_{fi}$ in Square Array .....	4-17
4.2	geometrical Parameters of Square Array Rod Bundles .....	4-17
5.1	Fuel Loading Assumptions Used in the SHARP Computer Code Calculations for the Haddam Neck Plant .....	5-2
6.1	Fuel Loading Assumptions Used in the Analysis .....	6-1

## EXECUTIVE SUMMARY

Once it is decided to permanently cease operation of a nuclear power plant, the reactor vessel will be defueled. Previous studies have concluded that the risk associated with decommissioning accidents that do not involve spent fuel is negligible. The primary source of public risk for these plants is associated with the accidents that involve the spent fuel stored in the spent fuel pool.

To assess the safety of the spent fuel storage pools, a low probability accident can be postulated in which all of the water drains from the pool, leaving the storage racks and their contents exposed to the air.

A methodology for predicting spent fuel heatup in the event of loss of water during storage has been formulated and implemented in a computer code called SHARP (Spent-fuel Heatup: Analytical Response Program).

The drained spent fuel pool is modeled as a vertical, parallel array of channels connected only at the base region beneath the racks and the large open volume above the spent fuel pool. The conservation equations are written to allow for downflow as well as upflow within the array of channels that include the spent fuel assemblies, the downcomer next to the edge of the pool, and empty slots (if any). The one dimensional conservation equations for buoyancy-driven air flows are solved numerically by using the subdomain method (control volume formulation) to discretize the equations. The heatup of the spent fuel elements is calculated by solution of the transient heat conduction equation in the axial direction. The boundary

conditions are obtained from the thermal hydraulic analysis within the base region beneath the racks, and within the spent fuel storage building. The hydrodynamic components of the boundary conditions are the zero net mass flow rate, the spent fuel storage building pressure, and the pressure gradient at the lower base region. In the present analysis, a fully mixed (i.e., isothermal and isobaric) base region is assumed. This is specifically the case if the flow Reynolds numbers are low and the base region equivalent diameter is large (i.e., large spacing at the bottom of the pool). The approximation of a fully mixed base region obviates the need for a multi-dimensional calculation of the temperature and pressure field in the base region. With the assumption of negligible pressure variation in the base region, the pressure drops across all channels become equal. It should be noted that for the situations with low spacing at the bottom of the pool, the SHARP code can also be applied to a certain region of the pool where the assumption of negligible pressure variation in the base region is more appropriate.

An analysis of spent fuel heatup, using representative design parameters and fuel loading assumptions has been performed. Sensitivity calculations were also performed to study the effect of fuel burnup, building ventilation rate, baseplate hole size, partial filling of the racks, and the amount of available space to the edge of the pool. The spent fuel heatup was found to be strongly affected by the total decay heat production in the pool, the availability of open spaces for air flows, and the building ventilation rate.

## FOREWORD

The SHARP computer code documented in this NUREG was developed for the NRC as a tool for making predictions of spent fuel heat up following a complete loss of water in the fuel pool. The code models an array of fuel channels which connect an upper and lower volume. Mass and energy conservation are ensured while mass flow rates are computed for each fuel bundle. Simplifying assumptions within the SHARP code allow the code to run quickly and give the user the ability to produce a

wide range of predictions. This NUREG documents the modeling assumptions and rationale for these modeling decisions. Potential users of this code should consider the assumptions and limitations built into the code when considering any code predictions. These assumptions and limitations can have a significant impact on the predicted results under some conditions. SHARP is not approved for licensing applications.

## NOMENCLATURE

### Latin:

A	Area
b	Thickness
$C_p$	Specific heat constant pressure
$D_H$	Hydraulic diameter
f	Friction factor
g	Acceleration of gravity (980 cm/sec <sup>2</sup> )
G	Mass flux
h	Specific enthalpy
$h_c$	Heat transfer coefficient
$h_g$	Gap conductance
K	Thermal conductivity
L	Length of a channel
$\dot{m}$	Mass flow rate
$\dot{m}_{leak}$	Leakage rate from spent fuel building to the external atmosphere
P	Pressure
$P_{max}$	Maximum pressure that can be sustained by the containment building
$P_H$	Heated perimeter
$q'''$	Volumetric heat generation rate
R	Gas constant for air (2.871 x 10 <sup>6</sup> dyn-cm/gm-°K)
T	Temperature
t	Time
u	Velocity
V	Volume
$\dot{V}_{vent}$	Volumetric venting rate
R	Radius
r	Radial distance
z	Axial distance

### Greek:

$\delta$	Gap thickness
$\rho$	Density

### Subscripts:

b	Base region
c	Cladding
f	Fuel
n	Channel
o	Outside atmosphere
r	Containment room
s	Structures

# 1. INTRODUCTION

## 1.1 Background

The spent fuel storage pools in light water reactors were originally designed to accommodate the amount of spent fuel expected to be awaiting shipment to a reprocessing facility. With the current United States moratorium on spent fuel reprocessing and the absence of either a permanent geological high-level waste repository or an interim Monitored Retrievable Storage (MRS) facility, utilities had few alternatives but to store spent fuel at the reactor site. This resulted in increasingly large inventories of spent fuel being stored in reactor spent fuel pools. The interim solution to the increased inventories has been a modification of spent fuel storage racks to further increase the ultimate capacities of most reactor fuel pools.

Currently, several nuclear power plants with years, sometimes decades, left on their operating licenses are permanently shutdown in various stages of the decommissioning process. Once it is decided to permanently cease operation of a nuclear power plant, the reactor vessel will be defueled. In parallel (or perhaps in anticipation of permanent shutdown) the licensee will apply for a license amendment to withdraw the authority to operate the plant. The amendment to remove the authority to operate also provides a basis to reduce the regulatory requirements during permanent shutdown.

Previous studies<sup>1,2</sup> have concluded that the risk associated with decommissioning accidents that do not involve spent fuel is negligible. The primary source of public risk for these plants is associated with the accidents that involve the spent fuel stored in the spent fuel pool.

To assess the safety of the spent fuel storage pools and to develop a basis for regulatory relief for Possession Only Licensees (POLs), a low probability accident can be postulated in which all of the water drains from the pool, leaving the storage racks and their contents exposed to air. The fuel elements subsequently heat up, usually reaching a steady state temperature distribution where the thermal power produced by radioactive decay is balanced by natural convection and thermal radiation. The release of radioactive materials to the environment will occur only if the attained temperature is high enough to cause the Zircaloy clad to rupture as a result of internal pressure, or to undergo rapid exothermic oxidation leading to clad melting. The likelihood and the timing of reaching a maximum allowable local cladding temperature depend, among other factors, on the amount of time that has elapsed since shutdown of fission power and fuel removal from the reactor (i.e., decay power).

Benjamin et al.,<sup>3</sup> investigated the heatup of spent fuel following drainage of the pool. A computer code, SFUEL, was developed to analyze thermal-hydraulic phenomena occurring when the spent fuel assemblies become exposed to air. Computations were performed to assess the effect of decay time, fuel element design, storage rack design, packing density, room ventilation and other variables on the heatup characteristics of the spent fuel.

Pisano et al.,<sup>4</sup> modified the SFUEL code to increase the calculational stability and to extend the code ability to analyze pool wide propagation of the self sustaining zirconium oxidation. This version of the code, SFUEL1W, was used to assess the propagation of Zircaloy "fires" from high power to low power assemblies.

## 1. Introduction

The major limitations and assumptions embodied in both SFUEL and SFUEL1W include the two dimensional modeling of the spent fuel pool and the requirement of the placement of the hottest elements in the middle of the pool and the cooler elements progressively toward the ends of the pool.

These simplifying assumptions may be reasonable for the scoping calculations for current storage practices where a number of spent fuel pools are approaching their design capacity. However, the ability of these codes to realistically predict the heatup characteristics of the actual case specific spent fuel pool conditions is questionable. For example, the impact of partial filling of the racks on the peak clad temperature cannot be addressed.

A computer code, SHARP, (Spent-fuel Heatup: Analytical Response Program), has been developed for the U.S. Nuclear Regulatory Commission (NRC) to predict the spent fuel heatup in the event of loss of water during storage. The SHARP computer program has not been approved for licensing purposes.

## 1.2 Scope and Organization of This Report

The objective of this document is to specify the overall structure of the computer code SHARP. Section 2 presents a general description of the design characteristics of spent fuel storage pools including rack configurations. An integrated structure somewhat similar to the one developed for severe accident technical issue resolution<sup>5</sup> has been adopted to assess the modeling requirements for the simulation of spent fuel heatup progression following loss of water during storage. The basic components for this physically based methodology and its application to the postulated spent fuel heatup scenario are discussed in Section 3. The code modeling framework, including the mathematical models and solution methods, are described in Section 4. Section 5 provides the code verification and validation activities. The computed results of the spent fuel heatup characteristics using representative PWR and BWR plant parameters are presented in Section 6. Section 7 presents a brief summary together with conclusions. The user manual of the code, which describes the code input and output, is included in Appendix A.

## 2. DESIGN CHARACTERISTICS OF SPENT FUEL STORAGE POOLS

Except for the capacity and the design of the racks, the configuration of spent fuel storage pools is similar for most nuclear power plants. Figure 2.1 shows a schematic of a typical spent fuel storage building. The pools are rectangular in cross section and approximately 40 ft. deep. Fuel assemblies are placed vertically in storage racks which maintain an adequate spacing to prevent criticality and to promote natural convective cooling in a water medium.<sup>3</sup> The pools themselves are constructed of reinforced concrete with sufficient thickness to meet radiation shielding and structural requirements. The spent fuel pool floor and walls are lined with 1/8" to 1/4" thick stainless steel liner plates to insure a leak tight system.<sup>6</sup>

Most boiling water reactors (BWRs) are designed for spent fuel storage within the secondary containment. In Mark I and Mark II plants, the spent fuel pool is located at the operating floor level, about 100 to 150 feet above grade. The thickness of the pool walls and floor is on the order of 4 to 6 feet. In Mark III design, however, the spent fuel pool is located on the ground level.

Pressurized water reactors (PWRs) use a ground level spent fuel storage pool which is located in the auxiliary building. Both BWR and PWR spent fuel storage pools typically range from 30 to 60 feet in length and 20 to 40 feet in width.<sup>3</sup>

The design of storage racks, fuel element cell (holder) configurations and total fuel element capacity varies

from facility to facility. Figure 2.2 shows typical spent fuel storage racks currently in use. In the configuration which is in use in nearly all PWRs, and is referred to as high density storage, the fuel assemblies are tightly packed with neutron absorber material used in the rack structure to replace the reduced water moderator for criticality control. A baseplate hole is included in each cell for water circulation.

Most storage configurations do provide enough spacing around the sides and over the bottom to promote natural circulation and to prevent bulk boiling in the fuel. For some rack designs, an administrative control, such as checkerboard loading of the fresh fuel, is employed to assure that the effective multiplication factor ( $K_{eff}$ ) for the optimum moderation point is  $<0.98$ .<sup>(7)</sup>

The quantitative details of storage configuration considered in the present analysis are given in Table 2.1. These representative design characteristics have been specified, based on a review of a few plant specific configurations, to lead to a conservative estimate of fuel heatup.

The subassemblies considered in the present analysis consisted of 17 x 17 and 7 x 7 fuel pin arrays for a PWR and a BWR, respectively. The details of the design characteristics of fuel assemblies used in the calculations are similar to the ones used in Reference 3 (see Table 2.2).

## 2. Design Characteristics of Spent Fuel Storage Pools

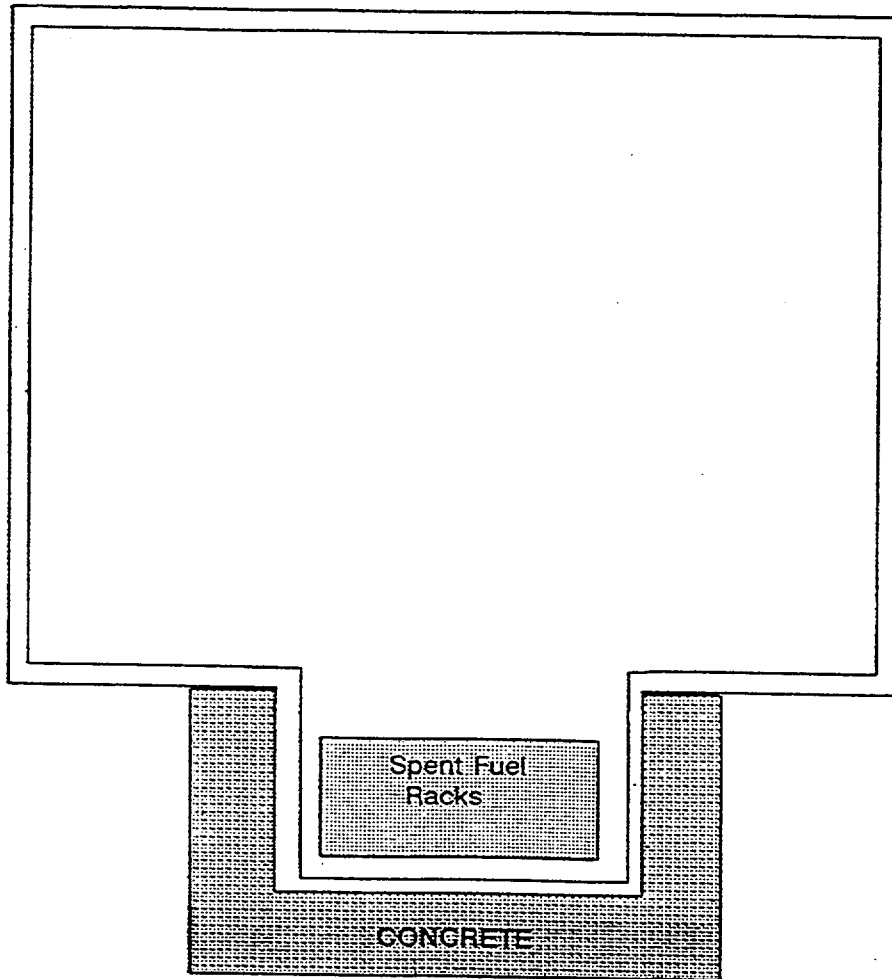


**Figure 2.1 Schematic view of a typical spent fuel storage building**

## 2. Design Characteristics of Spent Fuel Storage Pools

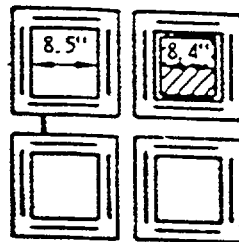
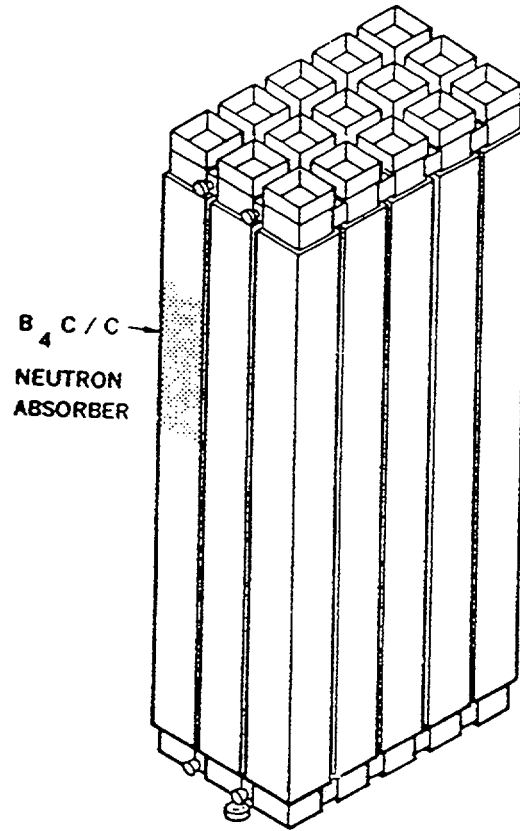


Figure 2.2 Typical spent fuel storage rack configuration

## 2. Design Characteristics of Spent Fuel Storage Pools

**Table 2.1 Design Characteristics of Spent Fuel Pool Used in the Analysis**

	<u>PWRs</u>	<u>BWRs</u>
Pool Dimension (Ft.)	32 x 32	30 x 30
Number of Cells	1460	3300
Cell Dimension (In.)	8.75x 8.75	6 x 6
Cell center-to-center pitch (In.)	10.40	6.255
Cell wall thickness (In.)	0.185	0.09
Cell orifice diameter (In.)	5	4
Module height (In.)	169	168
Module to wall space (In.)	3.	2.
Nominal plenum height (In.)	6	7.25

**Table 2.2 Design Characteristics of Fuel Assemblies Used in the Analysis**

	<u>PWRs</u>		<u>BWRs</u>	
Rod array	15 x 15	17 x 17	7 x 7	8 x 8
Number of fuel rods per assembly	208	264	49	63
Number of non-fuel rods per assembly	17	25	0	1
Active fuel height (In.)	144	144	144	148
Rod center-to-center pitch (In.)	0.558	0.496	0.738	0.64
Fuel rod outside diameter (In.)	0.420	0.374	0.563	0.493
Clad thickness (In.)	0.026	0.023	0.032	0.034
Metric tons uranium per assembly (MTU)	0.456	0.461	0.195	0.189
Number of assemblies per core	177	193	764	732

### 3. MODELING REQUIREMENTS

To provide a framework for assessment of modeling requirements for simulation of spent fuel heatup following loss of water during storage, a methodology somewhat similar to the one developed for severe accident technical issue resolution<sup>5</sup> was adopted. The basic components for this physically based methodology are illustrated in Figure 3.1. This approach assures that the analytical method used to resolve an issue is comprehensive, systematic, able to be audited, and traceable. In addition, the present approach assures that all important features of an issue are fully addressed. It should be noted that the focus here is to provide the "technical basis" for issue resolution (i.e., technical issue resolution). The full

process of resolving an issue encompasses more than just providing the technical basis and falls into the domain of licensing and regulatory efforts of the NRC.

This integrated structure has been also adopted previously<sup>8</sup> to assess the capabilities of existing codes (Component IV) for simulation of the spent fuel heatup progression. As illustrated in Figure 3.1, Component I (Phenomena Evaluation) provides the foundation for code development (Component II) and the entire technical issue resolution process and therefore its application to the postulated spent fuel heatup scenario is reproduced in detail in this section.

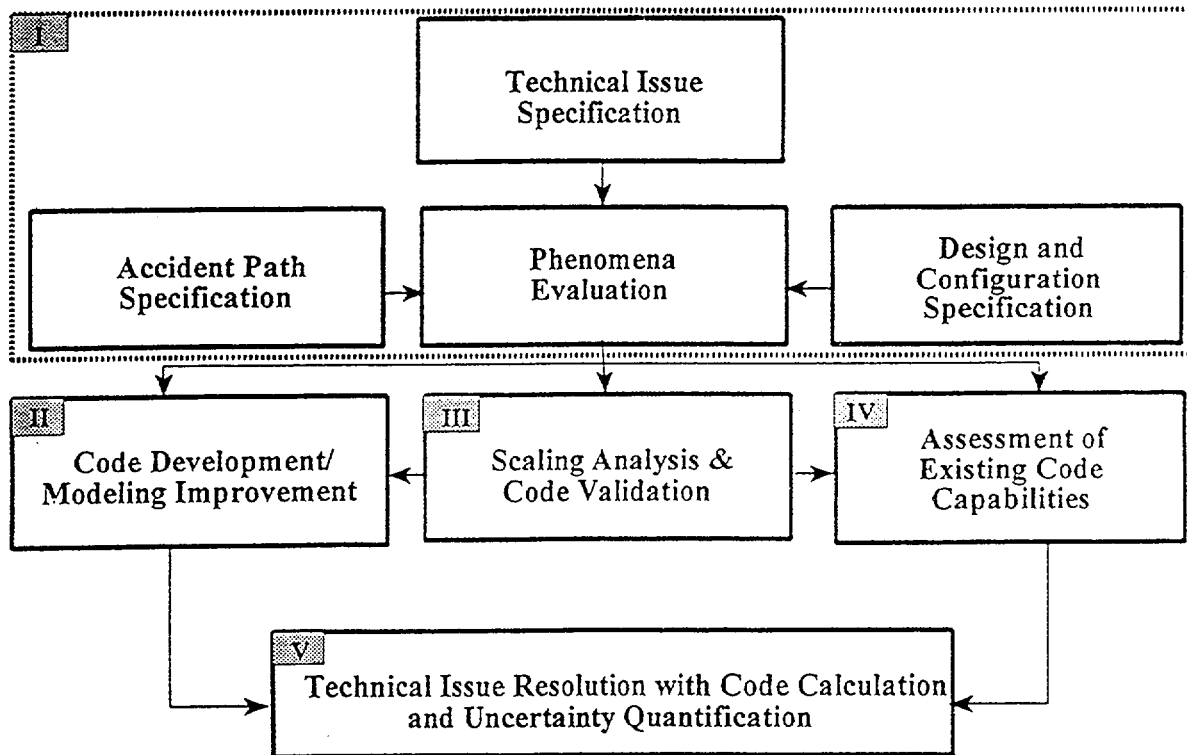


Figure 3.1 Basic components of the methodology for technical issue resolution

### 3. Modeling Requirements

#### 3.1 Technical Issue Specification

A statement of the technical issue provides the focus of the subsequent work. The heatup of the fuel has been postulated to occur when the water in the storage pool is drained due to certain accidents such as a beyond design basis seismic event. The issue here is to find the level of decay heat of the hottest assembly such that the fuel cladding will remain intact (i.e., no gap release) upon extended exposure to air. The release of radionuclide materials to the environment will occur only if the local cladding temperature is high enough to cause the Zircaloy clad to rupture as a result of internal pressure. The clad structural failure could occur at temperatures as low as 650°C if the thermal loading is sustained for several hours.<sup>9</sup>

#### 3.2 Accident Path Specification

The physical process important to one accident path may not have the same relevance to another path. Consequently, it is necessary to identify the specifications of the scenario and the accident path that need to be evaluated.

A number of accident initiators have been postulated which could result in draining or boiloff of the spent fuel pool and expose the relatively hot spent fuel assemblies to an air environment. A possible scenario is one initiated by a beyond design basis seismic event, where:

- The water drains instantaneously, leaving the pool completely void of water. It should be noted that the physical process of interest for incomplete drainage is different and will not be considered in the present study.
- For heat removal from the building two cases will be considered. In the first case, it is assumed that the ventilation provided through a powerful air ventilation system or through a chimney effect is sufficient to keep the room air at ambient

conditions. In the second case, it is assumed that no chimney effect exists. A leakage rate based on a prescribed building capability pressure and various building ventilation rates were assumed.

#### 3.3 Spent Fuel Pool Design and Configuration Specification

The spent fuel heatup characteristics following drainage of the pool will be affected by plant specific parameters such as pool geometry, storage rack configuration, loading pattern of fuel, and the availability of air ventilation systems.

In the present study, the modeling requirement will be assessed considering only the diversity in design and configuration of spent fuel storage pools currently in use. The phenomenology of spent fuel heatup for earlier storage rack designs consisting of open frame arrangements is different and will not be considered in the present assessment.

#### 3.4 Phenomena Evaluation

Phenomena evaluation provides a comprehensive framework to identify and prioritize the physical processes which need to be modeled in a code so as to ensure its capability to address the spent fuel heatup progression.

In order to identify and rank the processes important to spent fuel heatup progression, an approach similar to that discussed and developed in References 5, and 10 through 12 will be followed. The system (i.e., spent fuel pool storage facility) is decomposed into components. For each component, physical processes and phenomena are identified, and differentiated as to their cause and effects. This physically based decomposition of the spent fuel heatup progression in a cause and effect sequence, ensures that all aspects are considered and examined (albeit qualitatively). Subsequent to identification of the plausible

### 3. Modeling Requirements

phenomena, a ranking procedure is used since it is neither practical nor necessary to evaluate all phenomena in detail. The ranking technique is designed to direct the subsequent code development work to those phenomena having the most significant effect on the questions of concern (i.e., the likelihood and the timing of reaching an allowable peak clad temperature).

To facilitate the phenomena identification, the system was partitioned into five components:

1. Spent fuel rods.
2. Spent Fuel Storage Rack, including the cell and rack structures, tie plates and channel walls (BWRs).
3. Downcomer next to edge of the pool, including the sidewalls (liner and concrete).
4. Base region beneath the racks, including base floor (liner and concrete).
5. Spent fuel storage building - The large open space above spent fuel pool, including the structures (internal structures, walls and ceiling).

A review of sensitivity studies using the SFUEL code,<sup>3,4</sup> together with the basic knowledge about heat transfer and natural convection flows in parallel channel systems, was used to determine plausible phenomena and to judge their relative importance to overheating of the spent fuel. The initial importance ranking of plausible phenomena is summarized in Table 3.1. Three ranking categories were utilized for this initial screening:

1. High: The phenomenon in question could have a significant impact on peak clad temperature.
2. Medium: The phenomenon in question is expected to have at least a measurable impact on peak clad temperature.

3. Low: The phenomenon in question does not have significant impact on peak clad temperature.

It should be recognized that the present views held with respect to plausible phenomena and their relative ranks may be modified by evidence arising from any future code development, or assessment. Therefore, appropriate iteration is implied.

The ranking justifications and references, where possible, together with description of the phenomena in the context of their conceptualization by the authors is presented in the following subsections.

#### 3.4.1 Spent Fuel Rods

There is no fuel heatup without decay heat in the fuel rods; consequently this process was ranked as highly important.

The results of SFUEL calculations,<sup>3</sup> for cases where a steady state temperature distribution was obtained, indicate that most of the heat produced by decay heat is eventually removed by natural convection. The remainder of the energy is primarily accounted for by the temperature rise of the materials in the pool, with approximately 80% (for well-ventilated room conditions) of that energy going to the fuel rods. The energy stored in spent fuel rods is an important factor in determining the timing of the maximum steady state peak clad temperature.

Oxidation of Zircaloy clad by air is important only at elevated temperatures. As discussed in Section 3.1, clad structural failure could occur at temperatures as low as 650°C if thermal loading is sustained for several hours. The data for oxidation of Zircaloy in air<sup>13-15</sup> indicate a very low oxidation rate at temperatures below 650°C. Therefore, Zircaloy oxidation was ranked as low importance.

### 3. Modeling Requirements

**Table 3.1 Proposed Importance Rankings of Plausible Phenomena Related to Spent Fuel Heatup**

<u>Component/Phenomenon</u>	<u>Relative Importance<sup>a</sup></u>
<b>Spent Fuel Rods:</b>	
Decay heat	H
Stored energy	H
Zircaloy oxidation	L
Radial heat conduction	M
Axial heat conduction	H
<b>Spent Fuel Storage Rack:</b>	
Convective heat transfer from fuel rods to air flows through the cells	H
Radiative heat transfer between fuel rods and neighboring structures (i.e., holder walls, channel walls (BWRs), and tie plates)	M
Radiative heat transfer from one fuel rod to another	M
Heat conduction in structures (i.e., cell walls, channel walls (BWRs) and tie plates)	L
Stored energy in cell materials	M
Buoyancy induced flow of air through cells	H
Buoyancy induced flow of air in inter- cell/rack spaces	H <sup>b</sup>
Convective heat transfer between holder walls and air flow between holders	H <sup>b</sup>
Radiative heat transfer between adjacent holder walls	M

(a) L= Low importance, M= Medium importance, H= High importance

(b) Low importance if the inter-cell/rack spaces are closed to air flow

**Table 3.1 Proposed Importance Rankings of Plausible Phenomena Related to Spent Fuel Heatup  
(Cont'd)**

<u>Component/Phenomenon</u>	<u>Relative Importance<sup>a</sup></u>
<b>Downcomer Next to the Edge of the Pool:</b>	
Convective heat transfer between the air flows in downcomer and sidewalls liner	M <sup>b</sup>
Radiative heat transfer between peripheral holders and sidewalls liner	L
Convective heat transfer between peripheral cells and air flow in downcomer	M
Flow of air in downcomer	H
Heat conduction in concrete sidewalls	M <sup>b</sup>
Stored energy in concrete sidewalls	M <sup>b</sup>
Stored energy in sidewalls liner	L
<b>Base Region Beneath the Racks:</b>	
Convective heat transfer between lower tie plates and air flows in base region	L
Radiative heat transfer between lower tie plates and floor liner	L
Convective heat transfer between floor liner and air flow in base region	L
Pressure drop in base region	M

(a) L= Low importance, M= Medium importance, H= High importance

(b) Low importance in the presence of forced ventilation or a chimney effect

### 3. Modeling Requirements

**Table 3.1 Proposed Importance Rankings of Plausible Phenomena Related to Spent Fuel Heatup (Cont'd)**

<u>Component/Phenomenon</u>	<u>Relative Importance<sup>a</sup></u>
<b>Spent Fuel Storage Building:</b>	
Radiative heat transfer from upper tie plates to building atmosphere	L
Convective heat transfer from upper tie plates to building atmosphere	M
Heat exchange with outside by forced ventilation or chimney effect	H
Heat loss to outside by leakage through building	H <sup>b</sup>
Convective heat transfer from room atmosphere to building internal structures	M <sup>b</sup>
Convective heat transfer from room atmosphere to building walls	H <sup>b</sup>
Stored energy in building walls	L
Convective heat transfer from building (walls and ceiling) to outside atmosphere	H <sup>b</sup>
Building pressurization	H <sup>b</sup>
Thermal mixing and stratification	M <sup>b</sup>

(a) L= Low importance, M= Medium importance, H= High importance

(b) Low importance in the presence of forced ventilation or a chimney effect

In view of the fact that heatup time is on the order of hours, the radial temperature variations within the fuel rods may be small. Modeling of radial temperature dependence within fuel rods and cladding may not be necessary. A lumped model consisting of a fuel node and a cladding node connected by a simple gap conductance is adequate. Radial heat conduction in the spent fuel rods was ranked as medium importance to ensure its further assessment during code development work.

On the other hand, the axial conduction is potentially important. There is significant axial temperature

variation along fuel rods. The temperature of the air increases as it flows from the bottom to the top of the fuel element due to heat transfer from fuel rods. The heatup of the air in the flow channels results in less heat removal and consequently more heatup of the fuel rods toward the upper end of the flow channels.

#### 3.4.2 Spent Fuel Storage Rack

The phenomenology of the present system is similar to other natural circulation loops (thermosyphons), in which heat is convected from a heat source to a higher elevation heat sink.

### 3. Modeling Requirements

The spent fuel heatup is strongly affected by heat transfer from the fuel rods to flowing air and the heat removal in the spent fuel storage building due to ventilation, air leakages, or convective heat transfer to the outside atmosphere. The availability of open spaces for air flow is an important factor affecting the heatup of the spent fuel rods. Convection is the dominant mode of heat transfer between the fuel rods and the air flows through the cells. Radiation heat transfer is considered of lesser importance in view of the relatively low fuel rod temperatures (<650°C).

Thermal radiation from one fuel rod to another is also potentially important. Variations of temperature from rod to rod in an assembly may occur as a result of variations in decay heat. In view of the equalizing effect of thermal radiation from one rod to another, the simplifying assumption of neglecting the temperature variations in the horizontal direction across any fuel assembly may be considered adequate.

Buoyancy induced flow of air through holders and in inter-holder/rack spaces is judged to be highly important. A realistic prediction of air flows depends on accurate calculations of the pressure drop terms (i.e., buoyancy, shear stress dissipation, and orifice loss across base plate inlet hole).

#### **3.4.3 Downcomer Next to the Edge of the Pool**

The temperature of the returning flows of air into the downcomer is expected to be low especially in the presence of forced ventilation or a chimney effect in the spent fuel storage building. Therefore, heat transfer from the flowing air to the sidewalls is negligible. However, heat loss to sidewalls has been ranked as medium importance to ensure its consideration for further assessment in the absence of good ventilation.

#### **3.4.4 Base Region Beneath the Racks**

The temperature of flowing air into the base region, as well as the temperature of lower tie plates, is expected to be low. Therefore, all heat losses in this region have been ranked as having low importance.

The assumption of negligible pressure variation in the base region considerably simplifies both the modeling and the solution algorithm for determining the buoyancy induced flows in holders and in the downcomer region. The pressure drop in the base region is ranked as medium importance to ensure its further assessment.

#### **3.4.5 Spent Fuel Storage Building**

The extent of heat removal from the spent fuel building atmosphere strongly affects the heatup characteristics of the exposed spent fuel rods. Removal of heat from the spent fuel storage building under normal operation is accomplished by a forced ventilation system. However, as noted in Reference 3, under the accident conditions, this amount of ventilation will generally not be sufficient to remove all the decay heat transferred to the room atmosphere. Therefore, it is possible for the room air to heatup significantly and to adversely affect the natural convection processes. In the absence of a powerful air ventilation system (or a chimney effect) the building will pressurize until failure and result in the subsequent leakage of air to the outside atmosphere.

The thermal mixing and stratification in the spent fuel storage building has a potential impact on the natural convection flow structure within cells and the downcomer region. The presence of forced ventilation (or a chimney effect) would enhance mixing. However, thermal mixing and stratification in the storage building have been assigned a medium importance rank to ensure their assessment in the absence of any external auxiliary means of mixing (i.e., forced ventilation or chimney effects).

## 4. PHYSICAL MODELS

The physically based methodology discussed in Section 3 provides a valuable framework for the present code development effort. To conserve resources, the SHARP code has been structured to simulate the most important phenomena and processes, with lesser attention given to peripheral effects. Both an initial and subsequent interaction with the phenomena evaluation process discussed in Section 3 will assist in focusing the modeling on the key processes and phenomena required for technical issue resolution.

This section describes the mathematical models and their solution methods for predicting the thermal-hydraulic behavior of various system components following complete drainage of spent fuel pool.

### 4.1 Heat Transfer in Spent Fuel Elements

Figure 4.1 illustrates a general form of the right circular fuel rod with concentric clad, forming an annular gap of width  $\delta$ . The fuel pellet (subscript f) has the radius  $R_f$ , the volumetric heat capacity  $(\rho C)_f$ , thermal conductivity  $K_f$  and volumetric heat generation rate (decay heat)  $q'''_f$ . The gas in the gap is assumed to be stagnant with a gap conductance  $h_g$  to characterize the heat transfer (including radiation) through the gas. The clad (subscript c) has the inner radius  $R_{c,i}$  and outer radius  $R_{c,o}$ .

The air flow conditions in a fuel assembly are assumed to be such that the azimuthal flow condition is essentially the same around the fuel rod. The decay heat within the fuel rod is assumed to vary only in an axial direction. The above two conditions lead to the conclusion that no significant azimuthal temperature gradients exist in the fuel rod. Thus, the transient heat conduction equation reduces to:

$$\rho C_p \frac{\partial T}{\partial t} = \frac{1}{r} \frac{\partial}{\partial r} \left( rK \frac{\partial T}{\partial r} \right) + \frac{\partial}{\partial z} \left( K \frac{\partial T}{\partial z} \right) + q''' \quad (4.1)$$

By area averaging of Equation 4.1 for fuel pellet and clad separately, one finds

$$R_f^2 (\rho C)_f \frac{\partial \langle T \rangle_f}{\partial t} = 2 \bar{K}_f R_f \left. \frac{\partial T_f}{\partial r} \right|_{r=R_f} + R_f^2 \langle q''' \rangle_f + R_f^2 \frac{\partial}{\partial z} \left( \bar{K}_f \frac{\partial \langle T \rangle_f}{\partial z} \right) \quad (4.2)$$

$$R_{c,o}^2 - R_{c,i}^2 (\rho C)_c \frac{\partial \langle T \rangle_c}{\partial t} = 2 \bar{K}_c R_{c,o} \left. \frac{\partial T_c}{\partial r} \right|_{r=R_{c,o}} - 2 \bar{K}_c R_{c,i} \left. \frac{\partial T_c}{\partial r} \right|_{r=R_{c,i}} + (R_{c,o}^2 - R_{c,i}^2) \frac{\partial}{\partial z} \left( \bar{K}_c \frac{\partial \langle T \rangle_c}{\partial z} \right) \quad (4.3)$$

where the area-averaged temperatures  $\langle T \rangle_f$  and  $\langle T \rangle_c$  are defined as:

$$\langle T \rangle_f = \frac{2 \int_0^{R_f} T_f r dr}{R_f^2} \quad (4.4)$$

$$\langle T \rangle_c = \frac{2 \int_{R_{c,i}}^{R_{c,o}} T_c r dr}{R_{c,o}^2 - R_{c,i}^2} \quad (4.5)$$

The mean volumetric heat capacity  $(\rho C)$  and mean thermal conductivity  $K$  are evaluated at the area-averaged temperature. The appropriate boundary conditions are:

$$\left. \frac{\partial T_f}{\partial r} \right|_{r=0} = 0 \quad \text{at} \quad r=0, \quad (4.6)$$

4. Physical Models

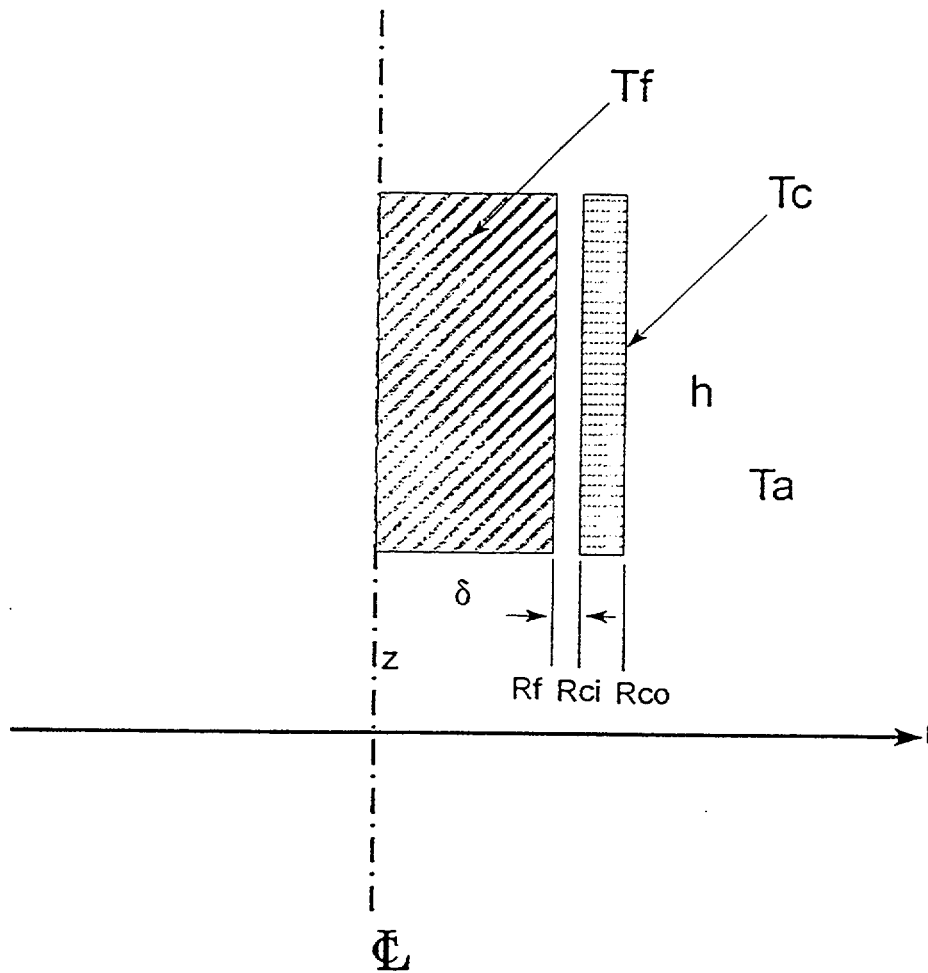


Figure 4.1 Fuel element geometry

#### 4. Physical Models

$$-\bar{K}_f \frac{\partial T_f}{\partial r} = h_g (T_{f,o} - T_{c,i}) \quad \text{at } r=R_f, \quad (4.7)$$

$$-\bar{K}_c \frac{\partial T_c}{\partial r} = h_g (T_{f,o} - T_{c,i}) \quad \text{at } r=R_{c,i}, \quad (4.8)$$

$$-\bar{K}_c \frac{\partial T_c}{\partial r} = h_g (T_{c,o} - T_a) \quad \text{at } r=R_{c,o}. \quad (4.9)$$

Where  $h_g$ ,  $h_c$ , and  $T_a$  are the gap unit thermal conductance, convective heat transfer coefficient and the air temperature, respectively.  $T_{f,o}$ ,  $T_{c,i}$  and  $T_{c,o}$  are the fuel surface temperature, clad inner surface temperature, and clad outer surface temperature, respectively.

Assuming a quasi-steady parabolic temperature profile across the fuel, the fuel temperature can be expressed as:

$$T_f = T_o + b \left( \frac{r}{R_f} \right) + c \left( \frac{r}{R_f} \right)^2 \quad (4.10)$$

Applying the conditions of Equations 4.6 and 4.7 to Equation 4.10 leads to  $b=0$  and

$$\frac{-2\bar{K}_f}{R_f} c = h_g (T_{f,o} - T_{c,i}) \quad (4.11)$$

when

$$T_{f,o} = c + T_o \quad (4.12)$$

Substituting Equation 4.10 into Equation 4.4 leads to:

$$\langle T \rangle_f = \frac{1}{2} c + T_o \quad (4.13)$$

Equations 4.11 through 4.13, after some algebra, yield the heat flux from fuel to cladding, in terms of area, averaged temperature of fuel.

$$h_g (T_{f,o} - T_{c,i}) = \frac{4 \frac{K_f}{R_f} h_g}{h_g + 4 \frac{K_f}{R_f} (\langle T \rangle_f - T_{c,i})} \quad (4.14)$$

Neglecting the radial thermal resistance in clad, we have:

$$T_{c,i} = T_{c,o} = \langle T \rangle_c \quad (4.15)$$

Using Equations 4.7 through 4.9 and 4.14, and ignoring the gap thickness ( $\delta = R_{c,i} - R_f \leq 10^{-2} R_f$ ) relative to radii  $R_f$  and  $R_{c,i}$ , the energy equations 4.2 and 4.3 can be expressed as:

$$R_f^2 (\bar{\rho c})_f \frac{\partial \langle T \rangle_f}{\partial t} = -2R_f h_{tot} (\langle T \rangle_f - \langle T \rangle_c) + R_f^2 \langle q''' \rangle_f + R_f^2 \frac{\partial}{\partial z} \left( \bar{K}_f \frac{\partial \langle T \rangle_f}{\partial z} \right) \quad (4.16)$$

and

$$(R_{c,o}^2 - R_{c,i}^2) (\bar{\rho c})_c \frac{\partial \langle T \rangle_c}{\partial t} = 2R_f h_{tot} (\langle T \rangle_f - \langle T \rangle_c) - 2R_{c,o} h_c (\langle T \rangle_c - T_a) + (R_{c,o}^2 - R_{c,i}^2) \frac{\partial}{\partial z} \bar{K}_c \left( \frac{\partial \langle T \rangle_c}{\partial z} \right) \quad (4.17)$$

Where the total effective fuel-cladding thermal conductance  $h_{tot}$  can be expressed (see Equation 4.14) as:

$$h_{tot} = \frac{4 \frac{K_f}{R_f} h_g}{h_g + 4 \frac{K_f}{R_f}} \quad (4.18)$$

Scoping analysis indicates that the radial temperature variations within the fuel and between the fuel and cladding, is very small (i.e.,  $\langle T \rangle = \langle T \rangle_f = \langle T \rangle_c$ ). Equations 4.16 and 4.17 then can be added to obtain the following single energy equation for fuel elements.

#### 4. Physical Models

$$\langle \rho c \rangle \frac{\partial \langle T \rangle}{\partial t} = \frac{R_f^2}{R_{c,o}^2} \langle q''' \rangle_f - \frac{2h_c}{R_{c,o}} (\langle T \rangle - T_a) + \frac{\partial}{\partial z} \left( \langle K \rangle \frac{\partial \langle T \rangle}{\partial z} \right) \quad (4.19)$$

Where:

$$\langle \rho c \rangle = \frac{R_f^2 (\overline{\rho c})_f + (R_{c,o}^2 - R_{c,i}^2) (\overline{\rho c})_c}{R_{c,o}^2} \quad (4.20)$$

and

$$\langle K \rangle = \frac{R_f^2 \overline{K}_f + (R_{c,o}^2 - R_{c,i}^2) \overline{K}_c}{R_{c,o}^2} \quad (4.21)$$

The fully implicit subdomain method<sup>16</sup> (control volume formulation) was used to derive the discretization equations. The solution of the resulting discretization equations was obtained by the standard Gaussian-elimination method. Because of the particularly simple form of equations, the elimination process turns into the convenient Thomas algorithm or the TDMA (Tri-Diagonal-Matrix Algorithm).

Figures 4.2 and 4.3 show the typical steady-state results for the clad temperature with normalized distance along a spent fuel element as a function of decay heat and inlet air velocity, respectively. For the axial variation of decay power, a chopped sine distribution having a peak-to-average variation of 1.5 was assumed. As shown in Figures 4.2 and 4.3, the axial location of peak temperature does not correspond to the location of the highest heat production ( $Z/L = 0.5$ ). This is due to a higher air stream temperature at the upper end of the spent fuel rods.

### 4.2 Buoyancy-Driven Air Flows

The drained spent fuel pool is modeled as a vertical, parallel array of channels connected only at plena<sup>17</sup> (i.e., base region beneath the racks and spent fuel storage building). In this section, the solution of the continuity, momentum, and energy equations of air

flow in the parallel channel system will be discussed. The physical basis for flow behavior will be stressed since the problem formulation allows multiple solutions for the flow in individual channels. The instability mechanisms will be discussed. The typical results for steady-state conditions will also be presented.

#### 4.2.1 One Dimensional Conservation Equations

Figure 4.4 illustrates the schematic of the drained spent fuel pool, modeled as multiple channels that are connected only at the base region beneath the racks and the large open space volume above spent fuel pool. It is assumed that the air flow patterns are one dimensional. In view of the fact the fluid transit time in the channel is much smaller than the inlet flowrate and heating time constants, a quasi-steady approach is adequate. The conservation equations are written to allow for downflow, as well as upflow within the array of channels that include the spent fuel assemblies, the downcomer next to the edge of the pool, and empty slots (if any). The sign convention adopted is positive for upflow and negative for downflow.

##### 4.2.1.1 Conservation of Mass

The relevant continuity equation is:

$$\frac{\partial \rho}{\partial t} + \frac{\partial}{\partial z} (G) = 0 \quad (4.22)$$

Where  $\rho$  is the fluid (air) density and  $G$  is the mass flux. Integrating Equation 4.22 along a channel under steady-state conditions and multiplying by the flow area yield:

$$G_n A_{fn} = \text{constant} \quad (4.23)$$

In a typical spent fuel pool with a large number of parallel channels (spent fuel assemblies), there are groups of channels with identical decay heat and geometries. For each channel type  $n$ , it is assumed that there are  $y_n$  identical channels. It is also assumed that each channel, in the sets of channels of type  $n$ , behave

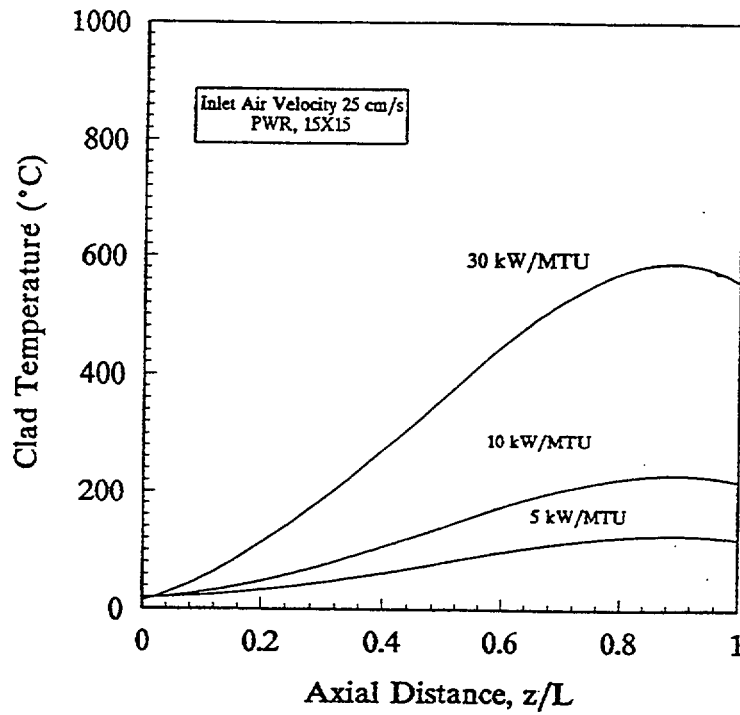


Figure 4.2 Effect of decay heat on axial variation of clad temperature

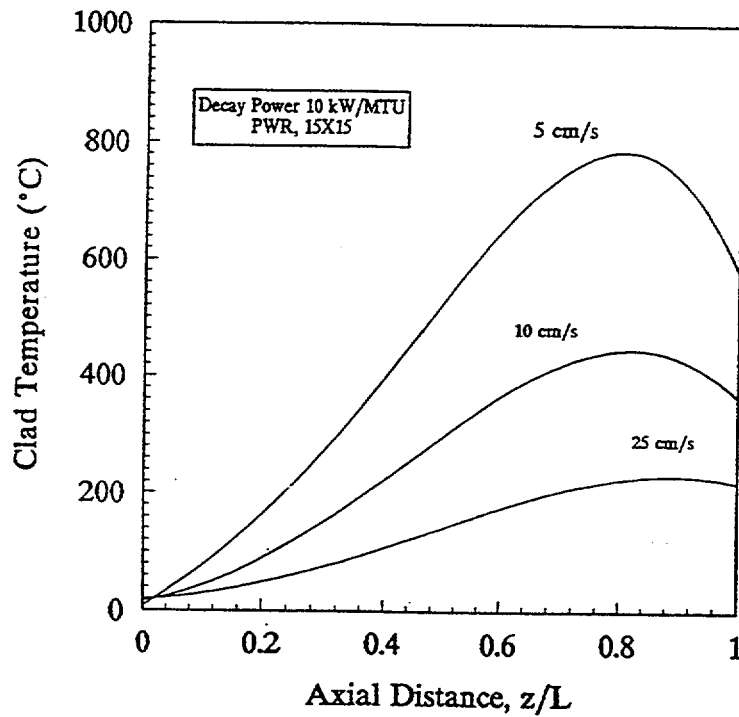


Figure 4.3 Effect of inlet air velocity on axial variation of clad temperature

4. Physical Models

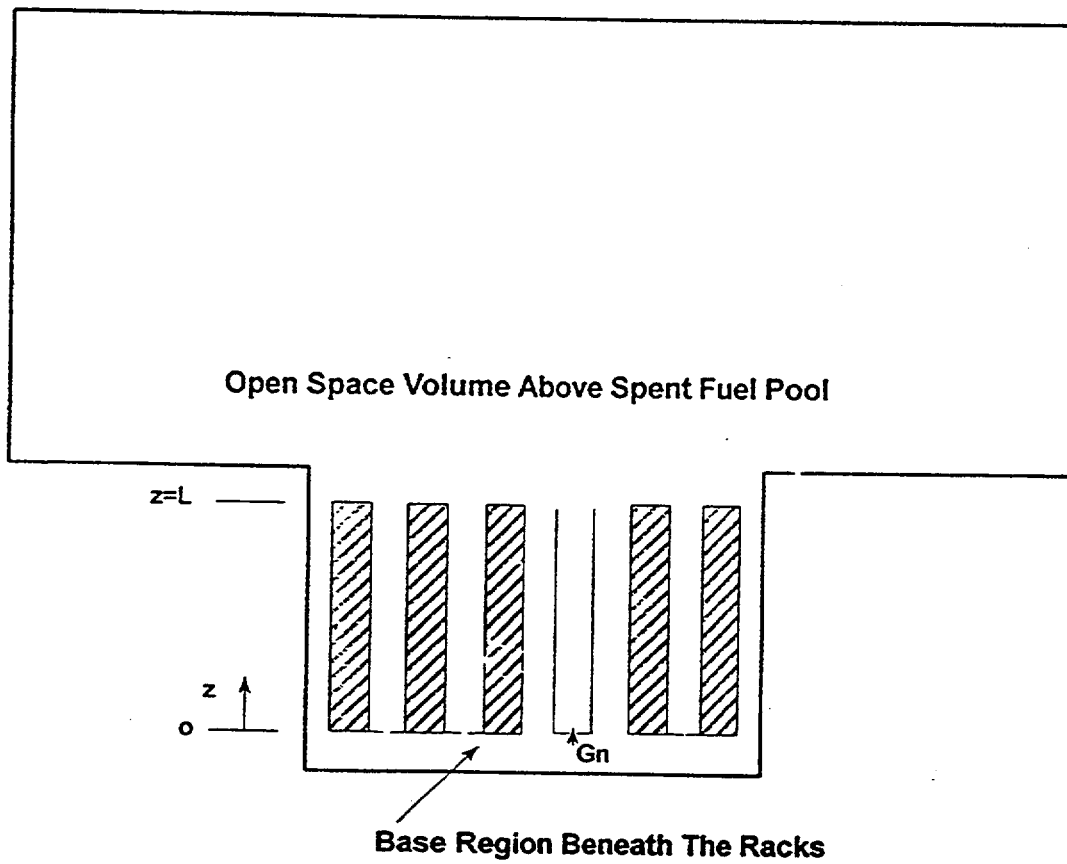


Figure 4.4 Schematic of spent fuel storage configuration modeled as parallel channels

identically. The net flow from the base region beneath the racks to the open space volume above the spent fuel pool is the algebraic sum of all channel flows which would be zero or:

$$\sum_{n=1}^N Y_n G_n A_{fn} = 0 \quad (4.24)$$

The subscript  $n$  refers to a channel type and not an individual channel so there are assumed to be  $N$  sets of channels.

#### 4.2.1.2 Conservation of Momentum

The relevant momentum equation is:

$$\frac{\partial G}{\partial t} + \frac{\partial}{\partial z} \left( \frac{G^2}{\rho} \right) = -\frac{\partial P}{\partial z} - \frac{fG|G|}{2D_H \rho} - \rho g \quad (4.25)$$

Integrating this momentum equation from the bottom of a channel ( $z=0$ ) to the top of channel ( $z=L$ ) under steady-state conditions and local losses across the base plate hole and spacer grids yields:

$$\begin{aligned} \Delta P_n = & g \int_0^L \rho_n dz + \int_0^L \frac{fG_n |G_n|}{2D_H \rho_n} dz + \sum_{k=1}^m \frac{k_{SG} G_n |G_n|}{2\rho_n(z_k)} \\ & + \frac{K_o G_n |G_n|}{2\rho_n(0)} + G_n^2 \left[ \frac{1}{\rho_n(L)} - \frac{1}{\rho_n(0)} \right] \end{aligned} \quad (4.26)$$

The channel pressure loss,  $\Delta P_n$ , is defined by:

$$\Delta P_n \equiv P_{b,n} - P_{u,n} \quad (4.27)$$

where  $P_{b,n}$  and  $P_{u,n}$  are the pressure at the lower and upper extremes of the channel ( $z=0$  and  $z=L$ ), respectively.

The right hand side of Equation 4.26 consists of the gravitational term, the frictional term, the local loss term due to spacer grids, the local loss term due to the base-plate hole, and the acceleration term, respectively. The gravity term is positive and independent of flow direction. The friction and local loss terms are positive for upflow and are negative for downflow as indicated by our sign convention on  $G_n$

because these terms cause the pressure decreases in the direction of flow. The acceleration pressure drop term for heated upflow or cooled downflow is positive, whereas for heated downflow is negative.

#### 4.2.1.3 Conservation of Energy

The one-dimensional energy equation, neglecting the terms due to pressure changes and wall friction forces, reduces to:

$$\rho \frac{\partial h}{\partial t} + G \frac{\partial h}{\partial z} = \frac{q'' P_h}{A_z} \quad (4.28)$$

Using the enthalpy-specific heat relationship and expressing the heat flux  $q''$  in terms of fuel elements and structural temperatures; the energy equation (4.28) for air flow in channel  $n$  becomes:

$$\rho_n A_{fn} C_p \frac{\partial T_n}{\partial t} + G_n A_{fn} C_p \frac{\partial T_n}{\partial z} = \sum_i h_{c,i} (T_{s,i} - T_n) P_{H,i} \quad (4.29)$$

The right hand side of Equation 4.29 represents the net convective heat transfer from structures (including the fuel elements) to air flow.

#### 4.2.2 Solution Procedure

The conservation equations formulated in the previous section are solved to predict buoyancy driven air flows in the drained spent fuel pool. The boundary conditions are obtained from the thermal hydraulic analysis within the base region beneath the racks and within the spent fuel storage building (see Section 4.3 and 4.4). The hydrodynamic components of the boundary conditions are the zero net mass flow rate (Equation 4.24), the spent fuel storage building pressure,  $P_r$  ( $P_{u,n} = P_r$ ), and the pressure gradient at the lower base region. To account for lateral pressure variation in the base region, it is assumed that each channel has a lateral pressure gradient correction term so that the channels will have the same pressure drop within an additive constant. The pressure drop across each channel is thus expressed as:

$$\Delta P_n = \Delta P + \Delta P'_{l,n} \quad (4.30)$$

#### 4. Physical Models

where the  $\Delta P'_{1,n}$  is the lateral pressure drop correction term which is obtained from the thermal-hydraulic analysis within the base region. It should be noted that with the assumption of negligible pressure variation in the base region, the pressure drops of all channels become equal ( $\Delta P_n = \Delta P$ ).

The momentum and energy equations (Equations 4.26 and 4.29) are coupled since the density,  $\rho$ , which is a function of temperature and pressure, appears in the momentum equation. The solution procedure can be simplified if the air is allowed to expand thermally, but is considered to be incompressible. The density  $\rho$  then can be expressed by:

$$\rho = \frac{P^*}{RT} \quad (4.31)$$

This approximation is valid because the pressure drops are small compared to system pressure  $P^*$ . Although the use of a reference pressure  $P^*$  does simplify the solution procedure, the energy and momentum equations are still coupled and are solved numerically by using the subdomain method<sup>16</sup> (control volume formulation) to discretize the equations. The power law scheme is used for convection-diffusion formulation which allows a uniform treatment of energy equation for both open and blocked channels.

The general solution procedure is shown in Figure 4.5. First, an initial estimate for  $\Delta P$  is chosen. Based on this  $\Delta P$ , the  $G_n$  values for each channel type are determined. Each value of  $G_n$  is obtained iteratively by solving the energy and momentum equations for each channel type  $n$ . The Secant method,<sup>18</sup> is used to find the values of  $G_n$  iteratively.

After the energy and momentum equations are used to solve for  $G_n$  for each channel, the system mass balance (Equation 4.24) must be satisfied. If this equation is not satisfied within a given tolerance a new value for  $\Delta P$  is chosen, and the procedure repeated until convergence is achieved. Here again, Secant method is used to find  $\Delta P$ .

The present solution procedure in principle is sufficient for obtaining the buoyancy-driven air flows. However, the momentum equation in particular leads to complexities because the channel pressure drop/flow rate behavior is not a simple monotonically increasing function. The channel hydraulic characteristic curve has a shape that can lead to multiple solutions and instabilities.

As a part of the present effort, a systematic study of these characteristics was performed to provide the physical basis essential to understanding and analyzing this complex system behavior.

Figures 4.6 and 4.7 illustrate the typical steady-state hydraulic characteristics of PWR and BWR spent fuel assemblies (cells), respectively. In these figures, a negative Reynolds number,  $Re$ , indicates downflow. These results were obtained by using the appropriate modules of the SHARP code, assuming an inlet air temperature of 20°C. The friction and the local pressure drop terms are scaled by  $\rho_o Lg$  while the dimensionless gravity pressure drop term,  $\Delta P^*_{grav}$ , is defined by:

$$\Delta P^*_{grav} = \frac{\Delta P_{grav} - \rho_o^{Lg}}{\rho_o^{Lg}} \quad (4.32)$$

The dimensionless total pressure drop,  $\Delta P^*_{tot}$ , then is expressed as:

$$\Delta P^*_{tot} = \frac{\Delta P_{tot} - \rho_o^{Lg}}{\rho_o^{Lg}} \quad (4.33)$$

The Reynolds number,  $Re$ , is defined by:

$$Re = \frac{\rho u D_H}{\mu} \quad (4.34)$$

where the equivalent hydraulic diameter,  $D_H$ , is defined by:

$$D_H = \frac{4A_f}{P_w} \quad (4.35)$$

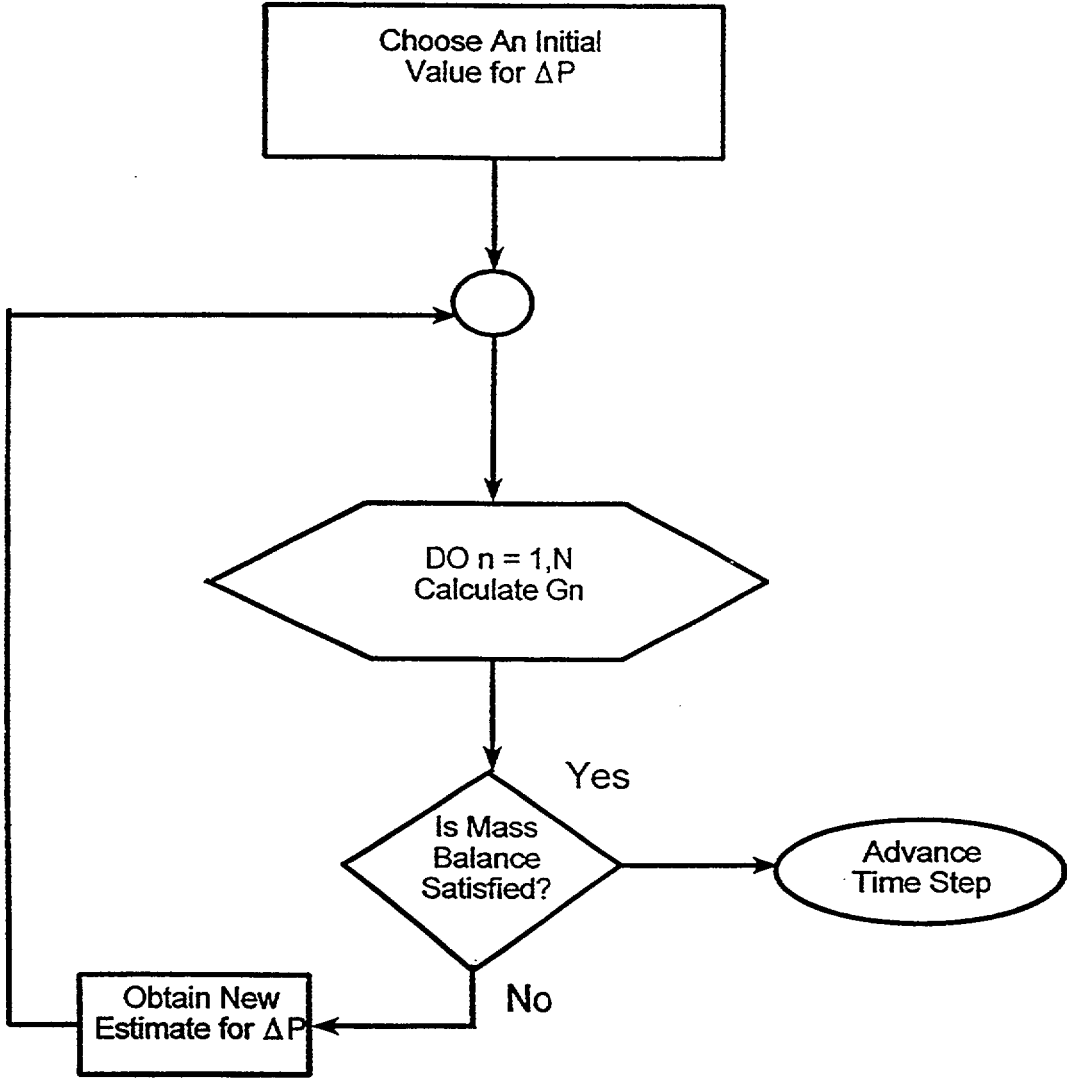


Figure 4.5 General solution procedure to obtain the buoyancy induced air flow

4. Physical Models

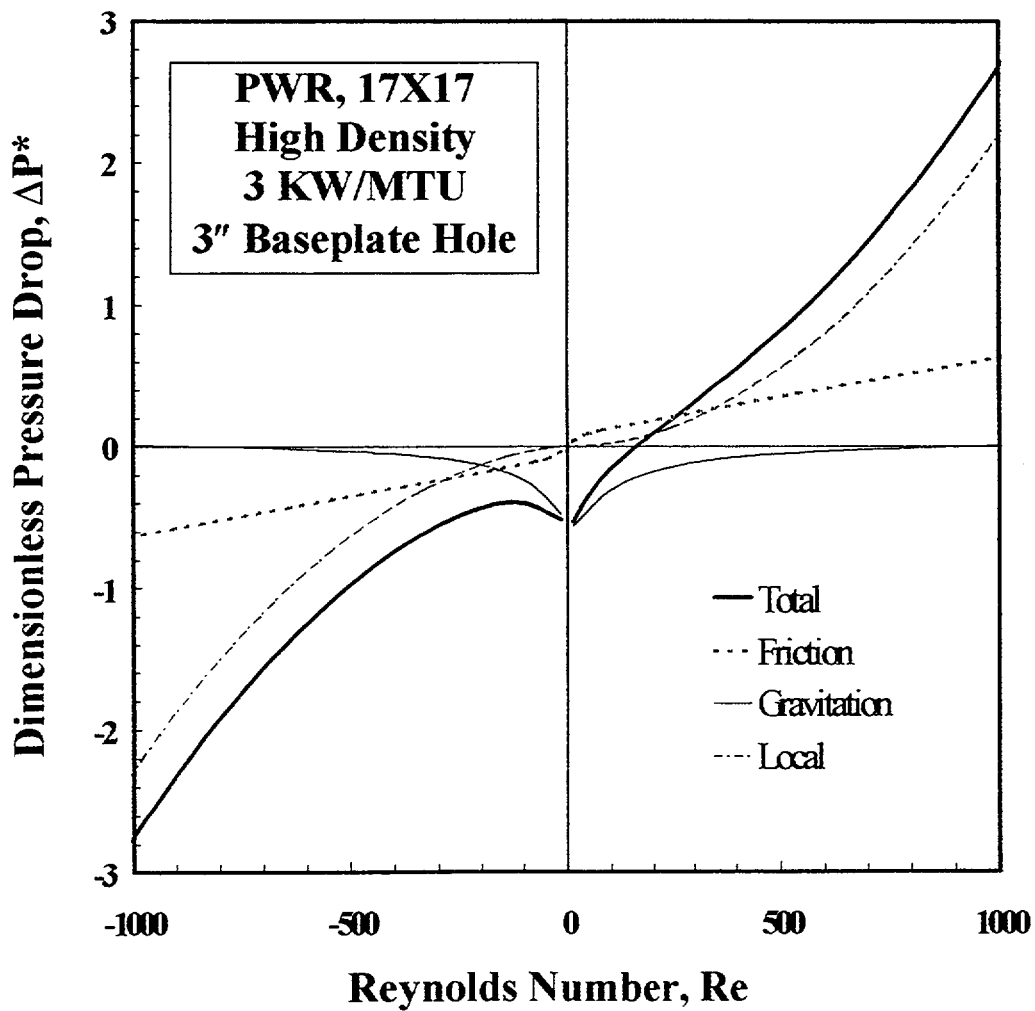


Figure 4.6 Typical hydraulic characteristics of a PWR spent fuel cell

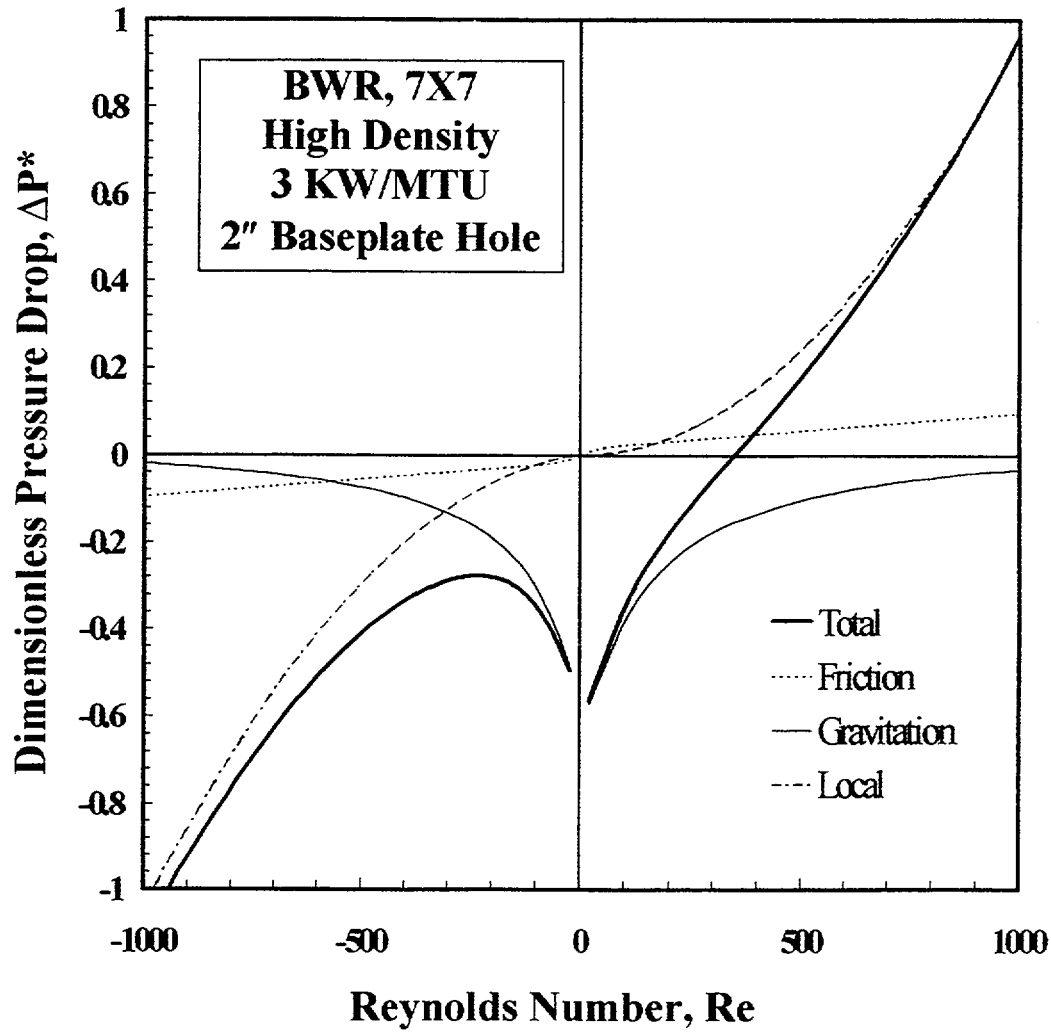


Figure 4.7 Typical hydraulic characteristics of a BWR spent fuel cell

#### 4. Physical Models

where  $A_f$  and  $P_w$  are the flow area and wetted perimeter, respectively.

As indicated in Figures 4.6 and 4.7, for certain prescribed  $\Delta P^*$ s, there can be three Reynolds numbers (flow rates) which satisfy the energy and momentum equations. Two in downflow, and one in upflow. For stable flow in a channel, the channel pressure drop must increase as the Reynolds number (flow rate) is increased. An equivalent requirement is that:

$$\frac{\partial(\Delta P^*)}{\partial Re_n} > 0 \quad (4.36)$$

Figures 4.8 and 4.9 show the typical steady-state hydraulic characteristics of spent fuel assemblies as a function of decay heat and the base-plate hole size, respectively. It should be noted that the intersections of hydraulic characteristic curves with the x-axis can be viewed as the corresponding values of air flows (in the presence of forced ventilation or a chimney effect) provided that there is large spacing around the side and bottom of the pool ( $\Delta P^* = 0$ ).

### 4.3 Thermal-Hydraulics of Spent Fuel Storage Building

As was discussed in Section 3, the extent of heat removal from the spent fuel building atmosphere strongly affects the heatup characteristics of the exposed spent fuel rods. Removal of heat from spent fuel storage buildings under normal operation is accomplished by a forced ventilation system. In the absence of a powerful air ventilation system (or chimney effect), the building will pressurize until failure and result in the subsequent leakage of air to the outside atmosphere. Assuming the building atmosphere is well mixed (i.e., isothermal and isobaric) the mass and energy conservation equations for the containment building can be expressed as:

$$V_r \frac{\partial \rho_r}{\partial t} = -\dot{m}_{leak} + \dot{V}_{vent} (\rho_o - \rho_r) \quad (4.37)$$

$$V_r \frac{\partial(\rho_r h_r)}{\partial t} = \sum (\dot{m}_n h_n)_{in} - (\sum \dot{m}_n)_{out} h_r - \dot{m}_{leak} h_r + \dot{V}_{vent} (\rho_o h_o - \rho_r h_r) - \sum h_s A_{r,s} (T_r - T_{rs}) \quad (4.38)$$

The right hand side of Equation 4.38 consists of enthalpy inflow from the spent fuel pool region, the enthalpy outflow to the spent fuel pool region, the enthalpy outflow due to leakage and the convective heat losses to heat sinks (structures), respectively.

The leakage rate,  $\dot{m}_{leak}$  at the constant failure pressure  $P_{max}$  can be expressed as:

$$\dot{m}_{leak} = \frac{1}{h_r} \left[ \sum (\dot{m}_n h_n)_{in} - (\sum \dot{m}_n)_{out} h_r + \dot{V}_{vent} (\rho_o h_o - \rho_r h_r) - \sum h_s A_{r,s} (T_r - T_{rs}) \right] \quad (4.39)$$

The energy balance for the structures is expressed by:

$$\rho_s C_{ps} b_s A_{r,s} \frac{dT_{r,s}}{dt} = h_{c,i} A_{r,s} (T_r - T_s) - h_{c,o} A_{r,s} (T_s - T_o) \quad (4.40)$$

where  $b_s$  and  $A_s$  are the thickness and heat transfer area of structures respectively.  $T_o$ ,  $h_{c,i}$  and  $h_{c,o}$  are the outside air temperature, inside convective heat transfer coefficient and outside heat transfer coefficient, respectively. Equations 4.37 through 4.40 together with the enthalpy-specific heat relationship and equation of state, are solved numerically to obtain the pressure and temperature of spent fuel building atmosphere.

### 4.4 Thermal Hydraulics of the Base Region Beneath the Racks

As discussed in Section 4.2.2, the temperature and pressure distributions within the base region beneath the racks are required to predict the buoyancy driven air flows within the spent fuel assemblies. Here, a fully mixed (i.e., isothermal and isobaric) base region is assumed. This is specifically the case if the flow

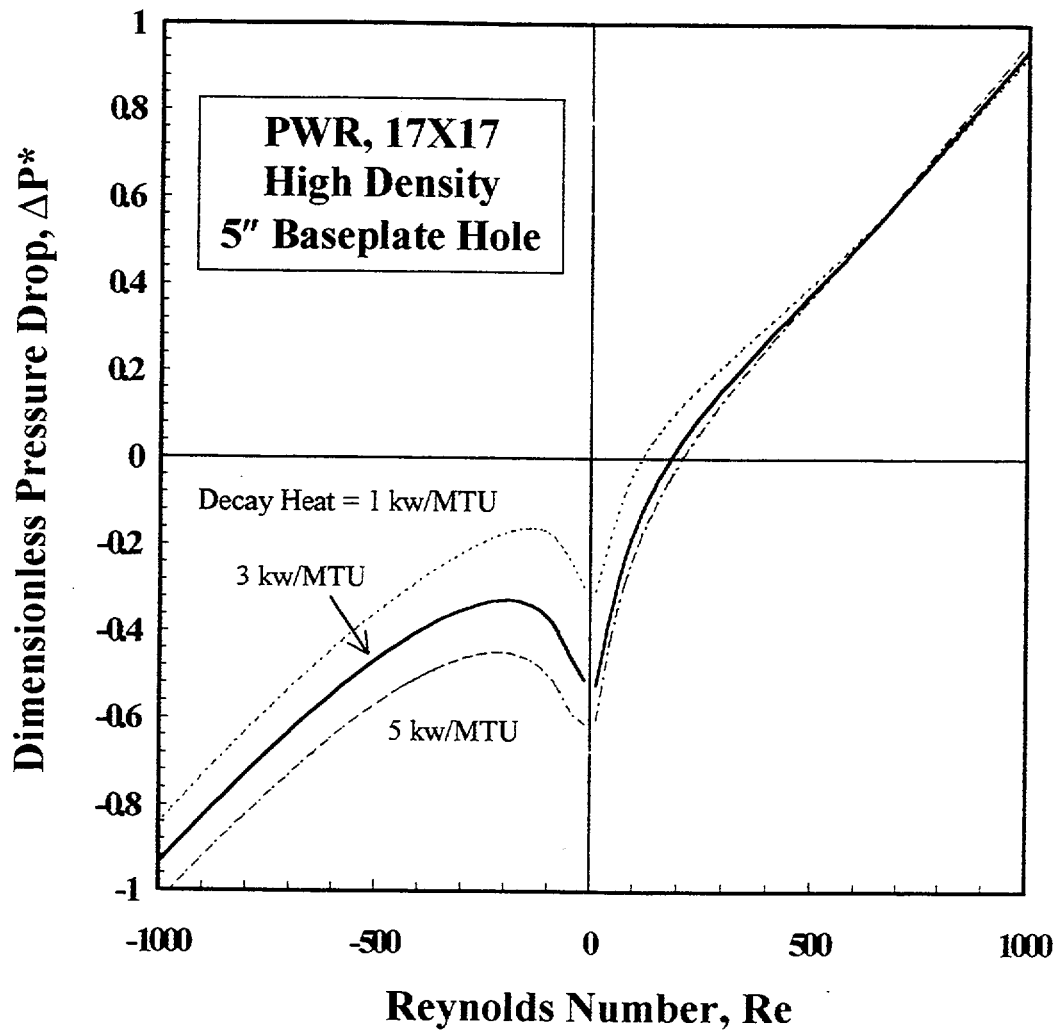


Figure 4.8 The effect of decay heat on the hydraulic characteristics curves

4. Physical Models

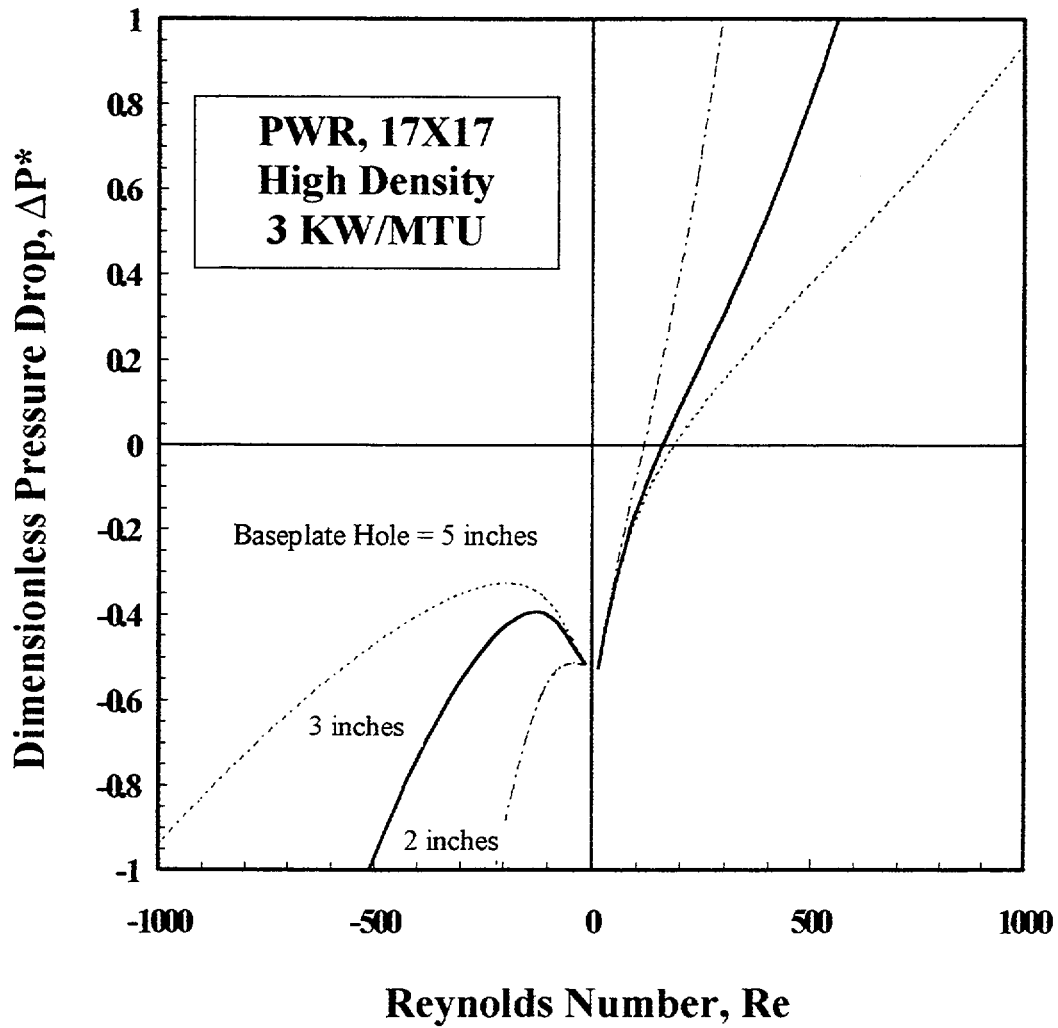


Figure 4.9 The effect of base-plate hole size on the hydraulic characteristics curves

Reynolds numbers are low and the base region equivalent diameter is large (i.e., large spacing at the bottom of the pool). The approximation of fully mixed base region obviates the need for a multi-dimensional calculation of temperature and pressure field in the base region. With a fully mixed base region, the lateral pressure gradient correction term,  $\Delta P'_{1n}$ , discussed in Section 4.2.2 is zero. The energy conservation equation can then be expressed as:

$$V_b \frac{\partial(\rho_b h_b)}{\partial t} = \sum (\dot{m}_n h)_{in} - \sum (\dot{m}_n)_{out} h_b - \sum h_c A_{bs} (T_b - T_{bs}) \quad (4.41)$$

The right hand side of Equation 4.41 consists of enthalpy inflow from the spent fuel pool region, the enthalpy outflow to the spent fuel pool region, and the convective heat losses to structures in the base region. Equation 4.41, together with the enthalpy-specific heat relationship and equation of state, are solved numerically to obtain the temperature of the base region.

## 4.5 Heat Transfer in Structures

Heat transfer within the structures of the pool region, such as cell walls, is modeled by heat conduction in one spacial dimension. The one dimensional heat conduction is reduced to:

$$A_{x,s} (\overline{\rho C})_s \frac{\partial T_s}{\partial t} = A_{x,s} \frac{\partial}{\partial z} \left( \overline{K}_s \frac{\partial T_s}{\partial z} \right) - \sum h_c (T_s - T) P_H \quad (4.42)$$

where  $A_{x,s}$  is the cross sectional area of structure,  $P_H$  is the heated perimeter,  $(\overline{\rho C})_s$  is the volumetric heat capacity (area averaged) and  $\overline{K}_s$  is the area averaged thermal conductivity.

The heat transfer into the concrete side and bottom of the pool is determined by the integral method.<sup>19</sup> The heat conduction equation for a semi-infinite concrete slab extending over the positive x direction is:

$$\frac{\partial T}{\partial t} = \alpha_{con} \frac{\partial^2 T}{\partial x^2} \quad (4.43)$$

where  $\alpha_{con}$  is the thermal diffusivity of concrete. Initially, the temperature  $T$  is  $T_o$  and at the surface  $x=0$  the heat flux,  $F(t)$ , for  $t>0$  is expressed by:

$$-K_{con} \frac{\partial T}{\partial x} \Big|_{x=0} = F(t) = h_c [T_a(t) - T(o,t)] \quad (4.44)$$

where  $T(o,t)$  is the concrete surface temperature which is assumed to be equal to the temperature of pool liner  $T_l(t)$ . The heat-balance integral obtained by integrating equation 4.43 over the thermal penetration distance,  $\delta(t)$ , becomes:

$$\frac{d}{dt} (\theta - T_o \delta) = \alpha_{con} \left[ \frac{\partial T}{\partial x}(\delta,t) - \frac{\partial T}{\partial x}(o,t) \right] \quad (4.45)$$

where:

$$\theta = \int_0^{\delta(t)} T dx \quad (4.46)$$

But, since there is no heat transferred beyond  $x=\delta$ ,

$$\frac{\partial T}{\partial x}(\delta,t) = 0 \quad (4.47)$$

Assuming a parabolic temperature profile across the thermal penetration distance, the slab temperature can be expressed as:

$$T = B_0 + B_1 x + B_2 x^2 \quad (4.48)$$

Applying Equations 4.44 and 4.47, and the condition  $T(\delta,t) = T_o$  to Equation 4.48 leads to:

$$T = T_o + \frac{F}{2K_{con} \delta} (\delta - x)^2 \quad (4.49)$$

Substituting Equation 4.49 into Equation 4.46 one obtains:

$$\theta = T_o \delta + \frac{\delta^2 F}{6K_{con}} \quad (4.50)$$

#### 4. Physical Models

Introducing Equations 4.44, 4.47, and 4.50 into the heat balance integral, Equation 4.45, leads to the following ordinary differential equation to be solved for  $\delta$ .

$$\frac{d}{dt} (\delta^2 F) = 6 \alpha_{con} F \quad (4.51)$$

By virtue of the initial condition,  $\delta(o)=0$ ,

$$\delta = \sqrt{6 \alpha_{con}} \left[ \frac{1}{F} \int_0^t F(u) du \right]^{1/2} \quad (4.52)$$

The surface temperature,  $T(o,t)$  is obtained by setting  $x=o$  in Equation 4.49 and applying Equation 4.52.

$$T(o,t) = T_o + \sqrt{\frac{3}{2} \alpha_{con}} \left[ F(t) \int_0^t F(u) du \right]^{1/2} / K_{con} \quad (4.53)$$

### 4.6 Friction Factor

As was noted previously, a realistic prediction of air flows depends on accurate calculations of the pressure drop terms. The expressions for the friction factor,  $f$ , used in Equation 4.26 are presented in this section.

The product of  $f Re$  for fully developed flow in the individual subchannels is available from Rehme.<sup>20,21</sup> The results have been fit by Cheng and Todreas<sup>22</sup> with polynomials for each subchannel type. The polynomial has the form:

$$C_{fi} = a + b_1(P/D - 1) + b_2(P/D - 1)^2 \quad (4.54)$$

where:

$$\hat{f}_i = \frac{C_{fi}}{Re_i^n} \quad (4.55)$$

where  $n=1$  for laminar flow and  $n=0.18$  for turbulent flow. When Equation 4.54 is used for edge and corner subchannels, pitch-to-diameter ( $P/D$ ) ratio is replaced by  $W/D$ , where  $W$  is the rod diameter plus gap between the rod and bundle wall. The effect of  $P/D$  (or  $W/D$ )

is separated into two regions;  $1.0 < P/D \leq 1.1$  and  $1.1 < P/D \leq 1.5$ . Table 4.1 presents the coefficients  $a$ ,  $b_1$ , and  $b_2$  for the subchannels of square arrays.

Bundle average friction factors are obtained from the subchannel friction factors by assuming that the pressure difference across all subchannels is equal and applying the mass balance condition for total bundle flow in terms of the subchannel flow. The resulting friction factor constant of a rod bundle,  $C_{fb}$ , is obtained by the following equation:<sup>17</sup>

$$C_{fb} = D_{Hb} \left[ \sum_{i=1}^3 S_i \left( \frac{D_{Hi}}{D_{HB}} \right)^{\frac{n}{n-2}} \left( \frac{C_{fi}}{D_{Hi}} \right)^{\frac{1}{n-2}} \right]^{n-2} \quad (4.56)$$

where  $S_i$  is the ratio of the total flow area of subchannels of type  $i$  to the bundle flow area. Table 4.2 lists the number of subchannels, their flow area, and their wetted perimeters for square arrays with the number of  $N$  rods in one row. The hydraulic diameter for each subchannel of Table 4.2 can be determined by:

$$D_{Hi} = \frac{4 A_i}{P_{wi}} \quad (4.57)$$

For fully developed flow in the downcomer next to the edge of the pool and empty holders, the friction factor can be obtained from Equation 4.55 where:

$$C_f = \begin{cases} 96 & \text{Laminar flow } (Re < 2100) \\ 0.184 & \text{Turbulent flow } (Re > 2100) \end{cases} \quad (4.58)$$

It should be noted that in the representative plant calculations reported in Section 6, the flow inside the spent fuel assemblies was governed by laminar fully-developed forced convection, whereas, in the downcomer along the side of the pool, the flow was dominated by turbulent fully-developed forced convection. In the SHARP Code, the correlations for friction factors are implemented in a separate module such that they can be easily overridden by a user for any future sensitivity calculations.

**Table 4.1 Coefficients in Equation 4.54 for Bare Rod Subchannel Friction Constants  $C_f$  in Square Array**

Subchannel	1.0 < P/D ≤ 1.1			1.1 ≤ P/D ≤ 1.5		
	a	b <sub>1</sub>	b <sub>2</sub>	a	b <sub>1</sub>	b <sub>2</sub>
Laminar flow						
Interior	26.37	374.2	-439.9	35.55	263.7	-190.2
Edge	26.18	554.5	-1480	44.40	256.7	-267.6
Corner	28.62	715.9	-2807	58.83	160.7	-203.5
Turbulent flow						
Interior	0.09423	0.5806	-1.239	0.1339	0.09059	-0.09926
Edge	0.09377	0.8732	-3.341	0.1430	0.04199	-0.04428
Corner	0.09755	1.127	-6.304	0.1452	0.02681	-0.03411

**Table 4.2 Geometrical Parameters of Square Array Rod Bundles**

Subchannel Type (i)	Number (n <sub>i</sub> )	Flow Area (A <sub>i</sub> )	Wetted Perimeter (P <sub>wi</sub> )
Central	(N - 1) <sup>2</sup>	$P^2 - \frac{\pi}{4}D^2$	$\pi D$
Wall	4(N-1)	$\left(W - \frac{D}{2}\right)P - \frac{\pi}{8}D^2$	$\frac{\pi}{2}D + P$
Corner	4	$\left(W - \frac{D}{2}\right)^2 - \frac{\pi}{16}D^2$	$\frac{\pi}{4}D + 2\left(w - \frac{D}{2}\right)$

#### 4. Physical Models

### 4.7 Local Form Loss Factor Due to Base-Plate Hole

The form loss coefficient,  $K_o$ , used in Equation 4.26 is obtained by the following expression:

$$K_o = \frac{A_c^2 - A_h^2}{C_D^2 A_h^2} \quad (4.59)$$

where  $A_h$  and  $A_c$  are the base-plate hole and cell cross sectional areas, respectively. The orifice discharge coefficient,  $C_D$ , is taken as 0.7.

### 4.8 Pressure Loss at Spacer Grids

Pressure losses across spacer grids are form drag-type pressure losses that can be calculated using pressure-loss coefficients.<sup>23</sup> Rehme<sup>24</sup> measured the pressure drop characteristics of a variety of spacer grids. He concluded that spacer grids pressure drop data may be correlated by:

$$\Delta P_{SG} = C_v \epsilon^2 \frac{G^2}{2\rho} \quad (4.60)$$

where  $C_v$  is the modified drag coefficient and  $\epsilon$  is the relative plugging defined by:

$$\epsilon = \frac{A_v}{A_s} \quad (4.61)$$

where  $A_v$  is the projected frontal area of spacer grid and  $A_s$  is the undisturbed flow area away from the spacer grid. Values of the modified loss coefficient  $C_v$  as a function of the Reynolds number  $Re$  for square arrays are available from Rehme.<sup>24</sup> The results were fit with the following correlation for use in the SHARP code:

$$C_v = \begin{cases} 9.3333 - 0.6667 \times 10^{-4} Re & Re < 5 \times 10^4 \\ 6 & Re > 5 \times 10^4 \end{cases} \quad (4.62)$$

It should be noted that the investigations of Rehme were performed for high Reynolds numbers only ( $Re > 3 \times 10^3$ ). However, for Reynolds numbers of interest

to the present fuel heatup calculations, the pressure losses at spacer grids were found to be negligible compared to the friction losses along the bare rod bundles.

### 4.9 Heat Transfer Coefficient

The heat transfer coefficient,  $h$ , is obtained through the non-dimensional Nusselt number:

$$Nu \equiv \frac{h D_H}{K} \quad (4.63)$$

where  $D_H$  is an appropriate length or lateral dimension. The value for Nusselt number,  $Nu$ , depends on the heat transfer regime (forced convection, natural convection, or mixed convection), flow condition (Turbulent vs. Laminar) and geometry.

For the laminar fully developed forced convection along rod bundles (inside fuel cells) the Nusselt number is taken as a constant value of 8. Here, Nusselt number is defined using the concept of equivalent heated diameter,  $D_H$ , where:

$$D_H \equiv \frac{4A_f}{P_h} \quad (4.64)$$

where  $A_f$  and  $P_h$  are the flow areas and the heated perimeter, respectively.

The Nusselt number for the turbulent fully developed forced convection,  $Nu_\infty$  is expressed as a product of  $(Nu_\infty)_{c.t.}$  for a circular tube multiplied by a correction factor:

$$Nu_\infty = \Psi (Nu_\infty)_{c.t.} \quad (4.65)$$

where  $(Nu_\infty)_{c.t.}$  is obtained by the Dittus-Boelter<sup>23</sup> correlation:

$$(Nu_\infty)_{c.t.} = 0.023 Re^{0.8} Pr^{0.4} \quad (4.66)$$

The correction factor,  $\Psi$ , in Equation (4.62) is obtained by the following formulation given by Presser.<sup>24</sup>

$$\Psi = 0.9217 + 0.1478 P/D - 0.1130 e^{-7(P/D-1)} \quad (4.67)$$

### 4.10 Decay Heat

The DOE High Level Radioactive Waste Management Database<sup>27</sup> was used as the source of the generic spent fuel decay power data for discharges one year or older. The data for decay power characteristics for PWR and BWR spent fuel assemblies for different amount of burnup are shown in Figures 4.10 and 4.11, respectively. These data are used internally in the SHARP code to obtain the decay power values based on the fuel burnup and decay time of each representative channel. Extrapolation was used to obtain the decay power data for discharges of less than a year. There are little differences between the decay power used in the present study and the ones tabulated in NUREG/CR-6525.<sup>28</sup> For the variation of decay power along the axis of a fuel rod, a chopped sine distribution having a peak-to-average variation of 1.5 was assumed.

It should be noted that in the SHARP code, with the proper choice of an input option, the decay power for each representative channel can be specified by a user.

### 4.11 Overview of SHARP Code

The model formulations and their solutions and their solution methods described in the previous sections have been implemented in a computer code called SHARP (Spent fuel Heatup: AnalYTical Response Program). The code allows analysis of the spent fuel heatup for a variety of storage practices including storing both PWR and BWR spent fuel assemblies in the same spent fuel pool during permanent shutdown.

Figure 4.12 presents the SHARP code structure. In addition to adequacy in modeling of the important processes and phenomena, a modular, highly structured and user friendly architecture was required to facilitate both the initial development of the code and any later modification and/or addition of models. Extensive internal documentation was also mandated for these same reasons. To avoid portability problems, adherence to ANSI standard FORTRAN 77<sup>29</sup> was desirable for the coding of SHARP. Finally, an architecture compatible with the short run-times necessary for sensitivity analyses was also required. A user's manual for the code is provided in Appendix A.

#### 4. Physical Models

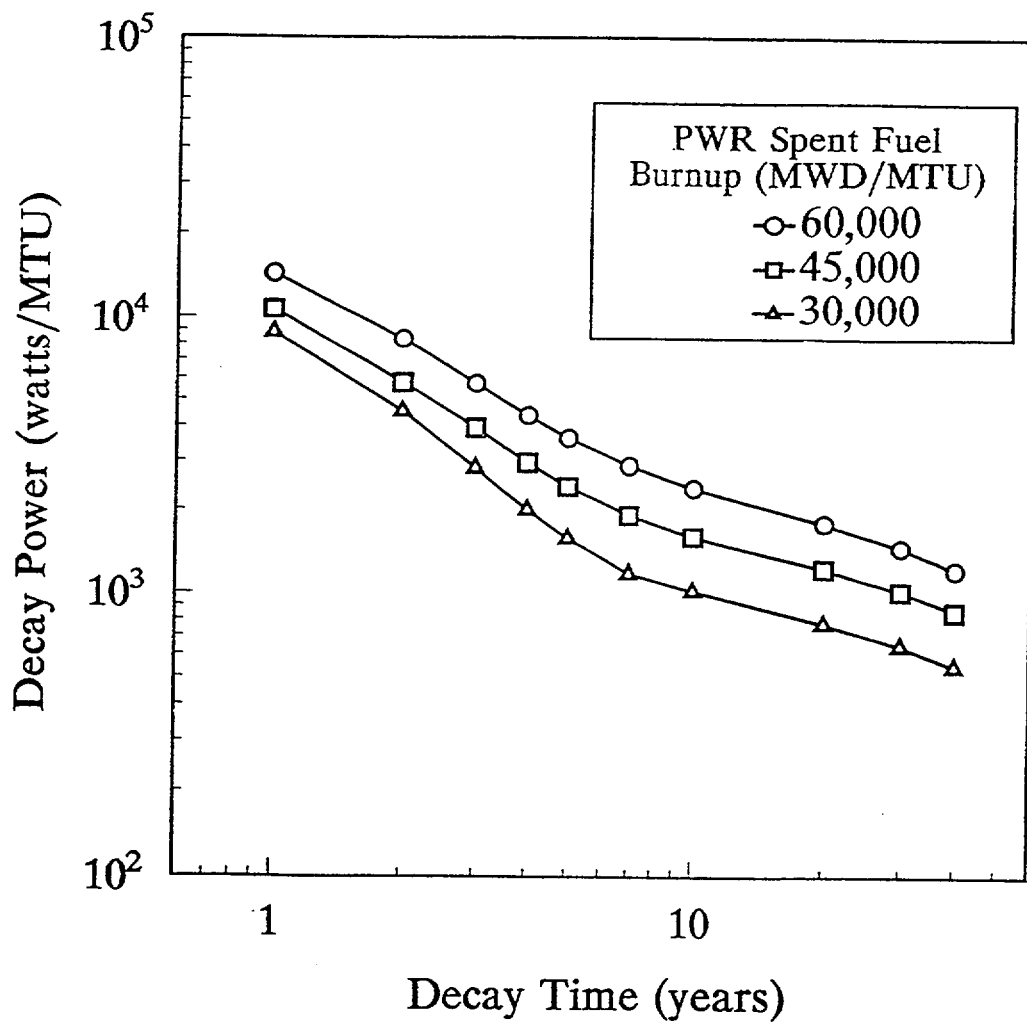


Figure 4.10 Decay power characteristics of PWR spent fuel assemblies

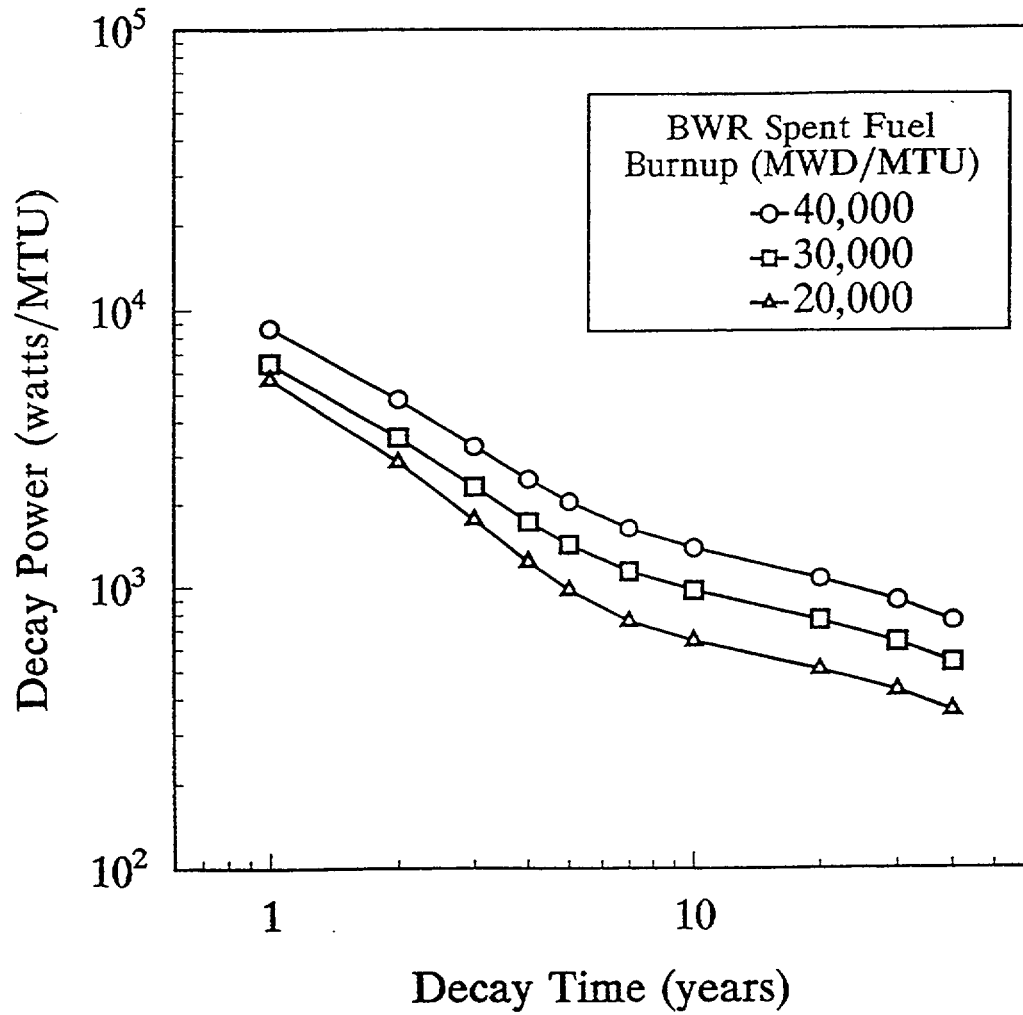


Figure 4.11 Decay power characteristics of BWR spent fuel assemblies

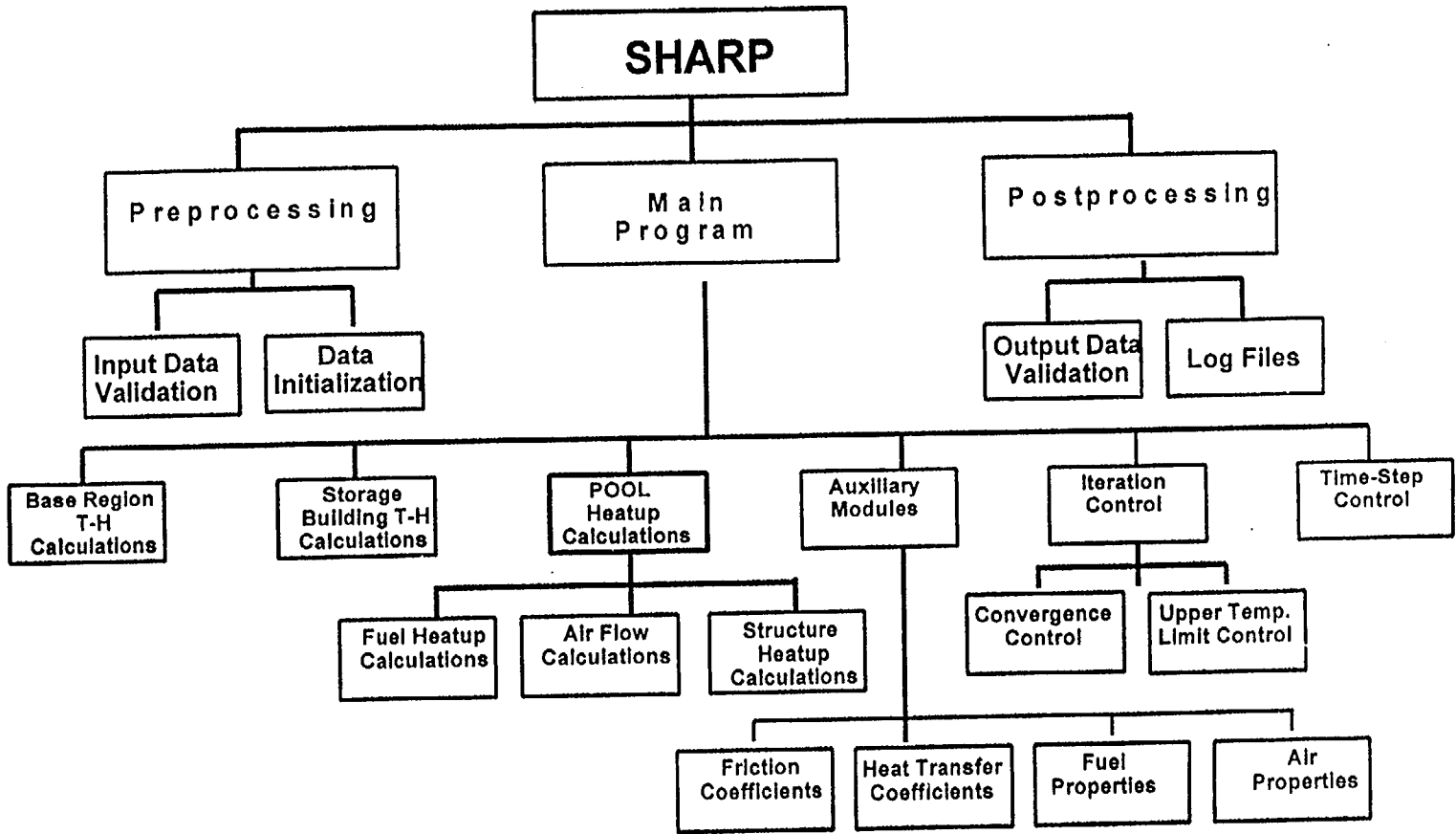


Figure 4.12 SHARP code structure

## 5. CODE VERIFICATION AND VALIDATION

The SHARP code has been subjected to a detailed line by line examination to ensure that models have been implemented as intended. Informal tests were performed to ensure each module and combination of modules are correct.

Except for limited data on an experiment performed by Chato<sup>30</sup> in a three parallel channel setup, no experimental studies on the behavior of natural convection flows in parallel-channel systems have been reported in the open literature.

To evaluate the technical adequacy of the SHARP code, the appropriate modules of the SHARP code were used to predict the heat up characteristics of a single cell (assuming constant inlet air velocity). The results were found to be consistent with the validated calculational results reported in References 3 and 4.

Multi-dimensional computational fluid dynamics (CFD) models, where equations of motion and transport are solved over the domain of interest with a variety of empirical approaches or approximations used to treat turbulence and transport properties, have been applied to spent fuel heatup and related thermal mixing problems. CFD model codes provide greater detail than the present simplified model of the SHARP code. However, due to the large dimensions of the calculational domain, establishing grid independence to resolve shear (mixing) layers is an extremely costly process. Computational expenses become even higher as the building ventilation rate decreases because of the increase in the time constant of the heatup transient. Therefore, these multi-dimensional codes are only feasible for steady state calculations and for a specific region of the entire spent fuel pool. The CFD codes also offer valuable tools for validation

and benchmarking of the present simplified SHARP model.

A heatup analysis of the Haddam Neck spent fuel pool was performed by Pacific Northwest National Laboratory (PNNL),<sup>31</sup> using the three dimensional TEMPEST<sup>32</sup> and COBRA-SFS<sup>33</sup> codes. Comparisons of SHARP code predictions with the results of COBRA-SFS/TEMPEST codes are discussed in this section.

### 5.1 Comparison with the COBRA-SFS/TEMPEST Codes Predictions

The PNNL also conducted an analysis of the Haddam Neck spent fuel pool.<sup>31</sup> Computer codes were used in the analysis to predict the peak cladding temperature following loss of all the water in the spent fuel pool.

A three-dimensional TEMPEST model was used to model heat transfer from the air space above the fuel racks to the ambient environment. The ventilation system was assumed to operate with a steady flow of 5.66 m<sup>3</sup>/s (12,000 cfm) of air at 31°C (88°F). Sensitivity calculations were also performed at a high ventilation flow rate of 18.87 m<sup>3</sup>/s (40,000 cfm). The average temperature obtained from the TEMPEST results was then applied as a uniform constant temperature boundary for the COBRA-SFS model.

A three-dimensional COBRA-SFS model was used to simulate heat removal from the four fuel racks in the northeast corner of the pool. The COBRA-SFS model assumed an adiabatic boundary existed between these four racks and the neighboring racks outside this region.

## 5. Overview of SHARP Code

For the SHARP analysis of Haddam Neck spent fuel heatup,<sup>34</sup> a total of eight representative channels, were assumed: five channels to represent the spent fuel assemblies with different decay heat, two channels to represent empty cells and one channel to represent the allowance space between the racks and the edge of the pool. The fuel loading assumptions used in the calculations are shown in Table 5.1. The decay power values used in the calculations were obtained internally by the SHARP code based on the burnup and decay time of each representative channel.

In the SHARP code calculations, the building was assumed to be capable of withstanding an internal gauge pressure of only 0.2 psi before any leakage occurs, and then was assumed to leak at the rate required in order to keep the pressure from exceeding 0.2 psig. All leakage was assumed to occur from the inside to the outside.

The SHARP code calculated results of the maximum clad temperature in the Haddam Neck pool as a function of time after pool drainage for different ventilation rates are presented in Figure 5.1. Also shown in Figure 5.1 are the steady state results obtained from the COBRA-SFS/TEMPEST analysis. As shown in Figure 5.1, the time to reach steady state increases when the ventilation rate decreases.

For a high ventilation rate case and decay heat loads corresponding to October 1, 1997 (approximately 14 months after reactor shutdown), the maximum clad temperature was predicted by the SHARP code to be 446°C as compared to 443°C obtained by PNNL using COBRA-SFS/TEMPEST. For a low ventilation rate case, the SHARP code predicted a peak cladding temperature of 583°C as compared to 515°C obtained from COBRA-SFS/TEMPEST analysis.

**Table 5.1 Fuel Loading Assumptions Used in the SHARP Computer Code Calculations for the Haddam Neck Plant**

Representative Channel (Region of the Pool)	Number of Cells (Assemblies)	Burnup (MWD/MTU)	Decay Time (years)
1 (Regions I & II)	104	40,000	t
2 (Region I)	53	14,400	t
3 (Region II)	53	35,000	t+1.5
4 (Region II)	161	35,000	t+3
5 (Region III)	649	35,000	t+9
6 (Regions I & II)	340 (empty cells)	NA	NA
7 (Region III)	108 (empty cells)	NA	NA
8 (Edge of the pool)	NA <sup>(a)</sup>	NA	NA

<sup>(a)</sup> NA = Not applicable

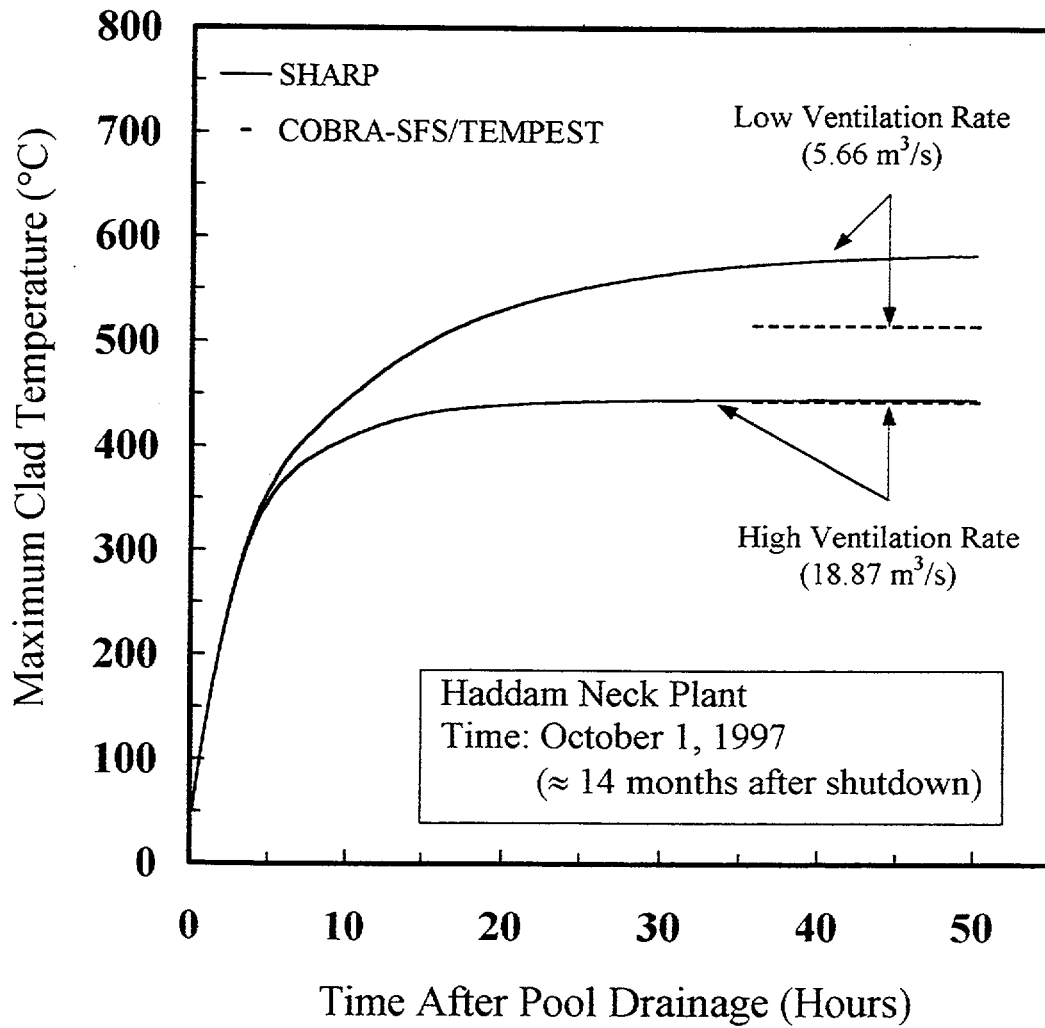


Figure 5.1 Comparison of SHARP code predictions with the steady state results of COBRA-SFS/ TEMPEST code for maximum clad temperature in the Haddam Neck spent fuel

## 5. Overview of SHARP Code

The COBRA-SFS model predicts the peak cladding temperature in the Region II racks that do not contain the fuel with the highest decay heat load. The SHARP code predicts the peak cladding temperature in the Region I racks that contain the fuel with the highest decay heat. One main reason for this difference in the location of peak cladding temperature is due to COBRA-SFS modeling of lateral holes in the bottom of the cell walls of the Region I racks, and heat

transfer between adjacent cells, which are not modeled in the SHARP code.

It should be noted that the capability of the SHARP code to address the local heatup characteristics of spent fuel assemblies has been tested here in an absolute prediction mode, without the benefit of any adjustable empirical input parameter.

## 6. RESULTS

In a typical spent fuel pool, there are a large number of parallel channels that include: the spent fuel assemblies, the downcomer next to the edge of pool; and empty slots (if any). However, there are groups of channels with identical decay heat and geometries. For each representative channel  $n$ , it is assumed that there are  $y_n$  identical channels. It is also assumed that each channel, in the set of representative channels of  $n$ , behaves identically. For the present drained pool heatup calculations, a total of four representative channels was assumed. Three channels were assumed

to represent the spent fuel assemblies with different decay heat and one channel to represent the allowance space between the racks and the edge of the pool (downcomer). The fuel loading assumptions used in the calculations are shown in Table 6.1. In order to envelope end of life shutdowns, this analysis assumed that the pools are full. The decay power values used in the calculations were obtained internally by the SHARP code based on the burnup and decay time of fuels in each representative channel.

**Table 6.1 Fuel Loading Assumptions Used in the Analysis**

Section of Pool (representative channel)	Number of Cells (Assemblies)		Burnup (MWD/MTU)	Decay Time
	Full Pool	20% storage capacity remaining		
<u>PWR</u>				
1	193 (1 full core)	193	60,000	t
2	634	634	60,000	t+1 yr.
3	633	341	60,000	t+2 yrs
4 (edge of the pool)	NA	NA	NA	NA
5 <sup>(b)</sup>	NA	292 (empty cells)	—	—
<u>BWR</u>				
1	764 (1 full core)	764	60,000	t
2	1268	1268	60,000	t+1 yr.
3	1268	608	60,000	t+2 yrs.
4 (edge of the pool)	NA	NA	NA	NA
5 <sup>(b)</sup>	—	660 (empty cells)	—	—

NA = Not Applicable

(b) Used only for the case of partial filling of the cells

## 6. Results

As discussed in Section 3, the extent of heat removal from the spent fuel building atmosphere strongly affects the heatup characteristics of the exposed spent fuel rods. Removal of heat from the spent fuel storage building under normal operation is accomplished by a forced ventilation system. In the absence of a powerful air ventilation system or a building design that promotes natural ventilation from the outside, such as from a chimney effect, the building will pressurize until failure and result in subsequent leakage of air to the outside atmosphere.

In the previous SHARP code calculations<sup>35,36</sup> using representative design parameters and fuel loading assumptions, it was assumed that ventilation provided through a powerful forced air system or through a chimney effect was sufficient to keep the room air at ambient conditions. The present representative calculations have been performed using a prescribed steady ventilation rate. An atmospheric air temperature of 30°C was assumed in the calculations.

In the present calculations, the building was assumed to be capable of withstanding an internal gauge pressure of only 0.2 psi before any leakage occurs, and then was assumed to leak at a rate required in order to keep the pressure from exceeding 0.2 psig. All leakage was assumed to occur from inside to the outside.

The typical results of the maximum temperature in the pool as a function of time after pool drainage for various room ventilation rates are presented in Figure 6.1. The calculations in this figure correspond to a PWR spent fuel pool at seven years after reactor shutdown. As shown in Figure 6.1, the time to reach steady state increases when the ventilation rate decreases. The results of building temperature predicted by SHARP code are presented in Figure 6.2. As expected, the building temperature decreases as the air flow rate through the building increases.

The results of representative PWR spent fuel heatup calculations are also presented in Figure 6.3, which depicts the maximum steady-state clad temperatures as a function of decay time of the most recently discharged

elements (time after reactor shutdown). Also shown in Figure 6.3 is the sensitivity of the results to the building ventilation rate. As expected, the maximum clad temperature increases as the ventilation rate decreases.

Calculations were also performed to study the sensitivity of the results to baseplate hole size, and to the downcomer space at the edge of the pool. As shown in Figure 6.4, the baseplate hole size can have a significant effect on the heatup of the spent fuel, since a small baseplate hole tends to constrict the flow at the inlet to the fuel assembly (see also Section 4.2). It should be noted that calculations were also performed with a 6" baseplate hole size. The heatup results for a 6" baseplate hole size were very close to the results for a 5" baseplate hole size.

As illustrated in Figure 6.5, the size of downcomer allowance space at the edge of the pool can also have a significant effect on the peak clad temperature. Large space at the edge of the pool leads to lower pressure drop across the cells with the subsequent result of higher flow through the assemblies and lower peak clad temperature. The result of calculations with 10" space at the edge of the pool were found to be almost identical to the results for 8" allowance space.

The effect of burnup on heatup of PWR spent fuel is illustrated in Figure 6.6. As expected, the peak clad temperature increases with the increase of fuel burnup.

In order to evaluate the impact of the partial filling of racks/cells on heatup characteristics, calculations were also performed assuming 20% of pool storage capacity remaining. The fuel loading assumptions used in these calculations are presented in Table 6.1. As shown in Figure 6.7, the peak clad temperature decreases with the presence of empty racks in the pool.

Similar results were obtained for BWR spent fuel assemblies, and they are presented in Figures 6.8-6.14. The heatup for BWR spent fuel tends to be lower than for PWR spent fuel, primarily due to the lower heat output per unit storage area.

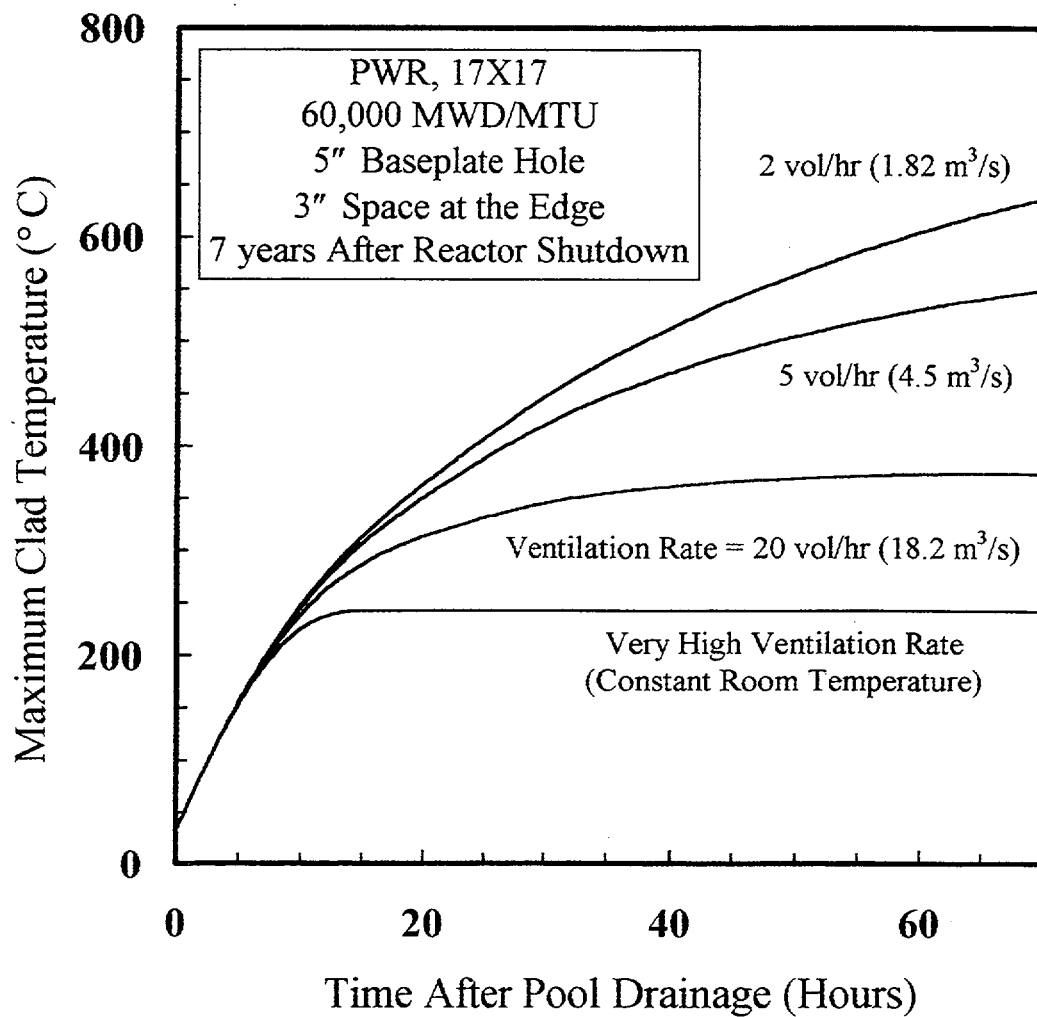


Figure 6.1 Maximum clad temperature versus time after pool drainage for PWR spent fuel

6. Results

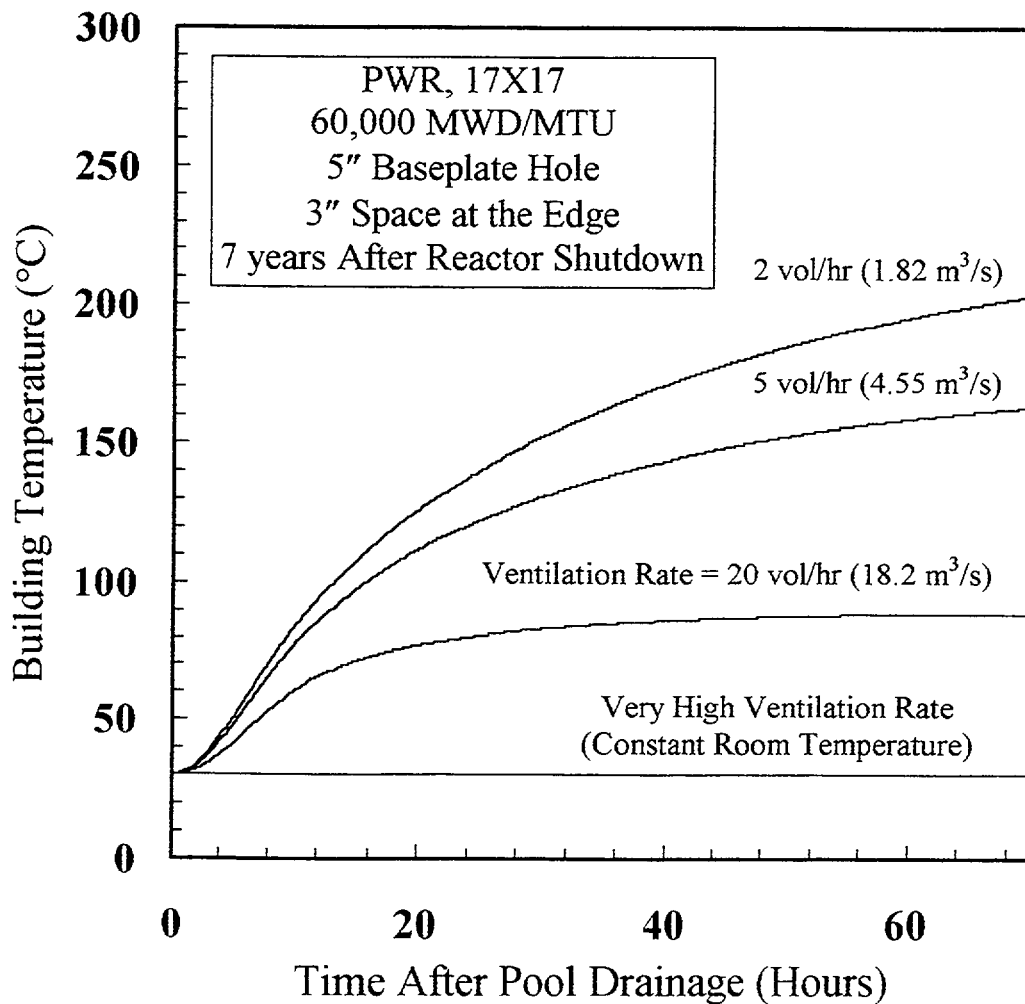


Figure 6.2 Building temperature versus time after pool drainage for PWR spent fuel

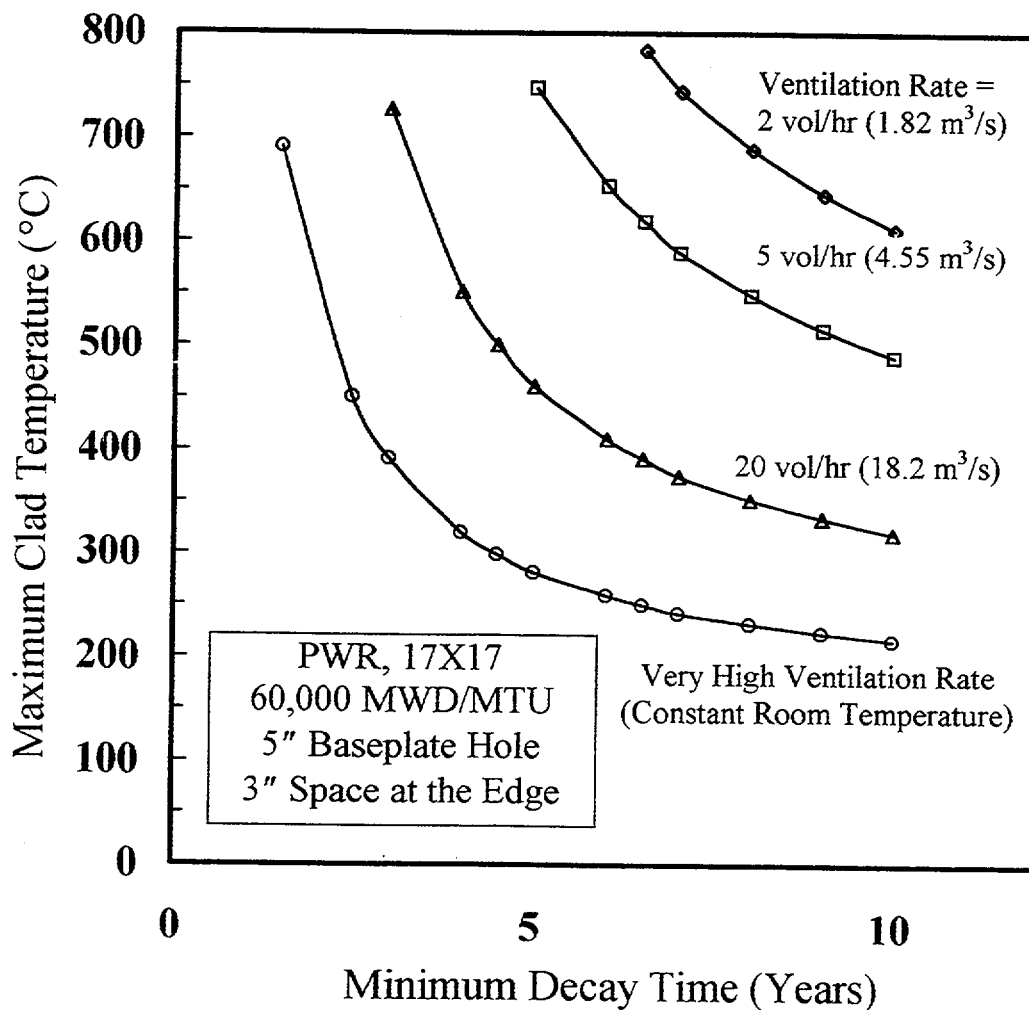


Figure 6.3 Effect of building ventilation rate on heatup of PWR spent fuel

6. Results

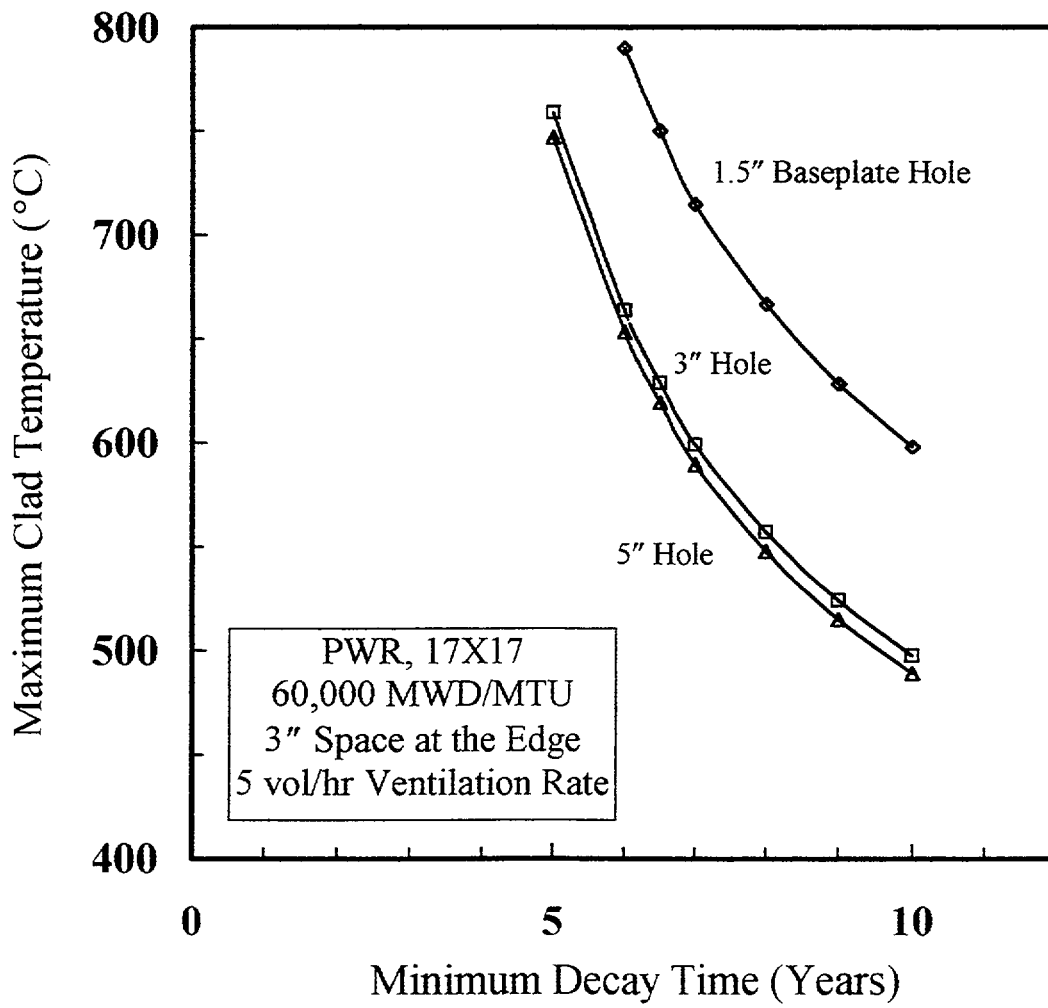


Figure 6.4 Effect of baseplate hole size on heatup of PWR spent fuel

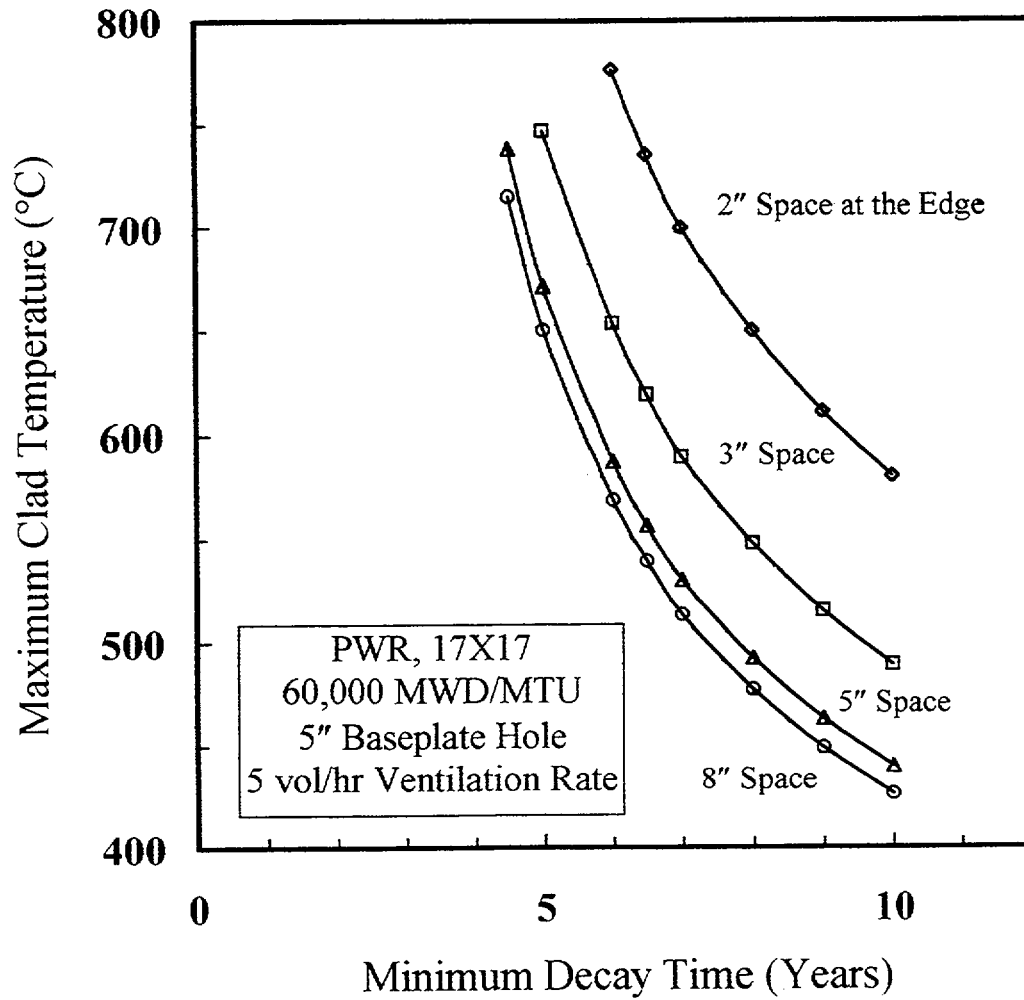


Figure 6.5 Effect of downcomer space at the edge of pool on heatup of PWR spent fuel

6. Results

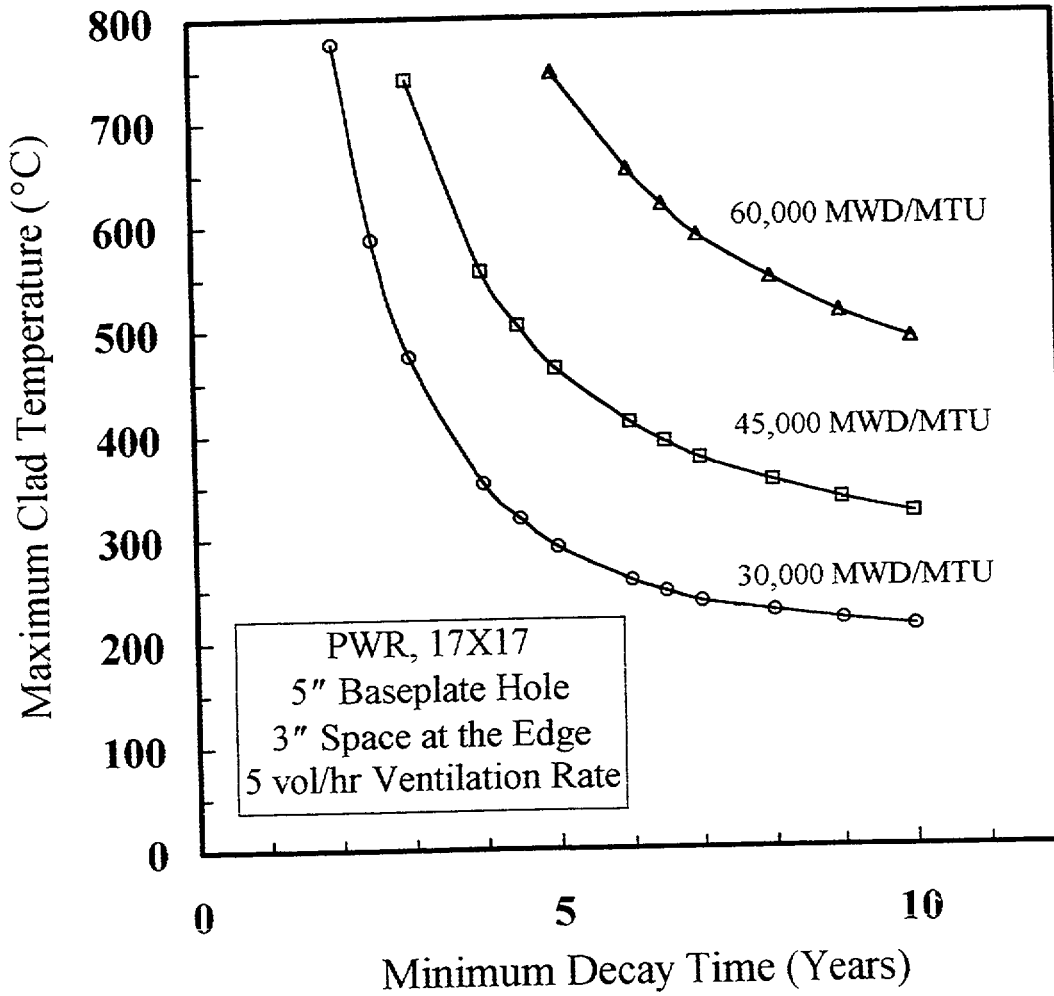


Figure 6.6 Effect of burnup on heatup of PWR spent fuel

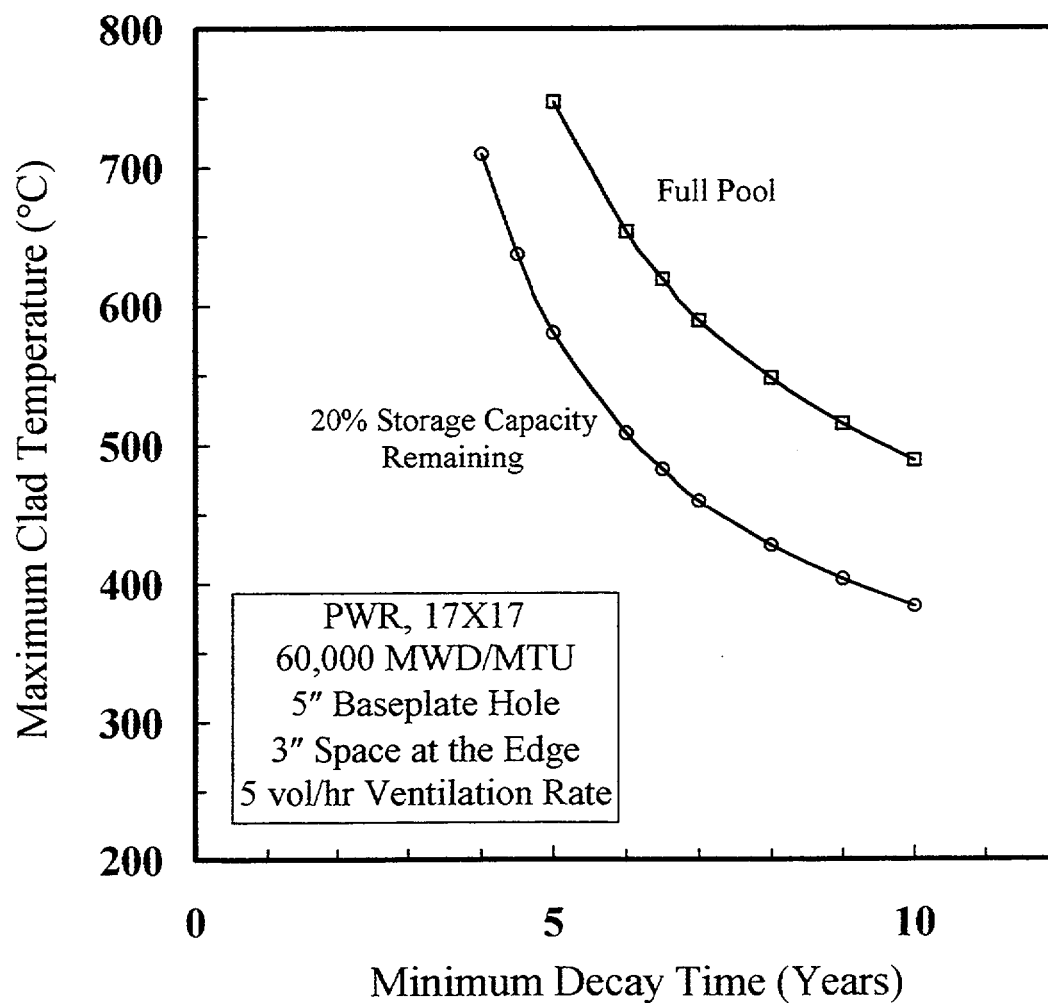


Figure 6.7 Effect of pool inventory on heatup of PWR spent fuel

6. Results

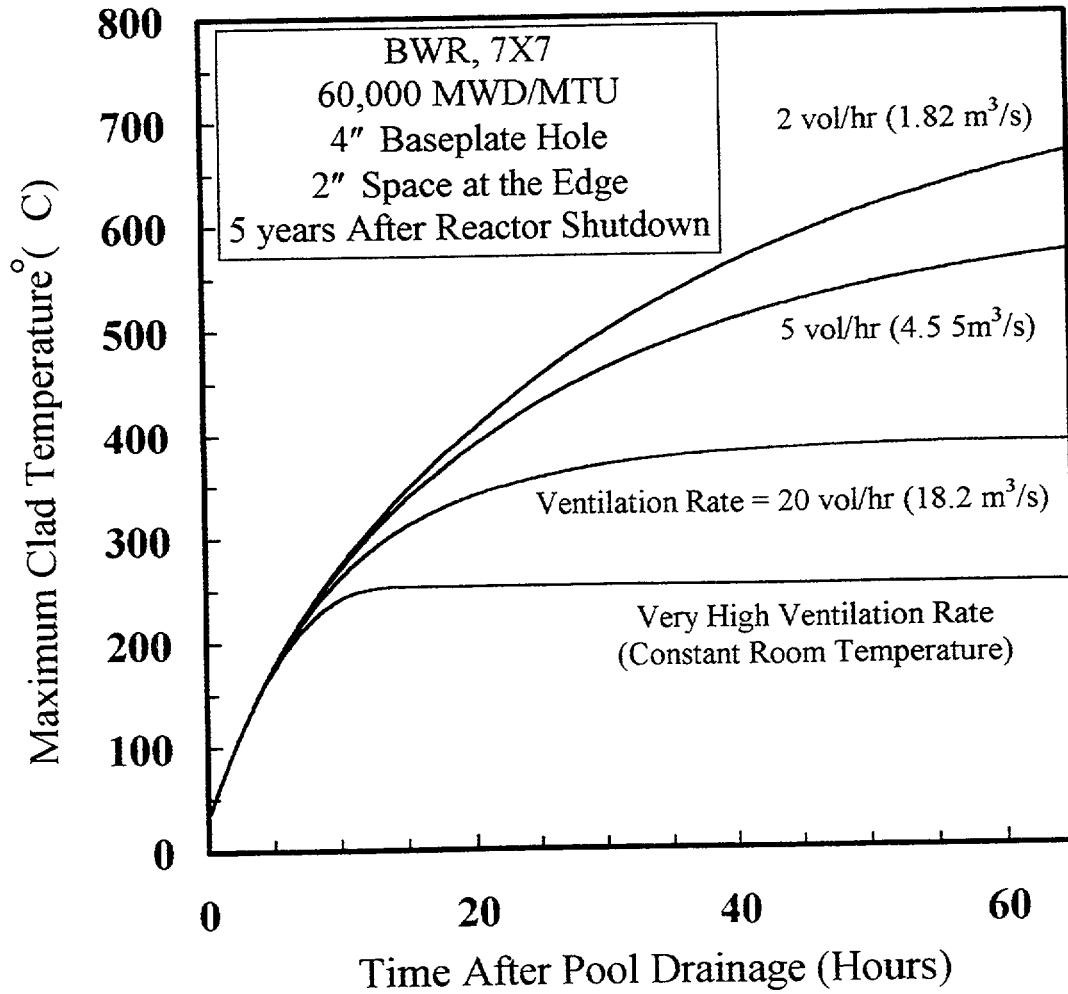


Figure 6.8 Maximum clad temperature versus time after pool drainage for BWR spent fuel

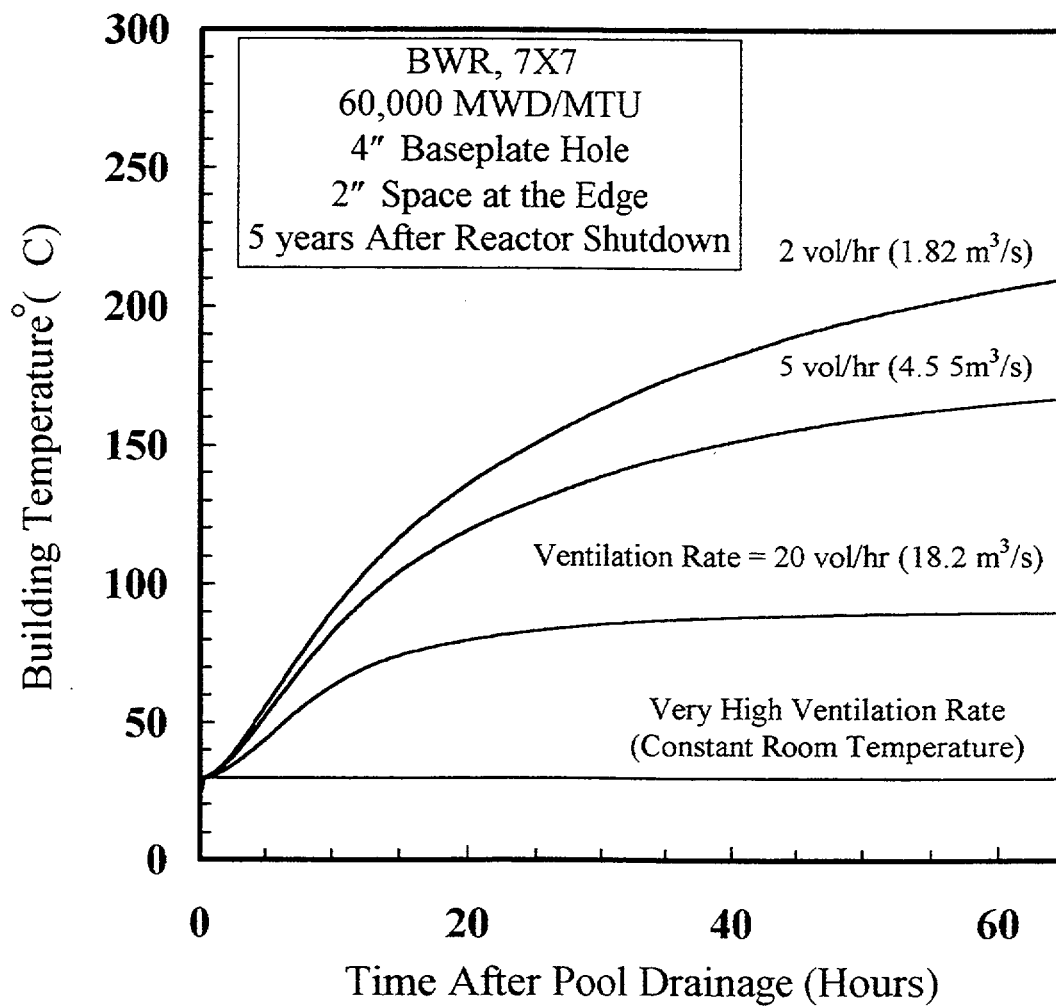


Figure 6.9 Building temperature versus time after pool drainage for BWR spent fuel

6. Results

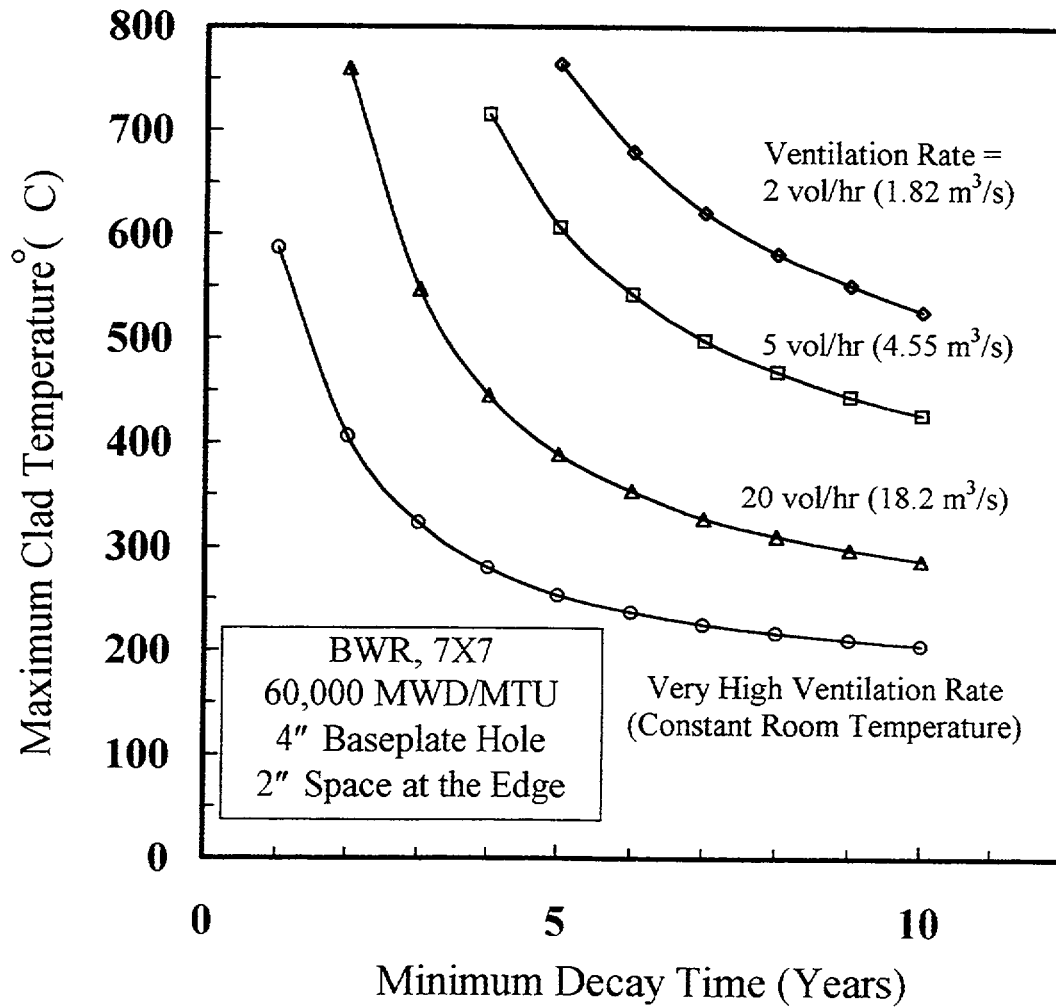


Figure 6.10 Effect of building ventilation rate on heatup of BWR spent fuel

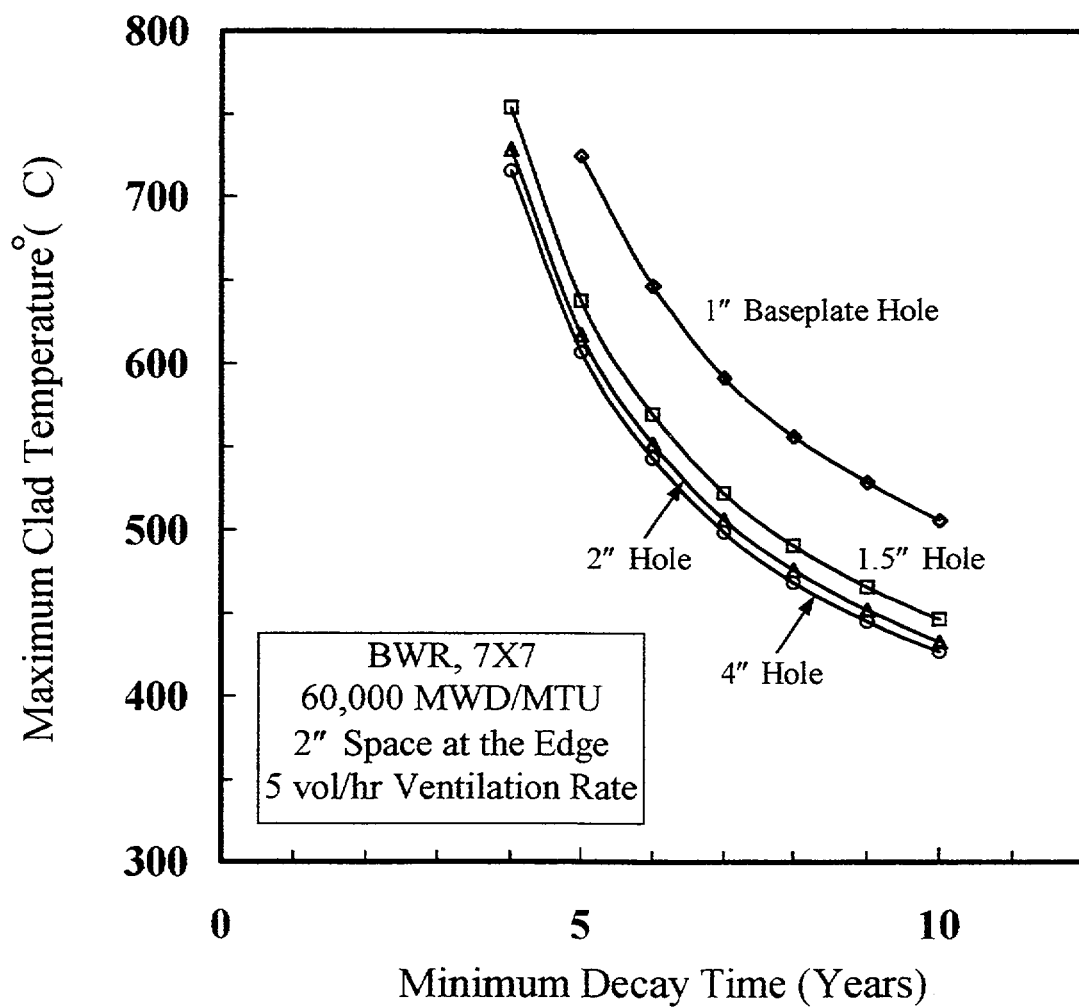


Figure 6.11 Effect of baseplate hole size on heatup of BWR spent fuel

6. Results

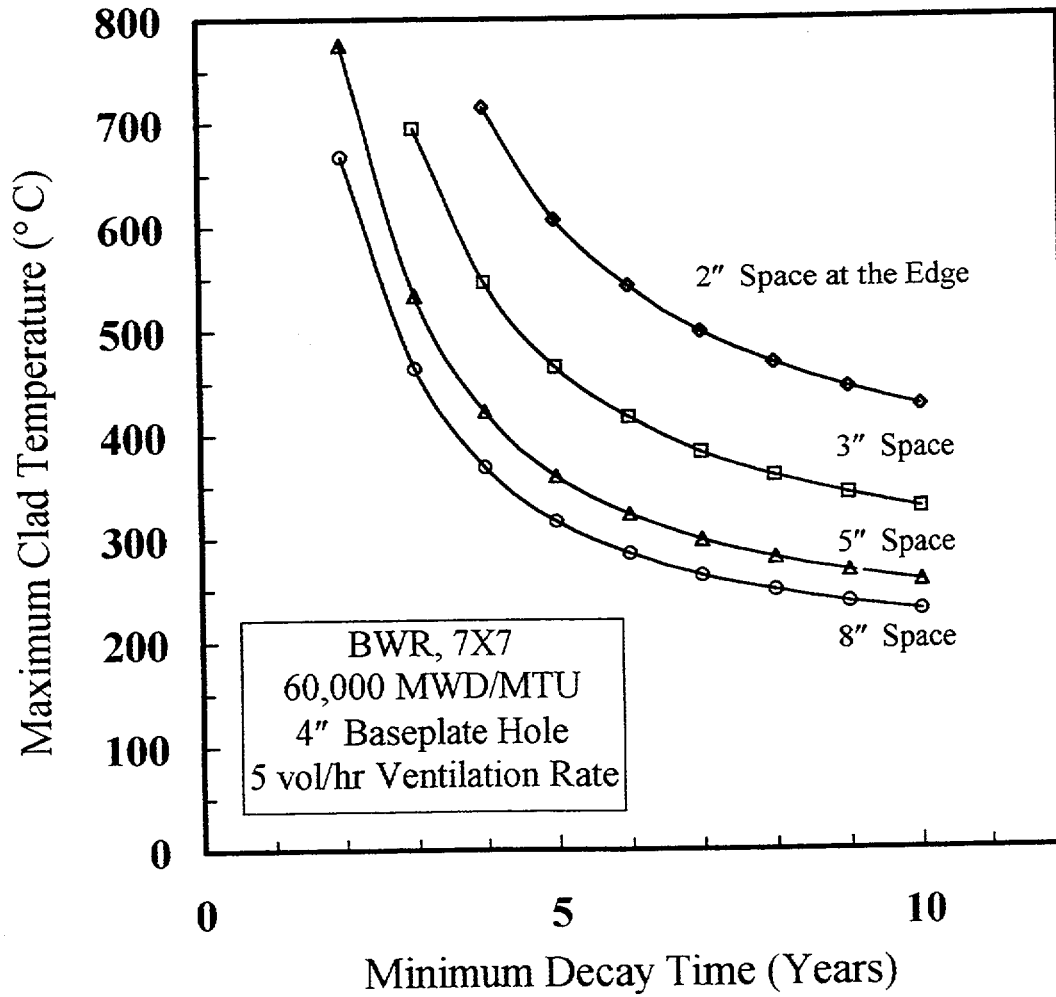


Figure 6.12 Effect of downcomer space at the edge of pool on heatup of BWR spent fuel

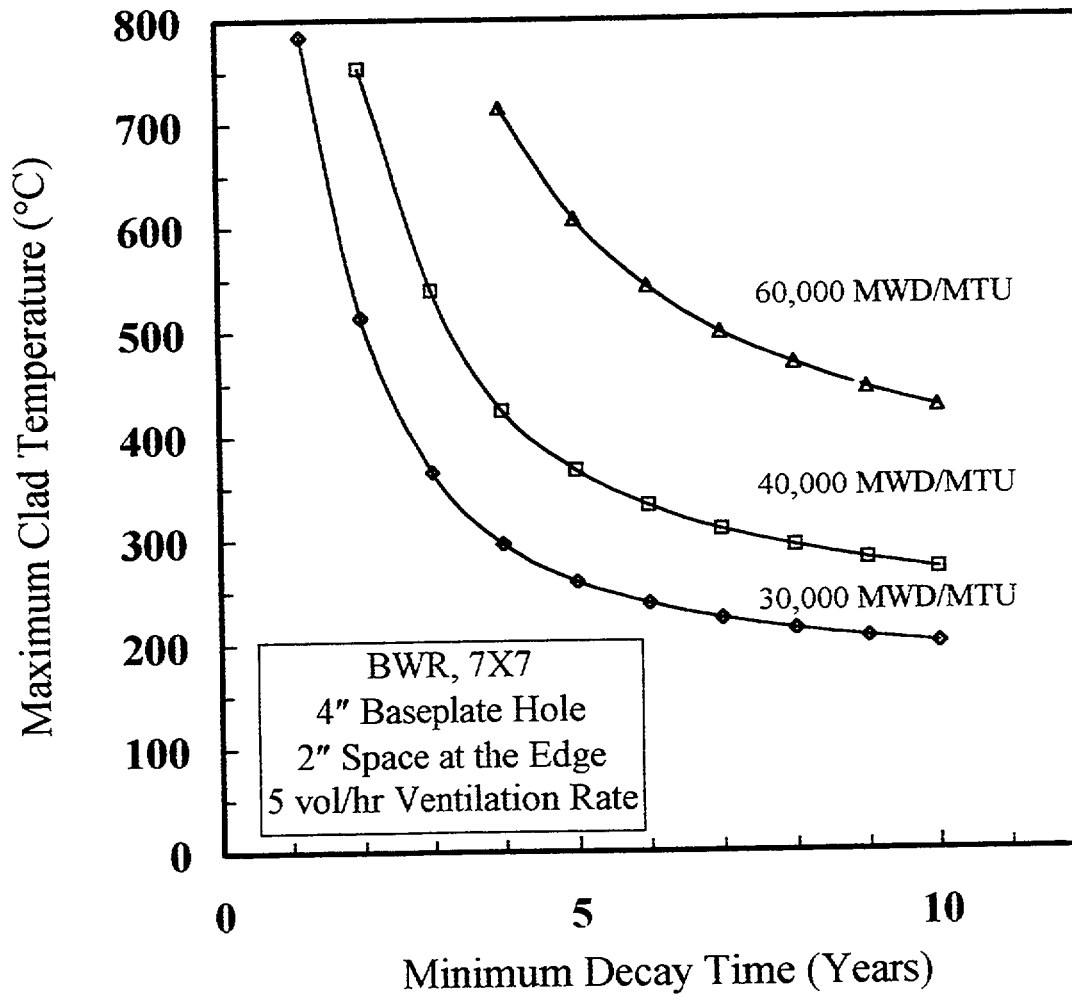


Figure 6.13 Effect of burnup on heatup of BWR spent fuel

6. Results

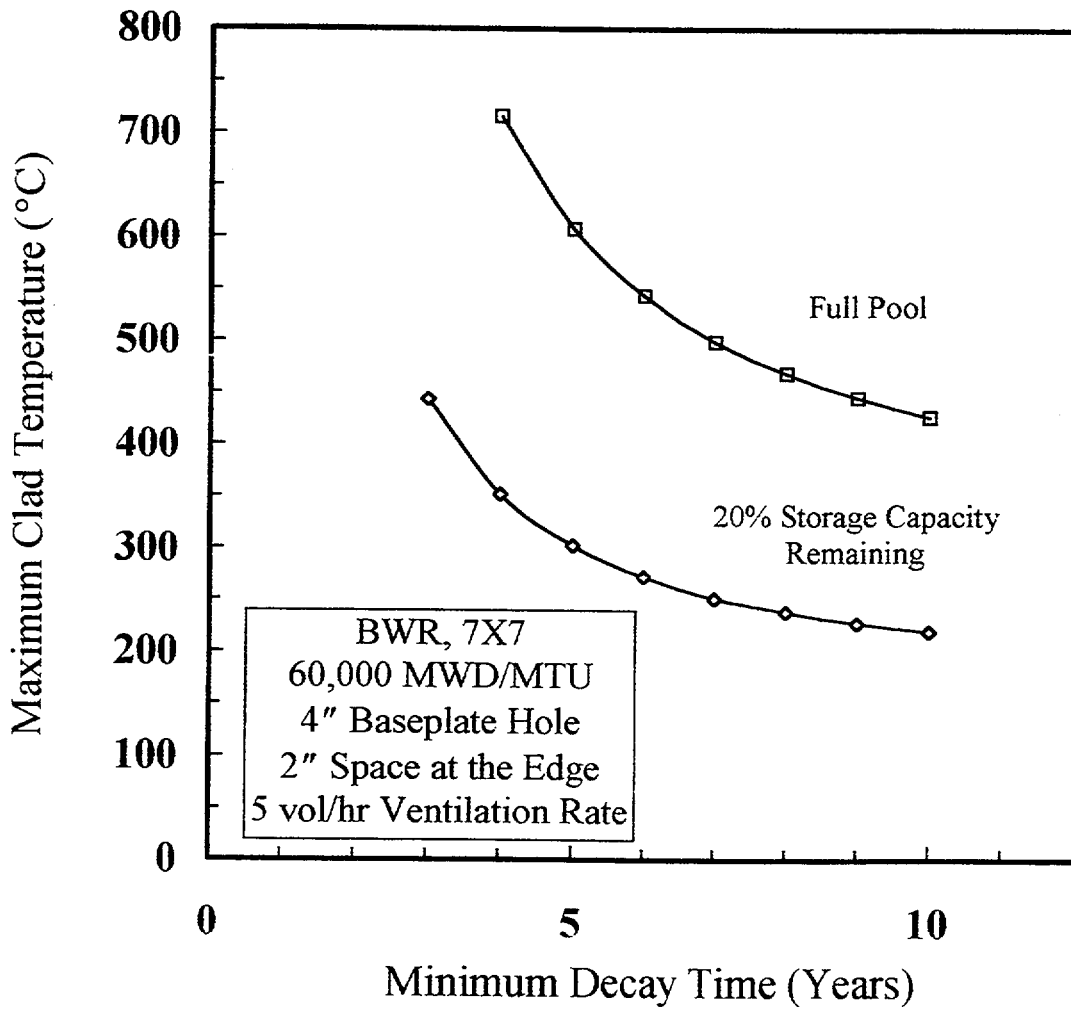


Figure 6.14 Effect of pool inventory on heatup of BWR spent fuel

## 7. SUMMARY AND CONCLUSIONS

A methodology for predicting spent fuel heatup in the event of loss of water during storage has been formulated and implemented in a computer code called SHARP, (Spent-fuel Heatup: Analytical Response Program).

The drained spent fuel pool has been modeled as a vertical, parallel array of channels connected only at the base region beneath the racks and the large open volume above the spent fuel pool. The conservation equations are written to allow for downflow as well as upflow within the array of channels that include the spent fuel assemblies, the downcomer next to the edge of the pool, and empty slots (if any). The one dimensional conservation equations for buoyancy-driven air flows are solved numerically by using the subdomain method (control volume formulation) to discretize the equations. The heatup of the spent fuel elements is calculated by solution of the transient heat conduction equation in the axial direction. The boundary conditions are obtained from the thermal hydraulic analysis within the base region beneath the racks, and within the spent fuel storage building. The hydrodynamic components of the boundary conditions are the zero net mass flow rate, the spent fuel storage building pressure, and the pressure gradient at the lower base region. In the present analysis, a fully mixed (i.e., isothermal and isobaric) base region was assumed. This is specifically the case if the flow Reynolds numbers are low and the base region

equivalent diameter is large (i.e., large spacing at the bottom of the pool). The approximation of a fully mixed base region obviates the need for a multi-dimensional calculation of the temperature and pressure field in the base region. With the assumption of negligible pressure variation in the base region, the pressure drops across all channels become equal. It should be noted that for the situations with low spacing at the bottom of the pool, the SHARP code can also be applied to a certain region of the pool where the assumption of negligible pressure variation in the base region is more appropriate.

As part of the present effort, a systematic study of the channel pressure drop/flow rate behavior (hydraulic characteristics) was performed to provide the physical basis essential to understanding and analyzing this complex system behavior.

An analysis of spent fuel heatup, using representative design parameters and fuel loading assumptions has been performed. Sensitivity calculations were also performed to study the effect of fuel burnup, building ventilation rate, baseplate hole size, partial filling of the racks and the size of the space at the edge of the pool. The spent fuel heatup was found to be strongly affected by the total decay heat production in the pool, building ventilation rate, and the availability of open spaces for air flows.

## 8. REFERENCES

1. Smith, R.I., et al., "Technology, Safety and Costs of Decommissioning a Reference Pressurized Water Reactor Power Station," NUREG/CR-0130, June 1978.
2. Oak, H.D., et al., "Technology, Safety and Costs of Decommissioning a Reference Boiling Water Reactor Power Station," NUREG/CR-0672, June 1980.
3. Benjamin, A.S., et al., "Spent Fuel Heatup Following Loss of Water During Storage," NUREG/CR-0649, March 1979.
4. Pisano, N.A., et al., "The Potential for Propagation of a Self-Sustaining Zirconium Oxidation Following Loss of Water in a Spent Fuel Storage Pool," Draft Report, 1984.
5. U.S. Nuclear Regulatory Commission, "An Integrated Structure and Scaling Methodology for Severe Accident Technical Issue Resolution," NUREG/CR-5809, Draft for Public Comment, November 1991.
6. Throm, E.D., "Regulatory Analysis for the Resolution of Generic Issue 82: Beyond Design Basis Accidents in Spent Fuel Pools," NUREG-1353, April 1989.
7. Spier, E.M., et al., "Westinghouse High-Density Spent Fuel Rack Design," Transactions of the American Nuclear Society, June 1977.
8. Nourbakhsh, H.P., "Realistic Simulation of Spent Fuel Heatup Following Loss of Water During Storage—Modeling Requirements and Existing Code Capabilities," BNL Technical Report, May 1994.
9. Sailor, V.L., et al., "Severe Accidents in Spent Fuel Pools in Support of Generic Safety Issue 82," NUREG/CR-4982, July 1987.
10. Shaw, R.A., et al., "Development of a Phenomena Identification and Ranking Table (PIRT) for Thermal Hydraulic Phenomena During a PWR Large-Break LOCA," NUREG/CR-5047, November 1988.
11. Theofanous, T.G., "Dealing with Phenomenological Uncertainties in Severe Accident Assessments and Probabilistic Risk Analysis," Proc. of the Third Intl. Topical Meeting of Nuclear Power Plant Thermal Hydraulics and Operation, Seoul, Korea, November 1988.
12. Ostrach, S., "Comments on Phenomenology and Modeling in NUREG-1150" in NUREG/CR-5113, UCID-21346, May 1988.
13. Hayes, E.T., and A.H. Roberson, "Some Effects of Heating Zirconium in Air, Oxygen, and Nitrogen," T. Electrochem. Soc. 96, 142, 1949.
14. Leistikow, S., et al., "Study in High Temperature Steam Oxidation of Zircaloy-4 Cladding Tubes," Nuclear Safety Project Second Semiannual Report, 1975, KFK-2262, Karlsruhe, 233, 1976.
15. White, T.H., reported in AEC Fuels and Materials Development Program, Progress Report No. 67, GEMP-67, General Electric Co., 151, 1967.
16. Patankar, S.V., *Numerical Heat Transfers and Fluid Flow*, Hemisphere Publishing Corporation, 1980.
17. Todreas, N.E. and M.S. Kazimi, *Nuclear Systems II Elements of Thermal Hydraulic Design*, Hemisphere Publishing Corporation, 1990.

## 8. References

18. Gerald, C.F., and P.O. Wheatly, *Applied Numerical Analysis*, Addison-Wesley Publishing Company, Inc., 4th ed., 1989.
19. Goodman, T.R., "Application of Integral Methods to Transient Non-linear Heat Transfer in *Advances in Heat Transfer*, Edited by T.F. Irvine, Jr. and J.P. Hartnett, Vol. 1, pp. 51-122, Academic Press, 1964.
20. Rehme, K., "Laminarstromung in Stabbundden," *Chem. Ingerieur Technik*, 43:17, 1971.
21. Rehme, K. "Simple Method of Predicting Friction Factors of Turbulent Flow in Non-Circular Channels," *Intl. J. Heat Mass Transfer*, 16:933, 1973.
22. Cheng, S.K., and N.E. Todreas, "Hydrodynamic Models and Correlations for Wire-Wrapped LMFBR Bundles and Subchannel Friction Factors and Mixing Parameters," *Nucl. Eng. Design*, 92:227, 1985.
23. Todreas, N.E. and M.S. Kazimi, *Nuclear Systems I: Thermal Hydraulics Fundamentals*, Hemisphere Publishing Corporation, 1990.
24. Rehme, K., "Pressure Drop Correlations for Fuel Elements Spacers," *Nucl. Technol.* 17:15, 1973.
25. Dittus, P.W., and L.M.K. Boelter, "Heat Transfer in Automobile Radiators of the Tubular Type," *University of California, Berkeley Pub. Eng.* 2:14, 443, 1930; reprinted in *Intl. Comm. Heat Mass Transfer*, 12, 3-22, 1985.
26. Presser, K.H., "Warmeubergang und Druckverlust and Reaktorbornelementen in From Langsdurchstromer Rundstabbundle," Jul-486-RB, KFA, Julich, 1967.
27. Office of Civilian Radioactive Waste Management, "Characteristics of Spent Fuel High-Level Waste, and Other Radioactive Wastes Which May Require Long-Term Isolation," DOE/RW-0184, U.S. Department of Energy, Washington, DC, December 1987.
28. Herman, O.W., C.V., Parks, and J.P. Renier, "Technical Support for Proposed Decay Heat Guide Using SAS2H/ORIGEN-S Data," NUREG/CR-5625, ORNL-6698, September 1994.
29. *American National Standard Programming Language FORTRAN*, ANSI X3.9-1978, ISO 1539-1980, American National Standard Institute, New York, NY, 1978.
30. Chato, J.C., "Natural Convection Flows in Parallel-Channel Systems," *Journal of Heat Transfer*, Vol. 85, pp. 339-345, November 1963.
31. PNNL, 1998, "Technical Evaluation of the Haddam Neck Spent Fuel Pool Analysis," TAC M99015; Docket No. 50-213.
32. Trent, D.S. and L.L. Eyler, "TEMPEST-A Computer Program for Three-Dimensional Time-Dependent Computational Fluid Dynamics, Volume 1: Theory and User's Manual, Version N, MOD34," PNL-4348, Pacific Northwest National Laboratory, Richland, WA, 1997.
33. Michener, T.E., D.R. Rector, J.M. Cuta, R.E. Dodge and C.W. Enderlin, "COBRA-SFS: A Thermal-Hydraulic Analysis Code for Spent Fuel Storage and Transportation Casks," PNL-10782, Pacific Northwest National Laboratory, Richland, WA, 1995.
34. Nourbakhsh, H.P., "SHARP Analysis of Haddam Neck Spent Fuel Heatup Following Loss of All Water in the Spent Fuel Pool," *Energy and Environmental Science, Inc.*, EESI-BNL-1, February 1999.

## 8. References

35. Nourbakhsh, H.P., G. Miao, and Z. Cheng, "Modeling of Spent Fuel Heatup Following Loss of Water in a Spent Fuel Pool," *Proceedings of the Sixth Intl. Conf. On Nucl. Eng. (ICONE-6)*, San Diego, CA, May 1998.
36. Nourbakhsh, H. P., G. Miao, and Z. Cheng, "Analysis of Spent Fuel Heatup Following Loss of Water in a Spent Fuel Pool: A User's Manual for the Computer Code SHARP," Draft Report for Comment, NUREG/CR-6441, BNL-NUREG-52494, May 1998.

**APPENDIX A**

**A USER'S MANUAL FOR THE SHARP COMPUTER CODE**

## A.1 Introduction

The Computer Code SHARP (Spent-fuel Heatup: Analytical Response Program), designed for use on a personal computer, has been developed for predicting spent fuel heatup in the event of loss of water during storage. The drained spent fuel pool is modeled as a vertical, parallel array of channels that include: the spent fuel assemblies, the downcomer next to the edge of the pool and empty slots (if any). The code allows analysis of the spent fuel heatup for a variety of storage practices including storing both PWR and BWR spent fuel assemblies in the same spent fuel pool during permanent shutdown. Depending on a user specified option the SHARP Code predicts:

- The transient spent fuel temperature following pool drainage; or
- The minimum decay time of the most recently discharged elements (time after reactor shutdown) so that the maximum clad temperature in the pool does not to exceed a certain value specified by the user.

This Appendix describes the code requirements, installation, input and output.

## A.2 Requirements

The SHARP Code runs on IBM-Compatible computers. Basic requirements are:

- DOS 3.0 or higher
- A Fortran compiler
- A monitor
- 640K of standard memory. Expanded or Extended memory is not required.
- A hard disk
- A math co-processor is recommended
- A printer (required only if printed output files are desired)

## A.3 Installation

The SHARP software is distributed on a single 1.44M, 3.5-inch diskette. The files contained on the diskette are the Fortran source code SHARP, FOR and the input data file INPUT.DAT. These files should be put together in a directory before generating the executable file SHARP.EXE.

## A.4 Input

The input for SHARP is somewhat similar to a name list. The following are the names of variables, their definition and units, together with some guidance for their specifications:

<b>ABORDER</b>	Cross-sectional area of the border channel (m <sup>2</sup> )
<b>AKCLAD</b>	Thermal conductivity of clad (W/m-K)
<b>AKCON</b>	Thermal conductivity of concrete (W/m-K)
<b>AKFRAME</b>	Thermal conductivity of holder walls (W/m-K)
<b>AKFUEL0</b>	Thermal conductivity of fuel (W/m-K)
<b>AKS</b>	Thermal conductivity of the storage building walls and ceilings (W/m-K)
<b>BURNUP(I)</b>	Fuel burnup for each representative channel, used for option 1 and 2 only (these burnup values are used internally by the SHARP code to calculate the decay power)
<b>CPCLAD</b>	Specific heat of clad (Joule/Kg-K)
<b>CPCON</b>	Specific heat of concrete (Joule/Kg-K)

Appendix A

<b>CPFRAME</b>	Specific heat of holder walls (J/Kg-K)	
<b>CPFUEL0</b>	Specific heat of fuel (J/Kg-K)	
<b>CPITCH</b>	Cell center-to-center pitch (m) (See Figure A.1)	
<b>CPS</b>	Specific heat of the storage building walls and ceilings (J/Kg-K)	
<b>DFUEL</b>	Fuel rod outside diameter (m)	
<b>DT</b>	Computational time step(sec)	
<b>ENDTIME</b>	Computation ending time used for options 1 and 3 only (It should be noted that the calculations may be terminated earlier if steady state conditions be reached)	
<b>EPS</b>	Relative plugging of flow area by spacer grids (refer to Section 4.8 of the report)	
<b>ICTYPE(I)</b>	Type of cell or assembly for each representative channel (This variable is used for identification of the various designs of fuel assemblies or cells present in the pool)	
<b>IOPTION</b>	Option for various calculations performed by the code:	
<b>IOPTION = 1:</b>	SHARP Code predicts the transient spent fuel temperature following drainage. The decay power values used in the calculations are obtained internally based on the burnup and decay time of each representative channel.	
<b>IOPTION = 2:</b>	SHARP Code predicts the minimum decay time of the most recently discharged elements (time after shutdown) that the maximum clad temperature in the pool not to exceed	
		a certain value ( $T_{given}$ ) specified by the user. The decay power values used in the calculation are obtained internally. For this option, the code internally calculates the maximum steady state temperatures using a large time step for integration. This option was originally incorporated in the code for spent fuel analysis under a very high ventilation rate. However, for low ventilation rates the internal steady state calculations may not be stable for this option. Therefore, it is recommended that for low ventilation cases, the minimum decay time be obtained by a few code calculations, using options 1 or 3 .
		<b>IOPTION = 3:</b> This option is similar to $ioption = 1$ except that the decay power for each representative channel is specified by the user.
		<b>IPRINT</b> Number of time steps between printouts
		<b>IRTYPE</b> Reactor type IRTYPE=1: PWR IRTYPE=2: BWR
		<b>NACTIVE</b> Number of active fuel rods in each cell
		<b>NATYPE</b> Number of cell or assembly types in the pool
		<b>NTOTAL</b> Total number of rods in each cell
		<b>NR</b> Spent fuel array parameter
		<b>NCHANNEL</b> Number of representative channel
		<b>NSG</b> Number of spacer grids in each assembly

<b>NUMBER(I)</b>	Number of cells in each representative channel	<b>SURFS</b>	Total surface area of the storage building walls and ceilings (m <sup>2</sup> )
<b>NTYPE(I)</b>	Type of representative channel 0: border channel 1: fuel assemblies 2: empty slots	<b>TA</b>	Outside air temperature
<b>PACC</b>	Convergence criterion for pressure iteration	<b>TGIVEN</b>	The maximum allowable clad temperature (°C), used for option 2 only
<b>PFAIL</b>	Failure pressure of the building (Kg m <sup>-1</sup> sec <sup>-2</sup> )	<b>THCLAD</b>	Clad thickness
<b>PITCH</b>	Rod center-to-center pitch (m) (See Figure A.1)	<b>THCON</b>	Thickness of the pool concrete encasement (m)
<b>P0(I)</b>	Decay power for each representative channel (KW/MTU) used for option 3 only	<b>THICKS</b>	Average thickness of the storage walls and ceilings (m)
<b>RHOCLAD</b>	Density of clad (Kg/m <sup>3</sup> )	<b>TINI</b>	Initial temperature of the pool
<b>RHOCON</b>	Density of concrete (Kg/m <sup>3</sup> )	<b>UL</b>	Length of inactive part of fuel rod (m)
<b>RHOFRAME</b>	Density of holder wall (Kg/m <sup>3</sup> )	<b>VENT</b>	Volume exchange rate for the storage building ventilation system (m <sup>3</sup> /sec)
<b>RHOFUEL</b>	Density of fuel (Kg/m <sup>3</sup> )	<b>VOLLOW</b>	Volume of the base region beneath the racks (m <sup>3</sup> )
<b>RHOS</b>	Density of storage building walls and ceilings (Kg/m <sup>3</sup> )	<b>VOLS</b>	Volume of the storage building (m <sup>3</sup> )
<b>SBORDER</b>	Width of downcomer next to the edge of the pool (m) (see Figure A.1)	<b>XACCO</b>	Convergence criterion for velocity iteration
<b>SHOLE</b>	Diameter of baseplate hole (m)	<b>YEAR</b>	The time after reactor shutdown (yr), used for option 1 only
<b>SINNER</b>	Cell dimension (m) (see Figure A.1)	<b>YRO(I)</b>	Decay time for each representative channel at the time of permanent shutdown of the plant (yr), used for option 1 and 2 only.
<b>SL</b>	Length of active part of fuel rod (m)		
<b>SMTU</b>	Metric tons Uranium per assembly (MTU)		
<b>SSP(I)</b>	Positions of grid spacers (m)		
<b>STHICK</b>	Thickness of the holder wall (m)		
<b>SURFCON</b>	Total surface area of the base region walls and floor (m <sup>2</sup> )		

A sample input listing is shown in Table A.1. This particular case corresponds to a representative calculation for PWR spent fuel discussed in the result section of the present report (refer to Section 6).

The first three lines of input are reserved for the title of the calculation. This is followed by the specification of

## Appendix A

the calculation option. For example the calculation option of one is used in the sample input (IOPTION=1). For this option, the SHARP code predicts the transient spent fuel temperature following the pool drainage. Also the decay power values used in the calculations are obtained internally, based on the burnup and decay time of each representative channel.

The value for the maximum allowable clad temperature (TGIVEN) is only used internally in the code when the input option of 2 (IOPTION=2) is utilized. However, in order to have a unified input format for all code calculation options, this temperature is specified for other options.

The building is assumed to be capable of withstanding a specified internal pressure (PFAIL) before any leakage occurs, and then is assumed to leak at a rate (calculated internally) required in order to keep the pressure from exceeding this failure pressure. All leakage is assumed to occur from inside to outside.

An integration time step of 60 sec (DT=60) is used in the sample input. This value for the time step was found to be adequate for all the calculations reported in Section 6 of this report. However, it is recommended that sensitivity calculations be performed to assure that the code results are independent of the input time step.

The solution procedure used in the SHARP code involves iteration techniques to obtain both the pressure drop across the channels and the buoyancy induced air flows (refer to section 4.2.2 of the present report). Many iteration parameters are used in the internal calculations. All calculations presented in Section 6 were performed without changing any iteration parameter. However, under certain conditions, such as local heatup calculations, there may be a need for changing convergence criteria. Therefore, in the current version of the code, two iteration parameters, PACC (used in the pressure drop iteration), and XACC0 (used in the velocity iteration) are specified as input parameters to SHARP code.

The input format to the SHARP code is designed such that the characteristics of the modeled representative channels can be easily specified in a tabular fashion. As shown in the sample input, for each representative channel, I (identified in column 1), its type (NTYPE0), number of cells (NUMBER), decay time at the time of permanent shutdown (YR0), burnup (BURNUP), and its type of cell or assembly (ICTYPE) are specified in columns 2 through 7 respectively.

After specifying the number of cell or assembly types in the pool (NATYPE), the design specification and the physical properties associated with each particular cell or assembly type are then specified. For the sample input presented in Table A.1, only one type cell was used. A sample of the input listing when different designs of spent fuel assemblies are stored in the same spent fuel pool is also provided in Table A.2. This input listing corresponds to the Haddam Neck spent fuel pool analysis used as a part of the SHARP code validation (refer to section 5 of the present report).

### A.5 Output

The code generates two output files: OUTPUT.OUT and OUTPUT.DAT.

A sample short-format output (OUTPUT.OUT) for Option=1 is shown in Table A.3. These results correspond to the input of Table A.1. For a better quality assurance the input data used by the code is echoed in the output.

OUTPUT.DAT file provides data (for options 1 and 3 only) on times and corresponding maximum temperatures for each channel following pool drainage to be used for plotting purposes.

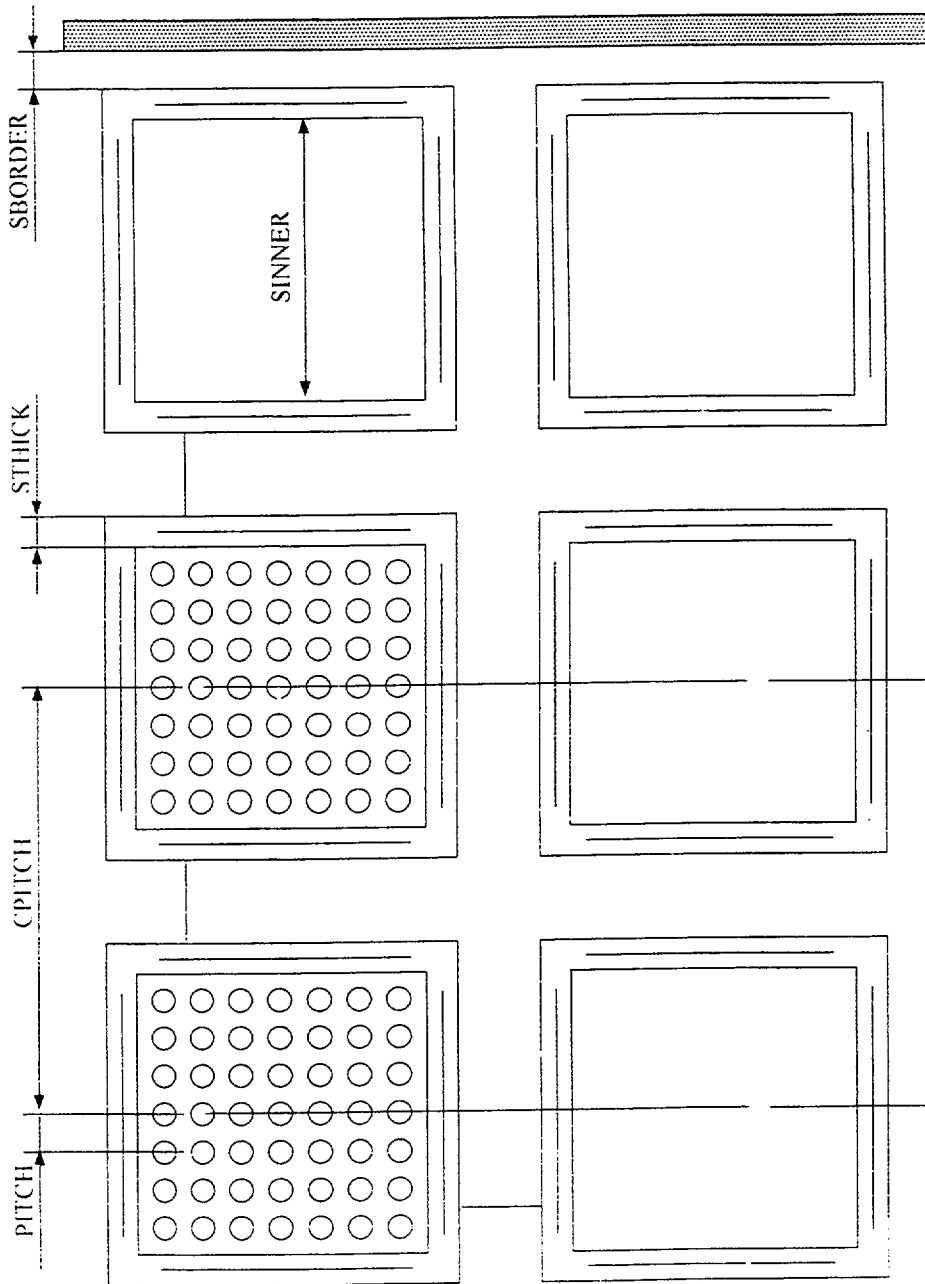


Figure A.1 Schematic of some geometric details for code input quantification

Appendix A

**Table A.1 Sample input listing using PWR representative design parameters**

```

=====
| PWR REPRESENTATIVE PARAMETERS: vent=20vol/hr,3"space,5"hole,OPTION 1 |
=====
ioption= 1
year= 6.
Tgiven= 565.
pfail= 1.027e5
Tini= 30.
Ta= 30.
vent= 18.2
dt= 60.
endtime= 14.4e4
Iprint= 120
Idata= 10
pacc= 1.e-5
xacc0= 0.00001
akcon= 1.2
akframe= 13.8
aks= 1.2
cpcon= 652.
cpframe= 460.
cps= 652.
rhocon= 2340.
rhoframe=7817.
rhos= 2340.
surfcon= 116.
surfs= 1100.
sborder= 0.0762
Aborder= 2.764
thcon= 3.0
thicks= 0.5
vollow= 14.5
vols= 3275.
sl= 3.6576
ul= 0.6096
nchannel=4


| I | P0(I) | Ntype(I) | Number(I) | Yr0(I) | Burnup(I) | Ictype(I) |
|---|-------|----------|-----------|--------|-----------|-----------|
| 1 | 14.4  | 1        | 193       | 0.     | 60.       | 1         |
| 2 | 8.31  | 1        | 634       | 1.     | 60.       | 1         |
| 3 | 5.72  | 1        | 633       | 2.     | 60.       | 1         |
| 4 | 0.0   | 0        | 1         | 0.     | 0.        | 1         |


natype= 1
----cell type 1-----
irtype= 1
nr= 17
ntotal= 289
nactive= 264
Dfuel= 0.0095
pitch= 0.0126
shole= 0.127
sinner= 0.22225
smtu= 0.461
cpitch= 0.2641
sthick= 0.0047
thclad= 5.842e-4
akfuel0= 5.77
cpfuel0= 240.67
rhofuel= 10970.
akclad= 13.

```

**Table A.1 Sample input listing using PWR representative design parameters (Cont'd)**

```
cpclad= 330.  
rho clad= 6500.  
esp= 0.25  
nsp= 8  
I spp(I)  
1 0.0  
2 0.52251  
3 1.04503  
4 1.56754  
5 2.09006  
6 2.61257  
7 3.13509  
8 3.6576
```

Appendix A

**Table A.2 Sample input listing for a case when different designs of assemblies are stored in the same spent fuel pool**

```

=====
| Haddam Neck Spent Fuel Pool Analysis,high vent,1.2years, OPTION 1 |
=====
ioption= 1
year= 1.19
Tgiven= 565.
pfail= 1.027e5
Tini= 31.
Ta= 31.
vent= 18.87
dt= 60.
endtime= 25.2e4
Iprint= 120
Idata= 10
pacc= 1.e-5
xacc0= 0.00001
akcon= 1.8
akframe= 19.
aks= 1.8
cpcon= 652.
cpframe= 502.
cps= 652.
rhocon= 2276.
rhoframe=8029.
rhos= 2276.
surfcon= 130.
surfs= 1081.
sborder= 0.13
Aborder= 3.872
thcon= 1.83
thicks= 0.2
vollow= 34.13
vols= 3271.
sl= 3.17
ul= 0.34
nchannel=8
I      P0(I)  Ntype(I)  Number(I)  Yr0(I)  Burnup(I)  Ictype(I)
1      0.0    1         104        0.       40.        1
2      0.0    1         53         0.       14.4       1
3      0.0    1         53         1.5      35.        1
4      0.0    1         161        3.       35.        1
5      0.0    1         649        9.       35.        2
6      0.0    2         340        0.       0.         1
7      0.0    2         108        0.       0.         2
8      0.0    0          1         0.       0.         1
natype= 2
----cell type 1-----
irtype= 1
nr= 15
ntotal= 225
nactive= 204
Dfuel= 0.0107
pitch= 0.0143
shole= 0.127
sinner= 0.22225
smtu= 0.411
cpitch= 0.227
sthistick= 0.00191
thclad= 6.17e-4

```

**Table A.2 Sample input listing for a case when different designs of assemblies are stored in the same spent fuel pool (Cont'd)**

```

akfuel0= 5.48
cpfuel0= 234.
rhofuel= 10410.
akclad= 15.
cpclad= 296.
rhoclad= 6554.
esp= 0.25
nsp= 8
I spp(I)
1 0.0
2 0.52251
3 1.04503
4 1.56754
5 2.09006
6 2.61257
7 3.13509
8 3.6576
----cell type 2-----
irtype= 1
nr= 15
ntotal= 225
nactive= 204
Dfuel= 0.0107
pitch= 0.0143
shole= 0.257
sinner= 0.2286
smtu= 0.411
cpitch= 0.27305
sthick= 0.00317
thclad= 4.19e-4
akfuel0= 5.48
cpfuel0= 234.
rhofuel= 10410.
akclad= 18.77
cpclad= 502.
rhoclad= 8029.
esp= 0.25
nsp= 8
I spp(I)
1 0.0
2 0.52251
3 1.04503
4 1.56754
5 2.09006
6 2.61257
7 3.13509
8 3.6576

```

Table A.3 Sample Short-Format Output For Option 1

```

*****
| PWR REPRESENTATIVE PARAMETERS: vent=20vol/hr,3"space,5"hole,OPTION 1 |
*****

```

```

-----
INPUT DATA

```

```

6.00 year(s) after reactor shutdown

```

```

-----
Failure pressure (pfail):                .103E+06 Pa
Initial temperature of the pool (Tini):  30.00    C
Outside air temperature (Ta):           30.00    C
Volume exchange rate for the storage
building ventilation system (vent):      .182E+02 m3/sec

```

```

-----control variable-----
Computational time step (dt):            60.00    sec
Computation ending time (endtime):      .144E+06 sec
Number of time steps between printouts
in output file OUTPUT.OUT (Iprint):    120
Number of time steps between printouts
in output file OUTPUT.DAT (Idata):     10

```

```

-----
Convergence criterion for pressure
iteration (pacc):                        .100E-04
Convergence criterion for velocity
iteration (xacc0):                       .100E-04

```

```

-----physical properties-----
Thermal conductivity of concrete (akcon): 1.20 W/m-K
Thermal conductivity of holder walls (akframe): 13.80 W/m-K
Thermal conductivity of the storage building
walls and ceiling (aks):                1.20 W/m-K
Specific heat of concrete (cpcon):       652.00 J/Kg-K
Specific heat of holder walls (cpframe): 460.00 J/Kg-K
Specific heat of the storage building walls
and ceiling (cps):                      652.00 J/Kg-K
Density of concrete (rhocon):            2340.00 Kg/m3
Density of holder walls (rhoframe):      7817.00 Kg/m3
Density of the storage building walls and
ceiling (rhos):                         2340.00 Kg/m3

```

Table A.3 Sample Short-Format Output For Option 1 (Cont'd)

-----configuration-----				
Total surface area of the base region walls and floor (surfcon):	116.00 m2			
Total surface area of the storage building walls and ceiling (surfs):	1100.00 m2			
Width of downcomer next to the edge of the pool (sborder):	.0762 m			
Cross-sectional area of the border channel (Aborder):	2.7640 m2			
Thickness of the pool concrete encasement (thcon):	3.0000 m			
Average thickness of the storage building ventilation system (thicks):	.5000 m			
vollume of the base region beneath the racks (vollow):	14.5000 m3			
vollume of the storage building (vols):	3275.0000 m3			
Length of active part of fuel rod (sl):	3.6576 m			
Length of inactive part of fuel rod (ul):	.6096 m			
-----				
Number of representative channel (nchannel):	4			
-----				
channel#	channel type	burnup	# of cells	cell type
	(Ntype)		(number)	(Ictype)
1	fuel assemblies	60.00	193	1
2	fuel assemblies	60.00	634	1
3	fuel assemblies	60.00	633	1
4	border channel	.00	1	0
-----				
Totally 1 cell type(s) in the pool.				
-----cell type 1-----				
Reactor type:	PWR			
Spent fuel array parameter (nr):	17			
Total number of rods in each cell (ntotal):	289			
Number of active fuel rods in each cell (nactive):	264			
Fuel rod outside diameter (dfuel):	.9500E-02 m			
Rod center-to-center pitch (pitch):	.1260E-01 m			
Diameter of baseplate hole (shole):	.1270E+00 m			
Cell dimension (sinner):	.2222E+00 m			
Metric tons Uranium per assembly (smtu):	.4610E+00 MTU			
Cell center-to-center pitch (cpitch):	.2641E+00 m			
Thickness of the holder wall (sthack):	.4700E-02 m			
Clad thickness (thclad):	.5842E-03 m			
Thermal conductivity of fuel (akfuel):	.5770E+01 W/m-K			
Specific heat of fuel (cpfuel):	.2407E+03 J/Kg-K			
Density of fuel (rhofuel):	.1097E+05 Kg/m3			
Thermal conductivity of clad (akclad):	.1300E+02 W/m-K			
Specific heat of clad (cpclad):	.3300E+03 J/Kg-K			
Density of clad (rhoclad):	.6500E+04 Kg/m3			
Relative plugging of the flow area by the spacer grid (eps):	.25			
Number of grid spacers (nsp):	8			
Spacer 1 position spp( 1):	.00			
Spacer 2 position spp( 2):	.52			
Spacer 3 position spp( 3):	1.05			
Spacer 4 position spp( 4):	1.57			
Spacer 5 position spp( 5):	2.09			
Spacer 6 position spp( 6):	2.61			
Spacer 7 position spp( 7):	3.14			
Spacer 8 position spp( 8):	3.66			

Appendix A

Table A.3 Sample Short-Format Output for Option 1 (Cont'd)

```

=====
*****
time= 2.00hours
          maximum temperature(C)    flow velocity(m/s)
channel#= 1          91.             .06
channel#= 2          85.             .06
channel#= 3          82.             .05
channel#= 4          --- border channel ---          -1.44
Air Temp. in the Storage Building    Air Temp. at the Base Region
                                   32.             32.
*****

time= 4.00hours
          maximum temperature(C)    flow velocity(m/s)
channel#= 1          145.            .08
channel#= 2          134.            .08
channel#= 3          128.            .07
channel#= 4          --- border channel ---          -1.95
Air Temp. in the Storage Building    Air Temp. at the Base Region
                                   38.             38.
*****

time= 6.00hours
          maximum temperature(C)    flow velocity(m/s)
channel#= 1          191.            .09
channel#= 2          177.            .08
channel#= 3          168.            .08
channel#= 4          --- border channel ---          -2.14
Air Temp. in the Storage Building    Air Temp. at the Base Region
                                   47.             46.
*****

time= 8.00hours
          maximum temperature(C)    flow velocity(m/s)
channel#= 1          229.            .09
channel#= 2          213.            .08
channel#= 3          203.            .08
channel#= 4          --- border channel ---          -2.19
Air Temp. in the Storage Building    Air Temp. at the Base Region
                                   55.             54.
*****

time= 10.00hours
          maximum temperature(C)    flow velocity(m/s)
channel#= 1          260.            .09
channel#= 2          243.            .08
channel#= 3          232.            .08
channel#= 4          --- border channel ---          -2.20
Air Temp. in the Storage Building    Air Temp. at the Base Region
                                   62.             60.
*****

```

Table A.3 Sample Short-Format Output for Option 1 (Cont'd)

```

time= 12.00hours
      maximum temperature(C)    flow velocity(m/s)
channel#= 1                    284.                .09
channel#= 2                    266.                .08
channel#= 3                    255.                .08
channel#= 4                    --- border channel ---    -2.20
Air Temp. in the Storage Building    Air Temp. at the Base Region
                                68.                66.
*****

time= 14.00hours
      maximum temperature(C)    flow velocity(m/s)
channel#= 1                    303.                .09
channel#= 2                    285.                .08
channel#= 3                    275.                .08
channel#= 4                    --- border channel ---    -2.20
Air Temp. in the Storage Building    Air Temp. at the Base Region
                                72.                70.
*****

time= 16.00hours
      maximum temperature(C)    flow velocity(m/s)
channel#= 1                    318.                .09
channel#= 2                    300.                .08
channel#= 3                    289.                .08
channel#= 4                    --- border channel ---    -2.20
Air Temp. in the Storage Building    Air Temp. at the Base Region
                                75.                73.
*****

time= 18.00hours
      maximum temperature(C)    flow velocity(m/s)
channel#= 1                    330.                .09
channel#= 2                    312.                .08
channel#= 3                    301.                .08
channel#= 4                    --- border channel ---    -2.20
Air Temp. in the Storage Building    Air Temp. at the Base Region
                                78.                76.
*****

time= 20.00hours
      maximum temperature(C)    flow velocity(m/s)
channel#= 1                    340.                .09
channel#= 2                    322.                .08
channel#= 3                    311.                .08
channel#= 4                    --- border channel ---    -2.20
Air Temp. in the Storage Building    Air Temp. at the Base Region
                                80.                78.
*****

time= 22.00hours
      maximum temperature(C)    flow velocity(m/s)
channel#= 1                    349.                .09
channel#= 2                    330.                .08
channel#= 3                    319.                .08
channel#= 4                    --- border channel ---    -2.20
Air Temp. in the Storage Building    Air Temp. at the Base Region
                                82.                80.
*****

```

Appendix A

Table A.3 Sample Short-Format Output for Option 1 (Cont'd)

```

time= 24.00hours
                maximum temperature(C)    flow velocity(m/s)
channel#= 1                358.                .09
channel#= 2                337.                .08
channel#= 3                326.                .08
channel#= 4                --- border channel ---        -2.20
Air Temp. in the Storage Building    Air Temp. at the Base Region
                        83.                81.
*****

```

```

time= 26.00hours
                maximum temperature(C)    flow velocity(m/s)
channel#= 1                365.                .09
channel#= 2                344.                .08
channel#= 3                332.                .08
channel#= 4                --- border channel ---        -2.20
Air Temp. in the Storage Building    Air Temp. at the Base Region
                        84.                82.
*****

```

```

time= 28.00hours
                maximum temperature(C)    flow velocity(m/s)
channel#= 1                371.                .09
channel#= 2                350.                .08
channel#= 3                337.                .08
channel#= 4                --- border channel ---        -2.20
Air Temp. in the Storage Building    Air Temp. at the Base Region
                        85.                83.
*****

```

```

time= 30.00hours
                maximum temperature(C)    flow velocity(m/s)
channel#= 1                377.                .09
channel#= 2                355.                .08
channel#= 3                343.                .08
channel#= 4                --- border channel ---        -2.20
Air Temp. in the Storage Building    Air Temp. at the Base Region
                        86.                84.
*****

```

```

time= 32.00hours
                maximum temperature(C)    flow velocity(m/s)
channel#= 1                382.                .09
channel#= 2                360.                .08
channel#= 3                347.                .08
channel#= 4                --- border channel ---        -2.20
Air Temp. in the Storage Building    Air Temp. at the Base Region
                        87.                85.
*****

```

```

time= 34.00hours
                maximum temperature(C)    flow velocity(m/s)
channel#= 1                386.                .09
channel#= 2                364.                .08
channel#= 3                351.                .08
channel#= 4                --- border channel ---        -2.20
Air Temp. in the Storage Building    Air Temp. at the Base Region
                        88.                86.
*****

```

Table A.3 Sample Short-Format Output for Option 1 (Cont'd)

```

time= 36.00hours
      maximum temperature(C)    flow velocity(m/s)
channel#= 1                    389.                .09
channel#= 2                    367.                .08
channel#= 3                    354.                .08
channel#= 4      --- border channel ---          -2.20
Air Temp. in the Storage Building    Air Temp. at the Base Region
                                   89.                87.
*****

time= 38.00hours
      maximum temperature(C)    flow velocity(m/s)
channel#= 1                    392.                .09
channel#= 2                    370.                .08
channel#= 3                    357.                .08
channel#= 4      --- border channel ---          -2.20
Air Temp. in the Storage Building    Air Temp. at the Base Region
                                   89.                87.
*****

time= 40.00hours
      maximum temperature(C)    flow velocity(m/s)
channel#= 1                    395.                .09
channel#= 2                    372.                .08
channel#= 3                    359.                .08
channel#= 4      --- border channel ---          -2.20
Air Temp. in the Storage Building    Air Temp. at the Base Region
                                   90.                88.

```

**BIBLIOGRAPHIC DATA SHEET**

*(See instructions on the reverse)*

1. REPORT NUMBER  
(Assigned by NRC, Add Vol., Supp., Rev.,  
and Addendum Numbers, if any.)

NUREG/CR-6441  
BNL-NUREG-52494

2. TITLE AND SUBTITLE

Analysis of Spent Fuel Heatup Following Loss of Water in a Spent Fuel Pool  
A User's Manual for the Computer Code SHARP  
Final Report

3. DATE REPORT PUBLISHED

MONTH	YEAR
March	2002

4. FIN OR GRANT NUMBER

N/A

5. AUTHOR(S)

H.P Nourbakhsh, G. Miao, and Z. Cheng

6. TYPE OF REPORT

Technical

7. PERIOD COVERED *(Inclusive Dates)*

N/A

8. PERFORMING ORGANIZATION - NAME AND ADDRESS *(If NRC, provide Division, Office or Region, U.S. Nuclear Regulatory Commission, and mailing address; if contractor, provide name and mailing address.)*

Energy and Environmental Science, Inc.  
25 East Loop Road  
Stony Brook, NY 11790

Under Contract to  
Brookhaven National Laboratory  
Upton, NY 11973-5000

9. SPONSORING ORGANIZATION - NAME AND ADDRESS *(If NRC, type "Same as above"; if contractor, provide NRC Division, Office or Region, U.S. Nuclear Regulatory Commission, and mailing address.)*

Division of Systems Analysis and Regulatory Effectiveness  
Office of Nuclear Regulatory Research  
U.S. Nuclear Regulatory Commission  
Washington, DC 20555-0001

10. SUPPLEMENTARY NOTES

P. Norian, NRC Project Manager

11. ABSTRACT *(200 words or less)*

A methodology for predicting the spent fuel heatup in the event of loss of water during storage has been formulated and implemented within a computer code called SHARP (Spent-fuel Heatup: Analytical Response Program). This report documents the overall structure of the computer code SHARP. The code modeling framework, including the mathematical models and solution methods are described in the report. The computed results of the spent fuel heatup characteristics using representative design parameters and fuel loading assumptions are presented. The results of sensitivity calculations to study the effect of fuel burnup, building ventilation rate, baseplate hole size, partial filling of the racks, and the amount of available space to the edge of the pool are also presented in this report.

12. KEY WORDS/DESCRIPTORS *(List words or phrases that will assist researchers in locating the report.)*

spent fuel pool  
spent fuel heatup  
computer code  
SHARP (Spent-fuel Heatup: Analytical Response Program)  
code modeling  
nuclear power plant

13. AVAILABILITY STATEMENT

unlimited

14. SECURITY CLASSIFICATION

*(This Page)*

unclassified

*(This Report)*

unclassified

15. NUMBER OF PAGES

16. PRICE



Federal Recycling Program

